Non-invasive imaging of neuronal activity using PET

Inaugural - Dissertation

zur

Erlangung des Doktorgrades

der Mathematisch-Naturwissenschaftlichen Fakultät

der Universität zu Köln

vorgelegt von

Melika Irani

aus Iran

Köln, Dezember 2024

Berichterstatter (Gutachter)	Prof. Dr. F. Thomas Wunderlich
	Prof. Dr. Peter Kloppenburg
Tag der mündlichen Prüfung	03.02. – 28.02.2025
Vorsitzender der Prüfungskommission	Prof. Dr. Matteo Bergami
Beisitzende	Dr. Heiko Backes

Contents

Abstract

Measuring neuronal activity *in vivo* is still a challenging approach, although it might have a huge impact on science and clinical therapy. *cfos*, an immediate early gene, is expressed in most brain regions in neurons and has low expression at the basal level, but it is activated rapidly in response to various stimuli, including neuronal activity. It is used in science as a marker for evaluating neuronal activation *in vivo*. However, it hasn't been yet possible to measure brain *cfos* activation *in vivo*. The ^{18}F-FHBG/PET system is extensively used in both science and clinics to measure the expression of Herpes Simplex Virus 1 thymidine kinase (*HSV1-TK*) *in vivo*. *HSV1-TK* is an enzyme that phosphorylates ^{18}F-FHBG to trap it in the cell, and using the PET system, helps to visualize the cells expressing *HSV1-TK*. When *HSV1-TK* expression is controlled by the *cfos* promoter, we are able to indirectly measure *cfos in vivo* using PET. However, the ^{18}F-FHBG/PET technique has its limitations for measuring *HSV1-TK* expression in the brain due to the lack of transporters and the presence of the blood-brain barrier (BBB). *SLC43A3* is a purine nucleobase transporter reported to work as a transporter for adenosine and guanosine analogs, including ^{18}F-FHBG. In this project, we aimed to develop a non-invasive PET imaging system to assess neuronal activity *in vivo* using the ^{18}F-FHBG/PET system. To this end, a *cfos*-BAC was modified such that a FLEx *HSV1-TK* cDNA together with a PGK promoter-driven *SLC43A3* transporter was inserted into the second exon of the *cfos* gene via CRISPR/CAS9 Red/ET recombination. The linearized *cfos-fl-HSV1-TK:PGK-SLC43A3* BAC was used in pronuclear injection experiments to generate founder lines. To identify the best founder line, mouse embryonic fibroblasts (MEFs) were generated and tested in *ex vivo* experiments. These tests showed that HTNCre activation triggered *HSV1-TK* expression under *cfos* control. Thus, founder mice were crossed with Cre deleter mice to activate *cfos-HSV1-TK* in all cells to investigate our PET system *in vivo*. However, although *HSV1-TK* expression was controlled by the *cfos* promoter, the ^{18}F-FHBG failed to enter the brain since *SLC43A3* was not expressed in lectin-positive BBB. To overcome this limitation, several AAVs were constructed with a strong CAG promoter driving *SLC43A3* expression. However, this also failed to be sufficiently expressed in the BBB. The inability to express *SLC43A3* in the whole brain, especially in endothelial cells of the blood vessels, might be a potential reason why *SLC43A3* doesn't facilitate ^{18}F-FHBG entrance into the brain. However, we also attempted to reproduce the published data regarding ganciclovir (GCV) tritium or ^{18}F-FHBG uptake in *SLC43A3*-expressing cells. Surprisingly, these experiments revealed that *SLC43A3* neither transports ^{3}H-GCV nor ^{18}F-FHBG, indicating that finding a new transporter for ^{18}F-FHBG to facilitate its entry into the brain without damaging the BBB is a precondition for measuring neuronal activity non-invasively *in vivo* with great precision.

Zusammenfassung

Die Messung der neuronalen Aktivität *in vivo* ist eine Herausforderung, die einen großen Einfluss auf die Wissenschaft und klinische Therapie haben könnte. *cfos*, ein unmittelbar frühes Gen (Immediate Early Gene), wird in Neuronen in den meisten Regionen des Gehirns exprimiert und weist ein niedriges basales Expressionsniveau auf. Die Expression des Gens steigt bei neuronaler Aktivität deutlich an, weshalb es in der Wissenschaft häufig als Marker zur Bewertung der neuronalen Aktivierung *in vivo* verwendet wird. Bisher war es nicht möglich, die Aktivierung von *cfos* im Gehirn *in vivo* zu messen. Das ^{18}F-FHBG/PET-System wird sowohl in der Wissenschaft als auch in der Klinik umfassend verwendet, um die Expression der Herpes-Simplex-Virus-1-Thymidinkinase (*HSV1-TK*) *in vivo* zu messen. *HSV1-TK* ist ein Enzym, das ^{18}F-FHBG phosphoryliert, wodurch dieses in der Zelle eingeschlossen wird. Mittels PET (Positronen-Emissions-Tomographie) kann die Expression von *HSV1-TK* detektiert werden. Wenn die *HSV1-TK*-Expression durch den *cfos*-Promotor gesteuert wird, kann *cfos in vivo* indirekt mittels PET gemessen werden. Die ^{18}F-FHBG/PET-Technik hat ihre Grenzen bei der Messung der *HSV1-TK*-Expression im Gehirn, da kein geeigneter Transporter für FHBG in die Blut-Hirn-Schranke (BBB) vorliegt. Es konnte gezeigt werden, dass *SLC43A3*, ein Purin-Nukleobase-Transporter, ^{18}F-FHBG als Substrat transportiert. Ziel dieses Projektes war es, ein nicht-invasives PET-Bildgebungssystem zu entwickeln, mit dem neuronale Aktivierung im Gehirn untersucht werden kann. Dazu wurde ein *cfos*-BAC so modifiziert, dass eine *FLEx-HSV1-TK*-cDNA zusammen mit einem PGK-Promotor-gesteuerten *SLC43A3*-Transporter in das zweite Exon des *cfos*-Gens mittels *CRISPR/Cas9 Red/ET*-Rekombination integriert wurde. Das linearisierte *cfos-fl-HSV1-TK:PGK-SLC43A3*-BAC wurde für pronukleare Injektionen verwendet, um Gründerlinien zu erzeugen. Um die beste Gründerlinie zu identifizieren, wurden embryonale Fibroblasten von Mäusen (*MEFs*) generiert und *ex vivo* analysiert. Diese Ergebnisse zeigten, dass durch *HTNCre*-Aktivierung die *HSV1-TK*-Expression unter der Kontrolle des *cfos*-Promotors induziert werden konnte. Die Gründerlinien wurden daher mit *Cre*-Deleter-Mäusen gekreuzt, um *cfos HSV1-TK* in allen Zellen zu aktivieren und unser PET-System *in vivo* zu untersuchen. Obwohl die *HSV1-TK*-Expression durch den *cfos*-Promotor gesteuert wurde, konnte ^{18}F-FHBG nicht in das Gehirn gelangen, da *SLC43A3* nicht in Lectin-positiven Endothelzellen der BBB exprimiert wurde. Zur Überwindung dieser Limitierung wurden mehrere *AAVs* mit einem starken *CAG*-Promotor zur Expression von *SLC43A3* konstruiert. Auch dies führte jedoch nicht zu einer ausreichenden Expression in der BBB. Die Tatsache, dass *SLC43A3* nicht in den Endothelzellen der BBB exprimiert werden konnte, könnte ein möglicher Grund dafür sein, dass ^{18}F-FHBG nicht in das Gehirn transportiert wird. Beim Versuch, die von Furukawa et al. (2016) publizierten Daten zu reproduzieren, konnte gezeigt werden, dass *SLC43A3* weder *GCV* noch ^{18}F-FHBG transportiert. Dies zeigt, dass die Suche nach einem neuen Transporter für ^{18}F-FHBG, der dessen Eintritt in das Gehirn ermöglicht, ohne die BBB zu schädigen, eine wesentliche Voraussetzung ist, um neuronale Aktivität *in vivo* nicht-invasiv messen zu können.

1 Introduction

1.1 *cfos* an Early Immediate Gene

Cells are constantly exposed to various stimuli, and they respond differently depending on their nature and intensity of the stimulus. Some of these responses are regulated through proto-oncogenes. Proto-oncogenes are genes involved in cell proliferation, and under certain conditions, they can become oncogenes that lead to cancer development. Among these proto-oncogenes, there are immediate early genes (IEG) like *cfos* and *cjun* which are rapidly and transiently activated in response to various stimuli. Their protein products, Fos and Jun, combine to form the Activator Promoter 1 (AP-1), a transcription factor complex. This complex is a key regulator of transcription controlling the expression of various downstream genes that are involved in processes like cell proliferation and differentiation. While these genes are essential for normal cellular function, their dysregulation is linked to tumor development through excessive cell proliferation and division[20, 32].

Cfos plays a crucial role in neuroscience research. Neuronal activation induces the synthesis of the *cfos* gene and its protein product, Fos, making it a valuable tool for studying neuronal circuits. *Cfos* expression is naturally low across most brain regions but highly sensitive to external stimulation with its mRNA and protein levels reaching their peak within minutes to hours, making it an effective marker for identifying activated neurons after the exposing. This low-cost, reliable tool has been widely used to study behavior, molecular activation, and neuronal mechanisms in the central nervous system (CNS). *cfos* is a key player in the early steps of cellular response to stress or stimulus. However, measuring whole-brain *cfos* expression has only been possible so far *ex vivo*, limiting the ability to capture real-time neuronal activity *in vivo*.

1.2 Positron Emission Tomography (PET)

Positron Emission Tomography (PET) is a non-invasive imaging technique that allows for the detailed *in vivo* monitoring of biological processes at the molecular level, offering precise and quantitative accuracy. Due to these capabilities, PET is extensively utilized in small-animal imaging, gene therapy research, and oncology diagnostics. It relies on monitoring the concentration and distribution of positron-emitting radiotracers (PET tracer) inside the body [12]. Figure 1 shows the application of PET for the functional mapping of brain structure. PET is one of the most effective imaging modalities, it exploits molecular probes containing positron-emitting isotopes, such as ^{11}C, ^{13}N, ^{15}O and ^{18}F, which have various half-lives depending on the substance and purpose. These isotopes result in the emission of positrons during their decay; the positron generated from the isotope annihilates with an electron, and their collision leads to producing two gamma

rays simultaneously that emit 180 degrees opposite to each other (Fig. 1) [19]. These gamma rays are visualized using a dedicated scanner which converts the measurements into detailed images illustrating the distribution of the original PET probe/tracer inside the body.

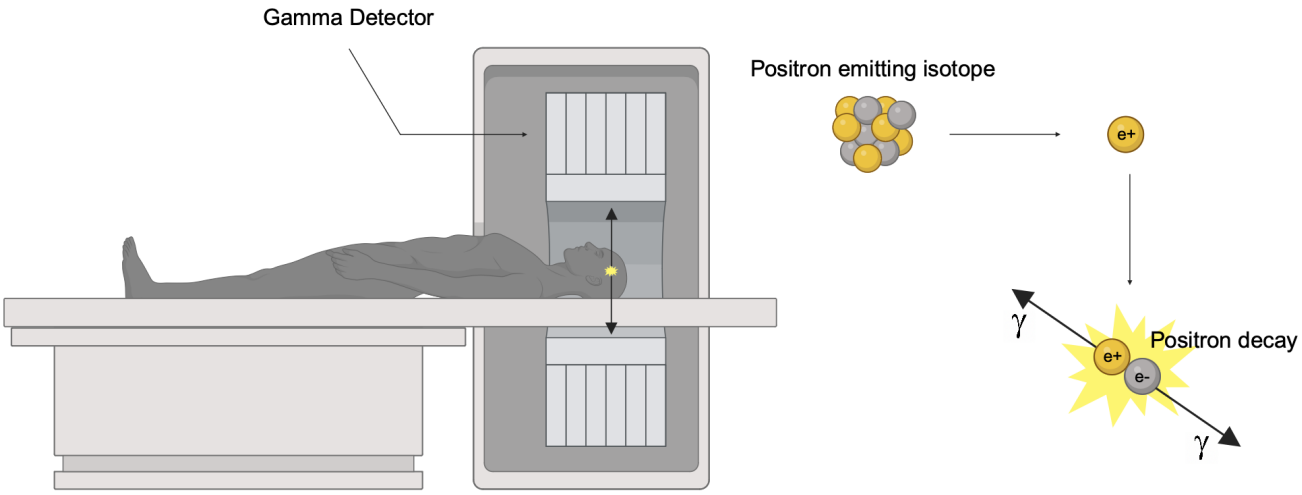

Figure 1: Principles of positron-emission tomography (PET) imaging. After intravenous injection, a positron-emitting probe circulated and is absorbed by tissues. The probe is sequestered where it either binds to target receptors or is converted by enzymes. Positron-electron collisions produce two photons gamma rays which are emitted 180° apart. These photons are detected as coincidence events, allowing the PET scanner to visualize the location and amount of the probe within the body [19] (BioRender.com).

During a PET measurement, a specific PET probe/tracer is injected into the subject's blood-stream. The probe spreads, diffuses into tissues, and binds to specific targets such as receptors or enzymes. Excess unbound probes are eventually cleared and washed out from the body, and then the PET scanner captures the target-specific accumulation of the radiolabeled probe in the body of the living subject.

Recent developments of PET probes that target specific gene expressions have been focused on making PET imaging more specific and sensitive for visualization and therapies. This includes designing new PET tracers that target specific cellular markers and combining PET with other modalities like Computed Tomography (CT) scan to get a complete picture of the therapeutic process. This has expanded the use of PET imaging to monitoring immune responses, tumor microenvironments and biodistribution of therapeutic agents. These probes are engineered to bind to specific proteins or receptors that are expressed as a result of gene activity. Once bound, they emit signals that can be detected by PET imaging and thus allows non-invasive monitoring of gene expression in real-time. So it helps to measure indirectly the target gene that has been reacted with the probe [1, 36].

PET is valuable in many fields, including oncology for its ability to monitor metabolic activities often altered in cancer cells. A commonly used tracer is ^{18}F-fluoro-2-deoxy-D-glucose (FDG), which is an analog of glucose. FDG is transported like glucose but is retained inside metabolically

active and fast glucose-consuming cells, such as the rapidly dividing cancer cells. This makes FDG/PET a very sensitive technique for cancer diagnosis or staging. PET scanners are usually combined with a CT scanner that can provide comprehensive diagnostics using both functional imaging capabilities and precise anatomical information.

Positron-emitting isotopes synthesized with a cyclotron usually have short half-lives; therefore, the labeled probes must be quickly synthesized and administered to the subject for study. Finally, the advent of small-animal PET (*micro-PET*) scanners has enabled scientists to expand the use of PET imaging in animal models before human clinical trials.

1.2.1 Neuronal Activity and PET Imaging

Beyond its clinical applications, PET has become an essential tool for studying neuronal activity and brain function in neuroscience. PET's ability to visualize metabolic processes is valuable to map areas of the brain that are active during specific cognitive tasks or in response to various stimuli. For example, tracers such as ^{18}F-fluorodeoxyglucose (FDG) can be used to visualize glucose metabolism in the brain, providing insights into the metabolic activity of neurons under different physiological and pathological conditions [33].

1.3 HSV1-TK as a PET Reporter Gene

Herpes simplex virus type 1 (HSV-1) is a virus that causes common oral and, sometimes, genital herpes infections. It belongs to the herpesviridae family and is distinguished by its latent infections in the host.*HSV-1* gene encodes the key enzme thymidine kinase (TK). TK plays a crucial role in the viral life cycle by phosphorylating nucleosides, which are necessary for DNA replication and division, particularly in infected cells. The HSV1-TK enzyme has a unique ability to phosphorylate a broad range of nucleoside analogs, which are not typically utilized by cellular thymidine kinases. This particular characteristic makes it beneficial for nucleoside-specific phosphorylation of the PET tracer in molecular imaging. The *HSV1-TK* enzyme is commonly used in research as a tool to monitor the expression of target genes. For this purpose, scientists place the expression of *HSV1-TK* and the target gene under the control of the same promoter. When the promoter initiates transcription, both the TK enzyme and the target gene are expressed proportionally.

1.4 ^{18}F-FHBG as the PET Reporter Probe/Tracer

In molecular imaging, *HSV1-TK* has been used as a PET reporter gene which can be visualized with a synthesized PET tracer called ^{18}F-FHBG (9-(4-^{18}fluoro-3-hydroxymethylbutyl)guanine).

Gambhir and his team conducted extensive research on ^{18}F-FHBG for visualization of *HSV1-TK* expression and developed a tracer kinetic model to quantify *HSV1-TK* activity *in vivo* effectively. They found ^{18}F-FHBG to be a highly effective and reliable tracer for *HSV1-TK* imaging.

This includes fast clearance from non-target tissues and high uptake in *HSV1-TK* expressing cells making ^{18}F-FHBG a great probe for high sensitivity and specificity imaging applications.

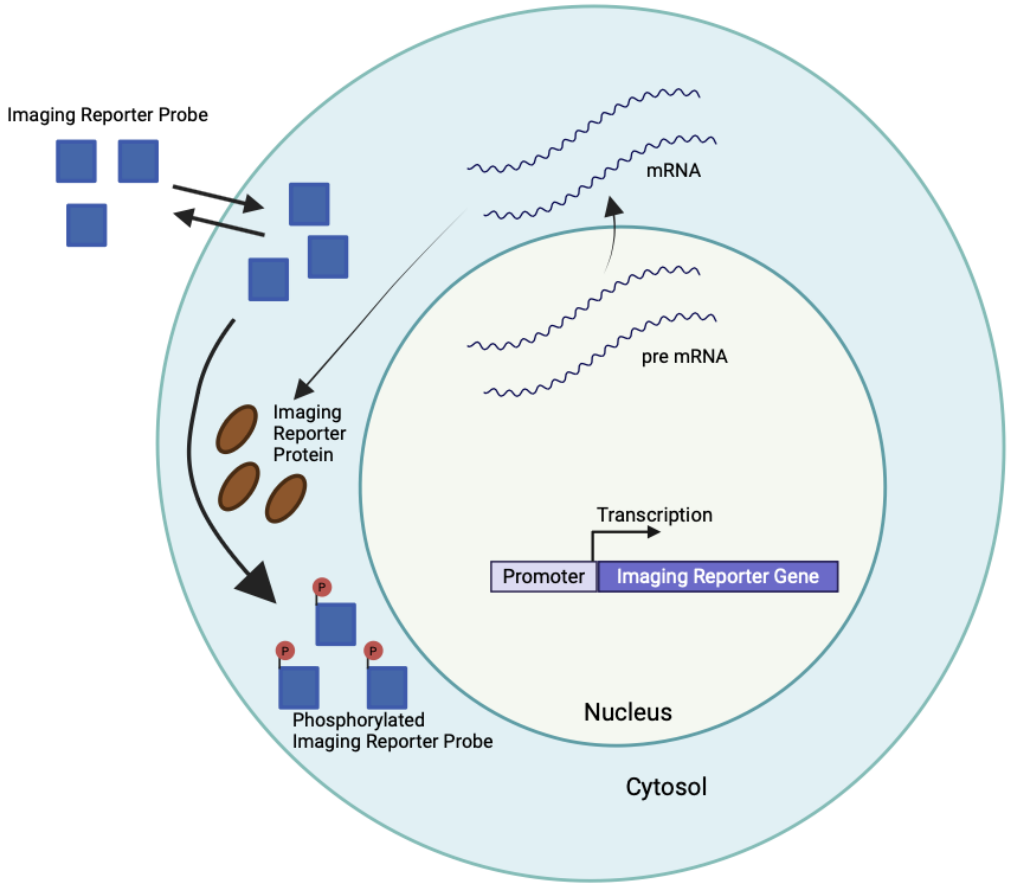

Figure 2: The mechanism of imaging the expression of the *HSV1-TK* enzyme-based PET reporter gene (PRG), Yaghoubi and Gambhir (2006), illustrating how the *HSV1-TK* gene allows for the specific trapping of radiolabeled substrates, enabling visualization through PET imaging [47](BioRender.com).

When *HSV1-TK* is introduced into target cells, the TK enzyme phosphorylates the injected radiolabeled ^{18}F-FHBG. The phosphorylated ^{18}F-FHBG by the TK protein is trapped inside the cells, allowing PET to visualize cells expressing the *HSV1-TK*. If the target gene is also expressed alongside TK under the same promoter, the expression of the target gene will be proportional to the TK expression. Hence, the expression of the target gene can be indirectly measured via the phosphorylated amount of ^{18}F-FHBG trapped in the cells (Fig. 2).

The *HSV1-TK*/^{18}F-FHBG system has been broadly studied for its effectiveness in tracking gene expression *in vivo*. Yaghoubi and Gambhir (2001) [48] [14] established its utility in both preclinical and clinical settings, showing that this ability to monitor cells expressing *HSV1-TK* non-invasively and in real time has made it a valuable tool for observing gene expression and evaluating the efficacy of gene therapy in living organisms [12] [48].

1.4.1 Limitations of ^{18}F-FHBG/PET Imaging in Quantifying *HSV1-TK* Expression in the Brain

Independent of all the valuable applications of the *HSV1-TK*/^{18}F-FHBG system in both science and clinical settings, there is a significant limitation for imaging *HSV1-TK* expression in the brain due to the lack of a transporter for ^{18}F-FHBG to cross the blood-brain barrier (BBB). The BBB is a selective barrier that restricts the passage of most substances from the bloodstream into the brain, including many radiolabeled probes like ^{18}F-FHBG, thereby preventing it from reaching brain tissues. Consequently, this restricts the use of ^{18}F-FHBG/PET imaging in monitoring *HSV1-TK* expression within the brain, making it unsuitable for studies involving gene expression in the central nervous system [46][45].

1.5 *SLC43A3*, a potential Transporter for the ^{18}F-FHBG

SLC43A3, a purine nucleobase transporter, was found by Furukawa and his team in 2016 [10]. Based on its known characteristics, *SLC43A3* is a good candidate to transport ^{18}F-FHBG into cells. This would be highly advantageous if ^{18}F-FHBG is effectively transported by *SLC43A3* into the brain. This would have enabled researchers to measure the *HSV1-TK* activity within the brain in future applications. *SLC43A3* has a fundamental role in the purine salvage pathway in mammals. Initially classified within a family of amino acid transporters comprising two other members named *SLC43A1* and *SLC43A2*, *SLC43A3* has been distinguished for its specificity in transporting guanine and adenine across cell membranes.

This transporter is crucial for maintaining intracellular nucleotide pools, enabling the uptake of these essential nucleobases for DNA and RNA synthesis, as well as for other metabolic activities. *SLC43A3* works as an equilibrative transporter, meaning it does not require energy input or ATP, and it passively facilitates the transport of nucleobases down their concentration gradient until reaching equilibrium across the membrane [10].

Furukawa also reported the mRNA distribution of *SLC43A3* across various organs ([10], Graph 6). Graph 6 in their publication demonstrates that *SLC43A3* is significantly expressed in organs such as the liver, kidneys, and spleen, while it is expressed the least in the brain and skeletal bones [10].

They also reported *SLC43A3*'s role in facilitating the transport of guanine analogs such as ganciclovir (GCV) [11]. GCV is extensively used in suicide gene therapy as a prodrug for the *HSV1-TK* enzyme. According to Figure 5 in Furukawa et al.[11], MDCKII cell lines stably expressing *SLC43A3* indicate the highest uptake of ^{3}H-GCV after 5 minutes of evaluation compared to control cell lines, while after 30 minutes, the cells expressing both *HSV1-TK* and *SLC43A3* show the highest uptake. They also presented a figure comparing the ^{3}H-GCV uptake in HEK293 cell lines transiently expressing *SLC43A3* and the two other members of the transporter family,

SLC43A1/A2, next to mock, which also shows the *SLC43A3* lines have the highest ^{3}H-GCV uptake. To conclude, *SLC43A3* plays an essential role in transporting ^{3}H-GCV into the cells, while *HSV1-TK* phosphorylates and traps the GCV in the cells [11].

Moreover, researchers have discovered that *SLC43A3* is involved in regulating free fatty acid flux within cells, which suggests that *SLC43A3* may have a role in lipid metabolism and general cellular energy balance. This multifunctionality positions *SLC43A3* as a critical player not only in nucleotide metabolism but also in broader metabolic processes [18].

Overall, *SLC43A3* is a purine equilibration passive transporter that plays essential roles in nucleotide and lipid metabolism. Its ability to transport both natural nucleobases and therapeutic analogs like GCV makes it valuable for enhancing the effectiveness of various medical treatments.

1.5.1 Applications of *HSV1-TK* and ^{18}F-FHBG/PET in Gene Therapy

Employing PET reporter genes and their corresponding PET reporter probes assists researchers in the non-invasive visualization of therapeutic gene expression in living subjects and in real time. This capability is essential for advancing human gene therapy trials and studying molecular and cellular therapies in animal models.

In addition, the *HSV1-TK* gene has been leveraged for therapeutic purposes, particularly concerning cancer treatment. Antiviral drugs like ganciclovir are substrates for the TK enzyme. TK initiates their phosphorylation, leading to the formation of toxic metabolites that selectively kill cells expressing *HSV1-TK*. This "suicide gene therapy" approach has been exploited to target and destroy cancer cells while simultaneously making it possible for the non-invasive monitoring of therapeutic effectiveness through PET imaging, as described by Karjoo, Chen, and Hatefi (2016)[23] (Fig. 3).

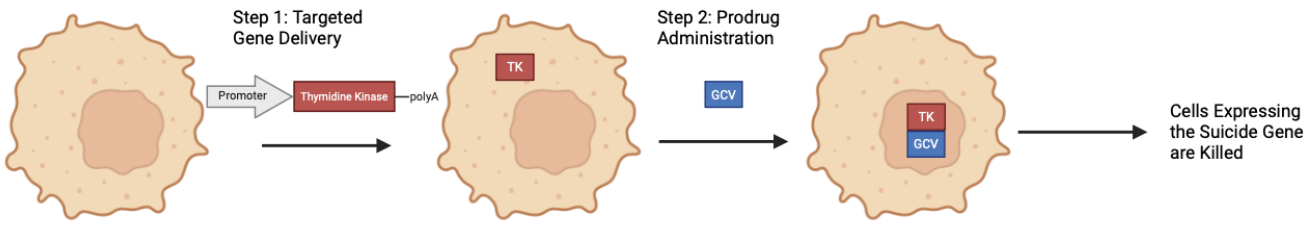

Figure 3: The two-step process in suicide gene therapy. First, cancer cells are targeted and transduced with suicide genes using a vector, resulting in the production of an enzyme. Next, a prodrug is administered, which is converted into a cytotoxic agent by the enzyme, leading to the destruction of the transduced cells [23](BioRender.com).

Advances in PET technology have improved the application of the *HSV1-TK* system. Improved scanner sensitivity and resolution enable the detection of even low levels of gene expression. Furthermore, the development and advent of more specific radiolabeled substrates have contributed to better imaging quality with high precision.

Overall, the *HSV1-TK*/^{18}F-FHBG system is a powerful tool in molecular imaging, offering a powerful method for visualizing gene expression and assessing the effectiveness of gene therapies.

1.6 Bacterial Artificial Chromosome (BAC) in Genetic Research

Bacterial Artificial Chromosomes (BACs), derived from the F-plasmid of *Escherichia coli*, are used in this study for generating the transgenic mouse line. BACs are crucial tools for CRISPR/CAS9 and nuclear injection in genetic engineering because they can carry large DNA fragments, up to 100-300 kb. This means they can include the target gene and all its regulatory elements, promoters and enhancers, so by using them we can get accurate and tissue specific expression. In addition, they are very stable so you don't get deletions or mutations during replication and handling which is critical when you are introducing complex constructs into the genome. With CRISPR/Cas9 techniques BACs are great templates for homology directed repair (HDR) because of their large homology arms. They are excellent tools for generating transgenic models. When introduced into mouse zygotes via pronuclear injection, they remain intact throughout the process, ensuring the preservation of large genomic regions. This makes them ideal for accurately modeling gene expression and regulatory elements *in vivo*. By including entire genomic regions BACs allow you to study tissue specific or activity dependent gene expression patterns, like the *cfos* gene, and to study gene function and regulatory networks *in vivo*. To this end, BACs are being used in science for different applications, such as transgenic animal model generation and for studying complex gene expressions that cannot be reached via other vectors [13][34].

1.7 Advancements in AAV Technology: Targeted Gene Delivery Using AAV-BI30 and AAV-PHP.eB

In this study, we used *AAV* vectors as an alternative approach to overexpress *SLC43A3* in the brains of mice, aiming to investigate the *SLC43A3* role in transporting ^{18}F-FHBG, a PET tracer, into the brain.

Adeno-associated viruses (*AAVs*) are vectors for delivering genetic material to specific cells, in research and therapy [30]. Recent advances in *AAV* engineering have given us new capsid variants that allow for more efficient and targeted delivery of genetic material. These engineered capsids expand the possibilities of *AAVs* to target specific tissues, increase transduction efficiency, and make gene delivery safer. They naturally infect many cell types and are not pathogenic, making them great for gene therapy [5].

Among the many *AAV* variants, *AAV-BI30* is discovered to be one of the most efficient for endothelial cells. Endothelial cells are key in vascular biology and of interest for both research and therapy. *AAV-BI30* has been engineered to target these cells specifically, allowing for efficient gene delivery to the endothelium. This specificity is achieved by modifications to the *AAV9* capsid

that improves binding and internalization in endothelial cells. It holds significant potential for vascular biology research and therapy for endothelial dysfunction diseases [27].

Another *AAV* variant used in this study is *AAV-PHP.eB*, which has been engineered for efficient crossing of the blood-brain barrier (*BBB*). The *BBB* is a major burden in delivering therapeutic agents to the central nervous system (*CNS*), and *AAV-PHP.eB* overcomes this by allowing gene delivery to neuronal and glial populations throughout the brain. This capsid variant has been shown to outperform many other *AAV* serotypes in brain-wide transduction, making it a valuable tool for neuroscience research and potential therapies for neurological diseases. Studies with *AAV-PHP.eB* have shown delivery of therapeutic genes in animal models of *CNS* diseases, highlighting its translational potential [5].

The invention and optimization of *AAV* capsids like *AAV-BI30* and *AAV-PHP.eB*, which we use in this study and are engineered variants of *AAV9*, showcase the progress in the field of viral vector engineering. These advances allow researchers to study specific cell populations with unprecedented precision and open up new gene therapy approaches. By combining the properties of engineered *AAVs* with specific targeting strategies, these vectors offer new ways to understand complex biology and address unmet medical needs. Their flexibility is a testament to the power of *AAV* technology in both research and therapy.

1.8 Significance of the Study

This project aims to address the limitation of imaging gene expression in the brain using the [^{18}F]-FHBG/*HSV1-TK* system. [^{18}F]-FHBG can't cross the blood-brain barrier because there is no appropriate transporter. Therefore, scientists cannot measure *HSV1-TK* expression, which prevents them from studying the target gene expression. The *HSV1-TK*/[^{18}F]-FHBG system is a potential technique to indirectly measure the expression of the gene of interest. Expressing the gene under the same promoter as *HSV1-TK* allows non-invasive measurement of the target gene. Traditionally, animals are sacrificed and perfused to dissect the brain tissue for immunostaining to analyze gene expression in the brain and understand neuronal activity. In this project, *cfos* is used as the target gene since it's one of the most commonly used genes in neuroscience to understand the role of neurons in response to different stimuli. To address this challenge, we tested our hypothesis by combining the *SLC43A3* transporter with the *HSV1-TK*/[^{18}F]-FHBG system. By genetically engineering ubiquitous expression of *SLC43A3* across all organs, including the brain, we aimed to facilitate the entry of [^{18}F]-FHBG into the brain, enabling measurement of *HSV1-TK* expression. This approach would allow us to assess *cfos* activity and other genes of interest in the future *in vivo*. To achieve this, we generated a custom reporter mouse model that expresses *HSV1-TK* under the *cfos* promoter, while *SLC43A3* is ubiquitously expressed under a selected promoter. This will be a new standard in neuroscience research and development of new therapeutic strategies. First, it allows scientists to measure target gene expression in the brain non-invasively in real time, reducing the risk of error and inconvenience of immunostaining or antibody selection and saving time. Second, it aligns with animal ethics by reducing the number of animals sacrificed, supporting the 3Rs (Replacement, Reduction and Refinement).

2 Materials and Methods

2.1 Animal Housing and Experimental Ethics

Animal housing and experiments followed approved protocols by local governmental authorities in Cologne (Bezirksregierung Köln). Ethics approval for breeding and experiments was granted by the Department for Environment and Consumer Protection - Veterinary Section Cologne North Rhine-Westphalia Germany (§11) 576.1.35.2.G 07/18 84-02.04.2017.A058). The animals in our study were housed in individually ventilated cages (IVCs) under a 12-hour light/dark cycle with the room temperature maintained at 22°C–24°C. They had a normal chow diet (NCD; Teklad Global Rodent 2018 Harlan). The pronuclear injection to generate the mouse line was conducted by Dr. Ronald Naumann at the Max Planck Institute of Molecular Cell Biology and Genetics in Dresden, Germany.

All mice used for staining underwent transcardial perfusion with 1X PBS, followed by ice-cold 4% paraformaldehyde (PFA; in 1X PBS; pH 7.4). After extraction from the skull, the brain was post-fixed in 4% PFA at 4°C for around 24 hours, then transferred to a 20% sucrose solution (in 1X PBS) at 4°C. The brains were cut at 20 μm on a sliding microtome (Leica Microsystems, model SM2010R) equipped with a stage for dry ice. For immunohistochemistry, sections were collected in bins containing anti-freeze solution (30% ethylene glycol and 20% glycerol in PBS), and subsequently stored at -20 °C until further processing. For RNA in situ hybridization, sections were mounted on SuperFrost Plus Gold slides (Cat No. FT4981Glp1LUS; ThermoFisher) and subsequently stored at -80 °C until further processing.

2.2 Materials

2.2.1 Primers list

All primers used in this study were purchased from Eurogentec company. In all naming cases the Fw stands for forward primer and Rev stands for revers primer.

Primer Name	**Sequence (5' to 3')**
55 FosTyp Fw	GCTCTCCTGTCAACACACAG
53 FosTyp Rev	AGACGGACAGACAGATC TGC GCA
35 FosTyp Fw	CAGAGCATCGGCCAGAAGGGG
33 Fostyp Rev	CGCTTGGAGTGTATCTGTCA

Primer Name	Sequence (5' to 3')
3xflag Rev	GTAGTCTCCGTCGTGGTCCT
55 new Fw	TGATGCCGAAGGGATAACGG
5 new correct Fw	GCCCCTTGAGCATCTGACTT
3 new correct Rev	CCATACCGACGATCTGCGAC
3NeoR Rev	CCTGCGTGCAATCCATCTTGTTC
SLC43A3.Fw	CCATCCCTGGTGTTCGTGTT
qPCR HSV1-TK.Fw	GCTCTCCTGTCAACACACAG
Fam Probe hsv1-tk	AATATCATGATCCTTGTAGTCTCCGTCGTGGTCCT
qPCR HSV1-TK.Rev	AACGCAGACGCGTGTTGATG
cFOS copy number FW	GGAGGGAGCTGACAGATACAC
cFOS copy number probe	CTGCTGCTCCTGAAACTTTATTAAAGTTGGAGC
cFOS copy number Rev	AAGGACCCTGCGCCCATAG
RT PCR,hsvtk FW	GCAGAAAATGCCCACGCTAC
RT PCR,hsvtk Rev	TGCCAGTAAGTCATCGGCTC
probe hsvtk	TTATATAGACGGTCCTCACGGGATGGGGAA
qPCR slc Rev	GGTCCGCACAGATCCTTGAA
qPCR slc Fw	CTGACAGGACTGCTGGAGTG

2.2.2 Antibody list

List of antibodies used in this study is brought in the table below.

Antibody Name	Dilution	Organism made in	Company
SLC43A3	1:50 IHC - 1:250 WB	Rabbit	Atlas Antibody

Name of Antibody	Dilution	Organism made in	Company
Lectin	1:200 IHC	Secondary Antibody	Vector Laboratory
NeuN	1:500	Rabbit	abcam
cFOS	1:500 IHC	Guinea pig	Syssys 108B5
GFAP	1:500	Chicken	Atlas Antibody
FLAG	1:700 IHC - 1:500 WB	Rabbit	abcam
Anti-GFP	1:1000	Chicken	abcam
NeuroTrace	1:200	Secondary	Thermo Fisher

2.2.3 Chemicals list

List of the all the chemicals used in this study shows in the table below.

Chemical	Supplier
β-mercaptoethanol	Applichem Darmstadt, Germany
Agarose	Merck Darmstadt, Germany
Ampicillin	Applichem Darmstadt, Germany
Bacillol	Bode Chemie Hamburg, Germany
Bovine serum albumin	Merck Darmstadt, Germany
Calcium chloride	Applichem Darmstadt, Germany
Chloramphenicol	AppliChem Darmstadt, Germany
Chloroform	Merck Darmstadt, Germany
DEPC	Applichem Darmstadt, Germany
Desoxy-ribonucleotide-triphosphates	Amersham plc, Little Chalfont, UK

DMSO	Merck Darmstadt, Germany
Ethanol	Applichem Darmstadt, Germany
Ethidium bromide	Merck Darmstadt, Germany
Ethylene diaminetetra acetate (EDTA)	Applichem Darmstadt, Germany
D-(+)-glucose	Merck Darmstadt, Germany
Glycerol	Merck Darmstadt, Germany
Glycine	Applichem Darmstadt, Germany
HEPES	Merck Darmstadt, Germany
Histodenz	Merck Darmstadt, Germany
Hydrochloric acid	Merck Darmstadt, Germany
IPTG	Thermo Fischer Scientific, Schwerte, Germany
Isopropanol	Roth Karlsruhe, Germany
Kanamycin	Applichem Darmstadt, Germany
LB	AppliChem Darmstadt, Germany
Magnesium chloride	Merck Darmstadt, Germany
N-Nitrosodiethylamine	Merck Darmstadt, Germany
Nitrogen (liquid)	Lide Pullach, Germany
Non-essential amino acids	Thermo Fischer Scientific, Schwerte, Germany
Phosphate-buffered saline (D-PBS)	Thermo Fischer Scientific, Schwerte, Germany
PMSF	Roche Mannheim, Germany
QIAzol	Qiagen Venlo, Netherlands

Sodium chloride	Merck Darmstadt, Germany
Sodium dodecyl sulfate (SDS)	Applichem Darmstadt, Germany
Sodium hydrogencarbonate	Merck Darmstadt, Germany
Sodium pyruvate	Thermo Fischer Scientific, Schwerte, Germany
Tissue freezing medium	Jung Heidelberg, Germany
Tris-(hydroxymethyl)-aminomethane	Merck Darmstadt, Germany
Triton X-100	Applichem Darmstadt, Germany
Trypsin inhibitor	Merck Darmstadt, Germany
Tween-20	Applichem Darmstadt, Germany
Western blocking reagent	Roche Basel, Switzerland

2.2.4 Bacterial strains and growth conditions

Various bacterial strains of *E. coli* were used depending on the experiment. Bacteria samples were grown on LB broth medium agar plates or LB broth medium liquid culture containing corresponded antibiotics. Samples were grown at 37 °C for 16-18 hours. Table below presents the information of the bacterial strains used in this study.

Strain	**Supplier**
Stbl3a	ThermoFisher Scientific, Invitrogen
DH5α	ThermoFisher Scientific, Invitrogen
XL10gold	In-house production

2.2.5 Kits list

All the kits used in this study are listed in the table below.

Kit	**Supplier**
Gel extraction kit	Qiagen, Germany
High capacity cDNA reverse transcription kit	Applied Biosystems, Darmstadt, Germany
Xtra Maxi	MACHEREY-NAGEL, Düren, Germany
Plasmid Mini prep	Applichem Darmstadt, Germany
Pierce BCA Protein assay kit	Thermoscientific, Schwerte, Germany
RNAScope kit	Advanced Cell Diagnostics (ACD), a Bio-Techne brand
RNase-free DNase kit	Qiagen, Hilden, Germany
RNeasy extraction kit	Qiagen, Hilden, Germany

2.2.6 Enzymes

All enzymes utilized in this study were sourced from New England Biolabs (NEB), known for their high quality and reliability. Enzymatic reactions were conducted using NEB-provided reaction buffers at recommended temperatures by the company, typically 37°C. The integrity and efficiency of the digestions were confirmed by agarose gel electrophoresis, ensuring successful DNA cleavage at the expected sites.

2.3 Methods

2.3.1 CRISPR/CAS9-Mediated Recombination

The *cfos* BAC (RP24-208N11 and RP24-233K8) was purchased from BacPac Resources as a bacterial stock. A small amount of the culture was streaked on a chloramphenicol plate to select single colonies. Subsequently, PCR was conducted using designed primers to verify the clones.

After confirming the correct colonies, mini-cultures containing 3 mL Luria-Bertani supplemented medium (LB) supplemented with chloramphenicol were prepared for transformation. The cultures were incubated for 16 hours at 37°C, after which the cells were pelleted by centrifugation and washed twice with ice-cold water. These cultures were then used to electroporate the CAS9 plasmid (Merck-Sigma Aldrich), which contains kanamycin resistance, into the bacteria. The

electroporated cells were then plated on chloramphenicol-kanamycin agar plates and incubated at 30°C for 18-24 hours.

Meanwhile, the *fl-HSV1TK:PGK-FRT-SLC43A3* gene construct, synthesized by GeneArt (Thermo Fisher) in a backbone plasmid (AMP), was transformed via heat shock into *XL10-Gold* competent cells for amplification. Subsequently, the BbsI restriction enzyme was used to excise the gene construct from the backbone plasmid.

Next, the linearized *fl-HSV1TK:PGK-FRT-SLC43A3* gene construct and custom designed CRISPRBACD plasmid, targeting the second exon of cfos (Merck-Sigma Aldrich), were electroporated into the cfos BAC CAS9 *E. coli* cells. Mini-cultures were prepared from the bacteria grown on chloramphenicol-kanamycin cultures for 3 hours at 30°C. The OD600 was measured until it reached the required value (0.3–0.5). Once the OD600 was achieved, 10% L-arabinose was added to induce the expression of the CAS9 plasmid to initiate the recombination process. After 3 hours, the cultures were centrifuged at 4°C to pellet the bacteria. The pellet was washed twice with sterile ice-cold water, and the linearized gene construct and CRISPRBACD plasmid were electroporated into the *E. coli* cells. The transformed cells were plated on chloramphenicol- 5% sucrose (Teknova, Catalog Number L5110) and incubate at 37 °C overnight (or for 8–12 hours). The gRNA plasmids can be removed through a counter-selection method utilizing SacB-sucrose, while the Cas9 Lambda Red Homologous Recombination Plasmid in *E. coli* can be eliminated by culturing the clone at 37 °C.

Subsequently, single colonies were picked and used with the designed primers (33 Fostyp Rev+5 new correct Fw and 55 new Fw+3 new correct Rev) to confirm the integration of the transgene in cfos BAC.

2.3.2 Cloning for the AAVs packaging

The CAG backbone plasmid and the gene of interest in the backbone plasmid were amplified by Maxi-Prep. Digestion control was performed for ITR sites afterwards for the CAG backbone plasmid.

Positive clones were digested with designated restriction enzymes matching the overhangs of the backbone and insertion.

The resulting digests were loaded into an agarose gel for electrophoresis. Gel purification was carried out using the kit. DNA concentrations were measured using Nanodrop, and the insertion and backbone in the ligation mixture were calculated using NEB Calculator (nebiocalculator.neb.com) as well as the NEB ligation kit. Heat shock transformation was performed by transforming 1 μl of the ligation mixture into *Stbl3* competent cells. Single colonies were picked and XmaI/SmaI enzyme digestion was used to check for the presence of ITRs while NcoI digestion was used to confirm the integration of the gene construct into the backbone.

2.3.3 AAVs Injection into the Brain

For direct brain transfection, we injected AAV-PHP.eB and AAV-BI30 into the mouse brain using a precise stereotaxic method.

The coordinates for the injections were set to (0.5, -1.94, -5.95). Using a surgical positioning system, the cannula was slowly inserted to a depth of z = -5.95 mm. A volume of 200 nL of the virus was injected at a rate of 50 nL/min. After the initial injection, the cannula was moved up by 0.5 mm in the z-direction, and the injection process was repeated. This procedure was continued incrementally until the cannula reached a final depth of z = -0.5 mm, resulting in a total injection volume of 2.4 μL of the virus across 12 positions.

After the final injection, the cannula was left in place for 10 minutes to allow for proper diffusion of the virus. The cannula was then slowly withdrawn to minimize tissue damage, and the injection site was closed with tissue adhesive to ensure proper healing.

2.3.4 Cell Culture

2.3.4.1 Passaging of Cells

Cells were maintained in an incubator at 37°C with 10% CO2 and 95% humidity. All cells were handled under a sterile hood (Hera Safe KS12, Heraeus Instruments). After the cells reached over 80% confluence, they were gently washed with PBS and then incubated for 5 minutes at 37°C in a trypsin solution (0.05% trypsin, 0.02% EDTA in PBS). To prevent cell damage, an equal volume of ES-cell medium was added to the trypsin solution. The cells were then centrifuged at 600g for 5 min RT and counted using the C-Chip from Thermo Scientific to determine the appropriate cell density for seeding onto new cell culture dishes.

2.3.4.2 Cell Freezing

For long-term storage, cells were frozen in FCS containing 10% DMSO (109678.0100, Merck, Darmstadt, Germany) and stored at -80°C. To thaw the cells, they were dissolved in EF medium (500 mL Dulbecco's Modified Eagle Medium (DMEM), 70 mL fetal calf serum (FCS), 6 mL sodium pyruvate (100 mM), 6 mL Minimum Essential Medium Non-Essential Amino Acids (MEM NEAA)) followed by immediate centrifugation at 600g for 5 minutes. Subsequently, the cells were seeded in fresh EF medium + p/s (Penicillin/Streptomycin) on cell culture dishes of the required size.

2.3.5 Generate Mouse Embryonic Fibroblast (MEF)

Mouse embryonic fibroblasts (MEFs) were isolated from 13.5-day-old embryos. Pregnant females were sacrificed by cervical dislocation. The uterus containing the embryos was collected and

transferred to a petri dish with PBS. Under the hood, the uterus was opened and the embryos were removed and transferred to a new petri dish with sterile PBS. The heads of the embryos were cut and saved for genotyping while all red and bloody parts were removed and discarded. The embryos were then cut into small pieces and 1 ml of 2.5% Trypsin (1 ml Trypsin per embryo) was added. The dish was then incubated at 37°C for 1 hour. To stop the reaction, 14 ml of EF media (500 mL Dulbecco's Modified Eagle Medium (DMEM), 70 mL fetal calf serum (FCS), 6 mL sodium pyruvate (100 mM), 6 mL Minimum Essential Medium Non-Essential Amino Acids (MEM NEAA)) plus 6 mL penicillin-streptomycin (Pen/Strep, 100 U/mL and 100 µg/mL, respectively) was added. The suspension was transferred from the mesh and plated in a 15 cm plate. The media was changed every day for 4 days for the primary MEFs.

2.3.6 Molecular Techniques

2.3.6.1 Polymerase Chain Reaction (PCR)

The PCR technique was utilized to amplify genomic DNA or plasmid DNA fragments for various purposes including genotyping and cloning. Depending on the amplicons's size, either GoTaq DNA polymerase (Promega, USA) or Phusion Hi-Fidelity polymerase (Thermo Scientific, USA) was employed.

2.3.6.2 Genotyping

The genotype of the mice was identified using polymerase chain reaction (PCR). Approximately 50 ng of isolated genomic DNA, DreamTaq PCR Master Mix, DNA Polymerase (Thermo Fisher Scientific, Schwerte, Germany), 25 pMol of each primer, and 25 µM dNTPs were combined in a 25 µl reaction mixture and incubated in a thermocycler with specific cycle protocols.

The genotyping PCR products were separated in agarose gels under a constant voltage of 130 V. Ethidium bromide in the gel was used to visualize the DNA. The size of the separated PCR products was determined by comparing them with a molecular weight marker (GeneRuler DNA Ladder Mix, Thermo Fisher Scientific, Schwerte, Germany).

2.3.7 RNA and Protein Extraction and Analysis

2.3.7.1 RNA Isolation

To extract RNA from tissue and cell samples, 500 µl of Quiazol lysis reagent was added to the tissue or 100 µl to the cell pellet, followed by thorough homogenization. After centrifugation at 1200 g for 10 minutes, the resulting supernatant was combined with 200 µl of chloroform for tissues and 100 µl for cells, then centrifuged for an additional 15 minutes at 12000 g at 4°C. Subsequently, the transparent upper phase was carefully transferred to a new reaction tube where

it was supplemented with 300 µl of 70% ethanol. To further refine RNA quality, the RNeasy Mini Kit (74106, Qiagen, Venlo, Netherlands) was utilized. The RNA mixture was loaded onto the RNeasy Mini spin column and centrifuged for 15 seconds at 8000 g. Following this, the column was washed with 350 µl of RW1 buffer. Any residual DNA was enzymatically digested by 30-minute RNase-free DNase kit (79254, Qiagen, Venlo, Netherlands) incubation at room temperature. Next, the column was washed with 350 µl of RW1 buffer and two additional washing steps with 500 µl of RPE buffer. Upon centrifugation for 2 minutes to dry the column, the elution of RNA in RNase-free water ensued and the concentration was subsequently determined using Nanodrop.

2.3.7.2 cDNA Synthesis

The High capacity cDNA reverse transcription kit was used to transcribe isolated mRNA into cDNA. Initially, 2 µg of isolated RNA was dissolved in 28.4 µl of ddH_2O. Subsequently, the mixture was supplemented with 4 µl of RT buffer, 1.6 µl of dNTP Mix (100 mM), 4 µl of Random Primer, and 2 µl of MultScribe™ Reverse Transcriptase (50 U/µl). The reaction was then incubated in a thermo block with the following temperature profile: 10 minutes at 25°C, 120 minutes at 37°C, followed by a final step at 85°C for 5 minutes. Finally, the samples were stored immediately at 4°C or -20°C for long-term storage.

2.3.7.3 Quantitative Real-Time PCR (qRT-PCR)

Quantitative Real-Time PCR (qPCR) was employed to measure the relative expression of genes at the mRNA level. Initially, isolated mRNA was reverse-transcribed into cDNA and subsequently amplified using a polymerase similar to conventional PCR methods. However, in qPCR, amplification is monitored in real time using a fluorescent dye. In this study, Taqman quantification and SYBR Green (SYBR® Select Master Mix, Thermo Fischer Scientific, Schwerte, Germany) were utilized. SYBR Green, functioning as a DNA intercalating dye, interacts with double-stranded DNA during annealing and elongation, thereby enabling relative quantification of the cDNA content. On the other hand, Taqman quantification employs a fluorescent dye attached to the 5' end of a specific probe and a quencher attached to the 3' end. As the Taq polymerase amplifies the targeted gene sequence, it degrades the probe, resulting in the separation of the fluorophore and quencher, emitting light measured as the cycle threshold (Ct). A higher Ct value corresponds to a lower initial DNA amount indicative of lower gene expression, while a lower Ct value indicates higher gene expression. The Ct values were normalized to a housekeeping gene assumed to be transcribed consistently under all experimental conditions. The qPCR experiments were conducted using the QuantStudio™ 7 Flex Real-Time PCR System (Applied Biosystems®, Foster City, USA). Tbp (TATA box binding protein) served as the housekeeping gene for normalization in most of the cases, and gene expression was calculated using the 2-ΔΔCt method (Livak and

Schmittgen 2001).

2.3.8 Detection of RNA Expression Using RNAscope In Situ Hybridization

Fluorescent in situ hybridization (RNAscope®) was employed to detect mRNA expression of *SLC43A3*. All required reagents were sourced from Advanced Cell Diagnostics (ACD, Hayward, CA), unless otherwise specified. Incubation steps were conducted at 40°C using the ACD HybEz hybridization system (Cat No. 321462). Sections were mounted on SuperFrost Plus Gold slides (Cat No. FT4981Glp1LUS; ThermoFisher) one day prior to the assay. After drying at room temperature, the slides were briefly rinsed in autoclaved Millipore water and air-dried, followed by incubation at 60°C for 4-6 hours. Subsequently, slides underwent Target Retrieval (Cat No. 322000) at 99.5°C for 10 minutes, followed by a rinse in autoclaved Millipore water and dehydration in 100% ethanol for 3 minutes. After air-drying for 5 minutes, a hydrophobic barrier was created around the sections using an ImmEdge hydrophobic barrier pen (Cat No. 310018), and slides were stored at room temperature until further processing.

The following day, slides were incubated with Protease Plus (Cat No. 322330) for 25 minutes. Subsequent steps, including probe hybridization, amplification, and detection, were carried out according to the manufacturer's protocol for RNAscope® Fluorescent Multiplex Detection Reagent kit v2 (Cat No. 323110). The probe was detected using tyramide-diluted Opal690 (1:2000), Opal650 (1:1500), Opal620 (1:1000), Opal570 (1:1000), Opal520 (1:750), or Cy3 (1:750). Sections were counterstained with DAPI and coverslipped with ProLong Gold Antifade Mountant (Cat No. P36931; ThermoFisher), then stored in the dark at 4°C until imaging.

2.3.8.1 Protein Isolation

The tissue or cells were snap-frozen in liquid nitrogen for preservation. Subsequently, a ceramic bead and 100 µl of the protein extraction mixture were added to the cells or tissue. This mixture comprised 1 ml of RIPA buffer (Cell Signaling Technology, Danvers, MA, USA) along with one tablet each of protease inhibitors (Complete Mini, Roche, Basel, Switzerland) and phosphatase inhibitors (PhosSTOP Phosphatase Inhibit. Cocktail, Roche, Basel, Switzerland) as well as 100 µl of PMSF. The tissue pieces were homogenized using an Ultra Turrax homogenizer. Following homogenization, the suspension was kept on ice for 30 minutes and then centrifuged at maximum speed for 10 minutes at 4°C. The resulting supernatant was carefully transferred into a new reaction tube and stored at -80°C for subsequent analysis.

2.3.8.2 Protein Quantification Using BCA Assay

The protein concentration of the cell lysates was determined using the Pierce BCA following the manufacturer's protocol. Absorption at 570 nm was measured to quantify the protein

concentration.

2.3.8.3 Western Blotting

SDS-PAGE was employed to separate proteins based on their molecular weight in an electric field. To achieve uniform negative charge on proteins and ensure equal loading, SDS was added to the protein solutions along with β-mercaptoethanol and incubated at 95°C for 10 minutes. The denatured proteins were then loaded into precast gels (Bio-Rad, Munich, Germany) and separated using SDS running buffer at 204 V. To estimate molecular weight, a PageRuler Prestained Protein Ladder was used.

Following SDS-PAGE, proteins were transferred onto a membrane for western blotting. The Trans-Blot®Turbo™ Transfer System (Bio-Rad, Munich, Germany) and Trans-Blot®Turbo™ Midi PVDF Transfer membranes (Bio-Rad, Munich, Germany) were utilized according to the manufacturer's recommendations.

After transfer, the PVDF membrane was washed with TBS-T and blocked with 1% blocking reagent (Roche, Mannheim, Germany) in TBS-T for 1 hour at room temperature. The membrane was then incubated with primary antibody diluted in 0.5% blocking solution overnight at 4°C. Subsequently, the membrane was washed three times, each for 10 minutes with TBS-T, and incubated with a secondary antibody conjugated to HRP for 1 hour at room temperature followed by another three rounds of 10 minutes TBS-T washing steps. Detection of the protein of interest was achieved using either Pierce ECL Western Blotting Substrate or SuperSignal Chemiluminescent Substrate (Thermo Fischer Scientific, Schwerte, Germany) depending on the expected signal intensity.

In western blotting, the primary antibody bound to a specific epitope on the protein of interest, while the secondary antibody. The secondary antibody was conjugated with horseradish peroxidase, which catalyzed the oxidation of luminol in the presence of H2O2, producing a luminescent signal that could be detected using a camera or light-sensitive films.

2.3.8.4 Immunohistochemistry (IHC)

To perform immunohistochemistry, brain tissue slices mounted on slides were surrounded by a hydrophobic barrier created using an ImmEdge hydrophobic barrier pen (Cat No. 310018) and allowed to air dry for 20 minutes. Subsequently, the slices were fixed using either 4% paraformaldehyde (PFA) or subjected to antigen retrieval as recommended by the antibody manufacturer. The slices were then washed twice for 10 minutes each with PBS. After washing, the slides were treated with 0.3% glycine for 10 minutes, followed by another 10-minute wash with PBS and a subsequent 10-minute incubation with 0.03% SDS.

Next, the slides were blocked for 1 hour in 3% serum from the animal species in which the

primary antibody was generated. Following blocking, the primary antibody, which was diluted in Signal Stain (Cell Signaling), was applied, and the slides were incubated overnight at 4°C. The following day, the slides were washed three times with PBS containing 0.1% Triton X-100 and then incubated for 1 hour at room temperature with the secondary antibody (ThermoFisher, 1:500 dilution) diluted in PBS with 0.25% Triton X-100. After incubation, the slides were washed three more times with PBS containing 0.1% Triton X-100 and dried. Finally, the sections were mounted in Vectashield DAPI-containing mounting medium (Vector Laboratories, #VEC-H-1200).

For the free-floating technique, brain slices in PBS were washed twice and subjected to the same procedure starting from the 0.3% glycine incubation. The slices were then treated with 0.03% SDS, blocked in 3% serum, and incubated with the primary antibody overnight at 4°C. The next day, the slices were washed with PBS containing 0.1% Triton X-100, incubated with the secondary antibody, and washed again. Finally, the sections were mounted in Vectashield DAPI-containing mounting medium (Vector Laboratories, #VEC-H-1200).

2.3.8.5 Imaging and quantification

Images were captured using a STELLARIS Confocal Microscope, equipped with a 40x/1.30 oil objective. Z-stacks were taken with optical sections of 0.9 μm. Laser intensities were kept constant throughout all related conditions. Images were imported into FIJI (NIH) where maximum intensities were projected. For representative images adjustments in brightness and contrast for each channel were kept constant throughout all related conditions.

In addition to confocal imaging, a slide scanner (Olympus Sideview VS200) was used to obtain full overviews of the slices. This allowed for capturing large-scale scans of tissue sections, complementing the high-resolution confocal images with a broader spatial context.

Images were imported into FIJI where maximum intensities were projected. For representative images adjustments in brightness and contrast for each channel were kept constant throughout all related conditions, whereas for quantification all channels were kept unmodified and approximately 4-6 sections were quantified per mouse. The software relies on the Dapi stain for cellular identification and calculates the cell intensity for each cell and probe

2.3.8.6 Recombinant expression of HTNCre

Recombinant expression of HTNCre began by inoculating LB-medium with a glycerol stock of *pTriEx-HTNCre* transformed into *E. coli*. These precultures were supplemented with 1% glucose, 100 µg/ml ampicillin, and 34 µg/ml chloramphenicol. The plasmid allows for IPTG-inducible expression of the Cre recombinase. Once the cultures reached an OD_{600} of 0.8, IPTG was added to induce HTNCre expression for 4 hours. After induction, the cultures were centrifuged, and the cell pellet was frozen at -20°C.

Upon thawing, cell lysis was initiated using lysozyme and benzonase, followed by sonication. TSB buffer was then added to the lysate, and the suspension was centrifuged. The supernatant was added to Ni-NTA agarose beads (Qiagen, Venlo, Netherlands) and incubated, followed by washing to remove weakly bound proteins. HTNCre, among the strongly bound proteins, was eluted using PTB containing 250 mM imidazole. The eluate was dialyzed overnight against a high-salt buffer and then against a buffer containing 50% glycerol for storage.

The concentration of HTNCre was determined by measuring absorption at 280 nm. Efficiency was assessed by incubating Ai14 mice-derived MEFs with different HTNCre concentrations and measuring fluorescence via flow cytometry (MACSQuantVYB, Miltenyi, Bergisch Gladbach, Germany). These MEFs carry a Cre reporter construct, which, upon Cre-mediated recombination, expresses a red fluorescent protein. The fluorescence level was used to determine the concentration of HTNCre that provided sufficient fluorescence without causing significant cell death.

3 Results

3.1 Generating of Conditional BAC *cfos-fl-HSV1-TK:PGK-FRT-SLC43A3* Transgenic Mice

In order to establish a mouse system allowing for cell type-specific non-invasive imaging of neuronal activity *in vivo*, we aimed at employing *cfos*-BAC transgenic mice with the ^{18}F-FHBG/PET imaging system. In our study, *cfos* was used as the target gene since its expression is tightly linked with neuronal activity under different conditions. To this end, we designed a conditional *cfos-HSV1-TK* gene construct (Fig. 4).

For this, the conditional *HSV1-TK* gene expression, one of the most widely used reporter genes, was placed under the *cfos* promoter. *HSV1-TK* expression is controlled by the FLEx (flip-excision) system. The FLEx system was used to express *HSV1-TK* in the target cells by crossing the mouse line with different Cre lines. This system involves two wild-type loxP and two mutant loxP cassettes flanking the *HSV1-TK* sequence, which was regulated by the *cfos* promoter.

Further, this mouse line was specifically designed to examine whether the ubiquitous expression of *SLC43A3* facilitates the entry of ^{18}F-FHBG into the brain.

In our model, *SLC43A3* is ubiquitously expressed throughout the mouse tissues via the phosphoglycerate kinase (PGK) promoter. At the same time, *SLC43A3* is flanked by two FRT sites, allowing for the removal of *SLC43A3* by crossing the founder mouse line with Del-flp, creating a control mouse line without the ubiquitous expression of *SLC43A3*.

On the other side, *SLC43A3* expression was designed to facilitate the radiotracer ^{18}F-FHBG to enter all cells, including those in the brain, while the FLEx-*HSV1-TK* system enables specific expression of *HSV1-TK* in target cells upon Cre-mediated flip. This specificity ensures accurate experiments for measuring *cfos* expression in specific neurons.

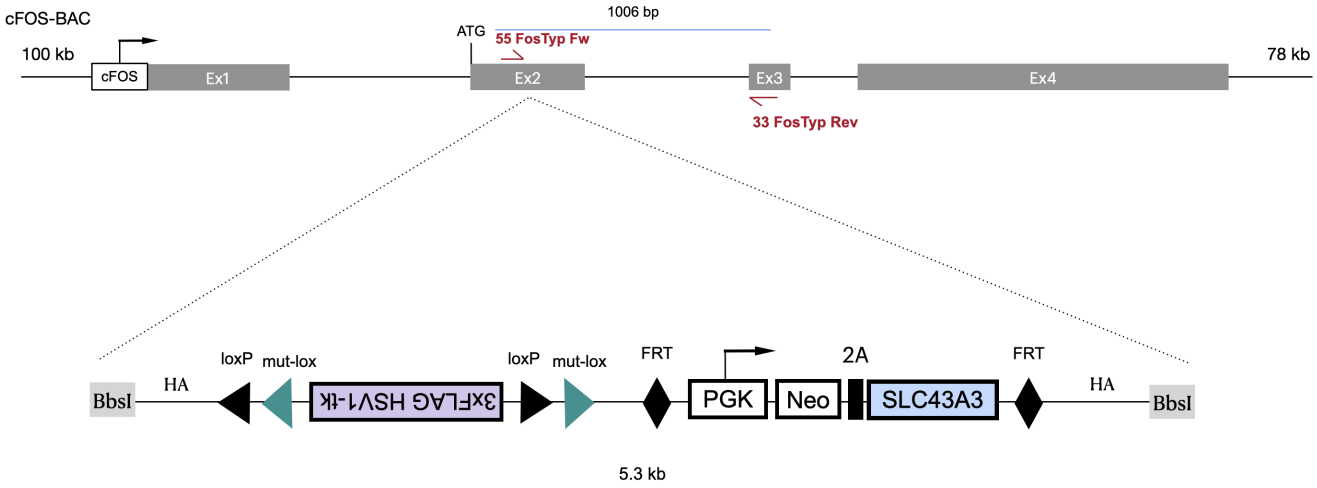

Figure 4: Designed *cfos*-fl-*HSV1-TK*:PGK-FRT-*SLC43A3*. The FLEX system is indicated by triangles with two wild-type and two mutant LoxP sites. *HSV1-TK* is FLAG-tagged and in reverse orientation, with its expression controlled by the FLEX system. *SLC43A3* expression is driven by the ubiquitous PGK promoter and flanked by two FRT sites, which can be crossed with Del-FLP mice to remove the sequence between these two FRTs. Two homology arms (HA) are positioned at each end of the fragment to facilitate the recombination steps. Additionally, BbSI was designed to cut the gene construct from the backbone. A 2A sequence is included to facilitate the cleavage of polypeptides during translation. Primers are shown in red, and the amplicon is indicated in blue

3.1.1 Modifying *cfos*-BAC using CRISPR/CAS9

cfos Bacterial Artificial Chromosomes (BACs) were modified using the CRISPR/CAS9 system. BACs are valuable tools in genetic research because of their stability in their host over many generations and their ability to maintain large DNA fragments.

cfos-BACs were specifically chosen for their inclusion of *cfos* within the genome. They carry a chloramphenicol resistance cassette to facilitate the selection of bacterial cultures carrying the BAC plasmid.

cfos-BAC *E.colis* were streaked on chloramphenicol agar plates from the delivered bacterial culture stab in a manner designed to isolate single colonies. Following colony isolation, primers were designed targeting the exon 2 of *cfos* (primers: 55 FosTyp Fw + 53 FosTyp Rev and 35 FosTyp Fw + 33 FosTyp Rev) to verify the presence of the correct cfos sequence in the BAC through PCR amplification, as depicted in Figure 5.

Once the clones were confirmed, a glycerol stock was made to save the BAC for subsequent experiments. The purified BAC DNA was then prepared for the CRISPR/CAS9 editing process.

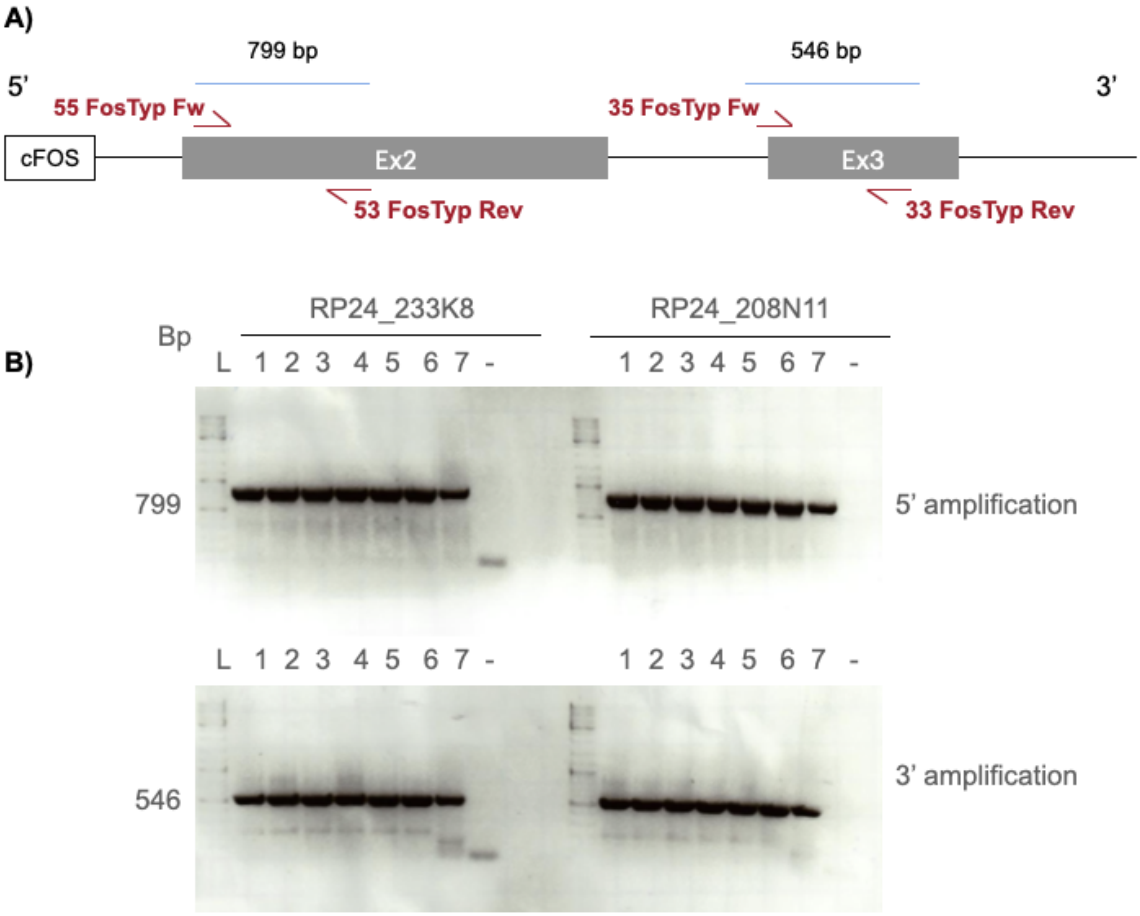

Figure 5: *cfos*-BAC verification. A) *cfos* gene and the position of the primers shown in red color while the amplicon region is in blue color. B) Agarose gel electrophoresis showing the PCR verification of two different *cfos*-BAC stocks. First and second rows show the amplification of the 5' and 3' ends, respectively. The expected PCR product sizes confirm the presence of the *cfos* gene in both BACs.

3.1.2 CRISPR/CAS9 Recombination using Red/ET enzymes

The CRISPR/CAS9 system, combined with RedET enzymes (*gam*, *bet*, and *exo*), was used to modify and insert the designed gene construct into the second exon of the BAC-*cfos*.

The Cas9 coding plasmid also contains a L-arabinose inducible promoter (*araBAD*) and the *araC* inhibitor, which is used to regulate the expression of the RedET enzymes. It also contains a *rep101ts*, a temperature-sensitive cassette that allows the plasmid to be removed at temperatures higher than 30°C, facilitating plasmid elimination after recombination. This plasmid was trasnformed via electroporation into *cfos*-BAC *E. coli* and selected by Kanamycin and Chloramphenicol (Fig 7).

At the same time, The designed *fl-HSV1TK:PGK-FRT-SLC43A3* construct, synthesized by Thermo Fisher Scientific GENEART GmbH in a plasmid vector with an ampicillin resistance cassette, was prepared for further use. To amplify the construct, it was first transformed into *XL10gold E. coli*, followed by a maxi-prep. Following amplification, to remove the backbone and obtain the linearized construct for the recombination step, the plasmid was subjected to overnight digestion with the restriction enzymes BbsI and ScaI, which were initially designed to cut the gene construct from the backbone. The digestion products were then separated by electrophoresis on a 1% agarose gel. A 5.3 kbp band, corresponding to the gene construct, was excised from the gel, and the DNA was purified using a gel extraction kit (Fig 6).

To confirm the successful linearization and purification of the gene construct, 3 µl of the cleaned DNA was loaded onto a 1% agarose gel for electrophoresis. The resulting gel image confirmed the presence and purity of the linearized gene construct, free from the plasmid backbone.

To proceed with the CRISPR/Cas9 recombination process, kanamycin- and chloramphenicol-resistant clones from the first electroporation were transformed with the linearized, purified gene construct and a customized gRNA plasmid (CRISPRBACD) (Fig. 7). The gRNA targets a specific protospacer adjacent motif (PAM) sequence and guides CAS9 to create a double-strand break at the target site.

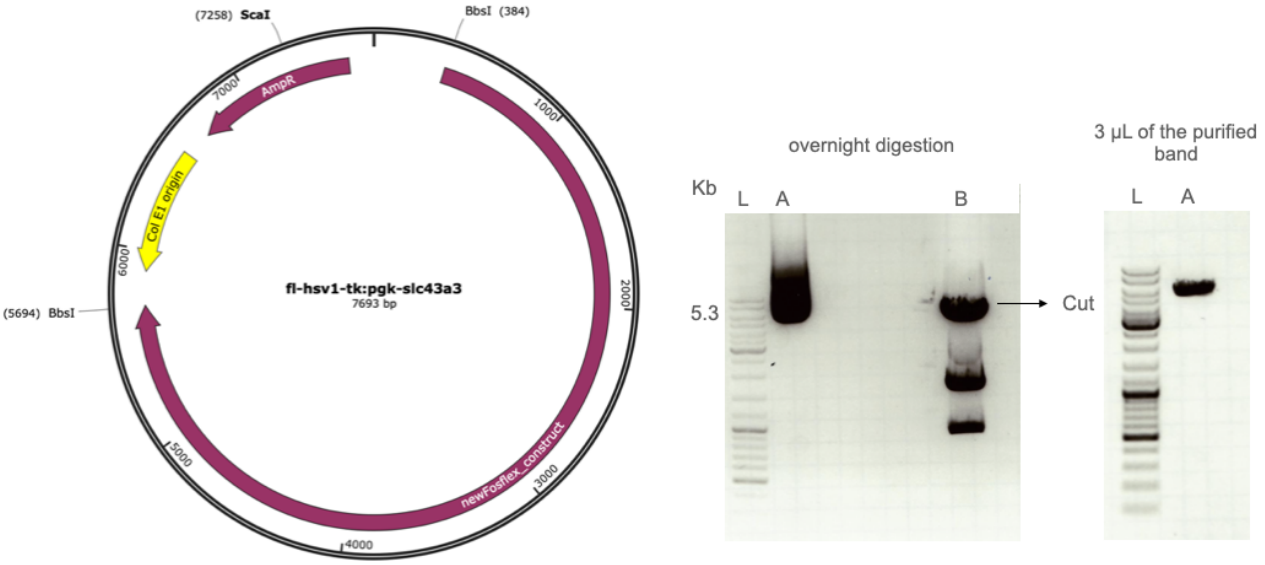

Figure 6: The left panel shows the plasmid map with the marked enzymes sites. On the right, the gel electrophoresis of the gene construct backbone plasmid digested with BbsI and ScaI has been shown. The sample was loaded into a 1% agarose gel. Sample B was purified and reloaded, as seen on the right side of the picture, verifying the cleanliness of the band.

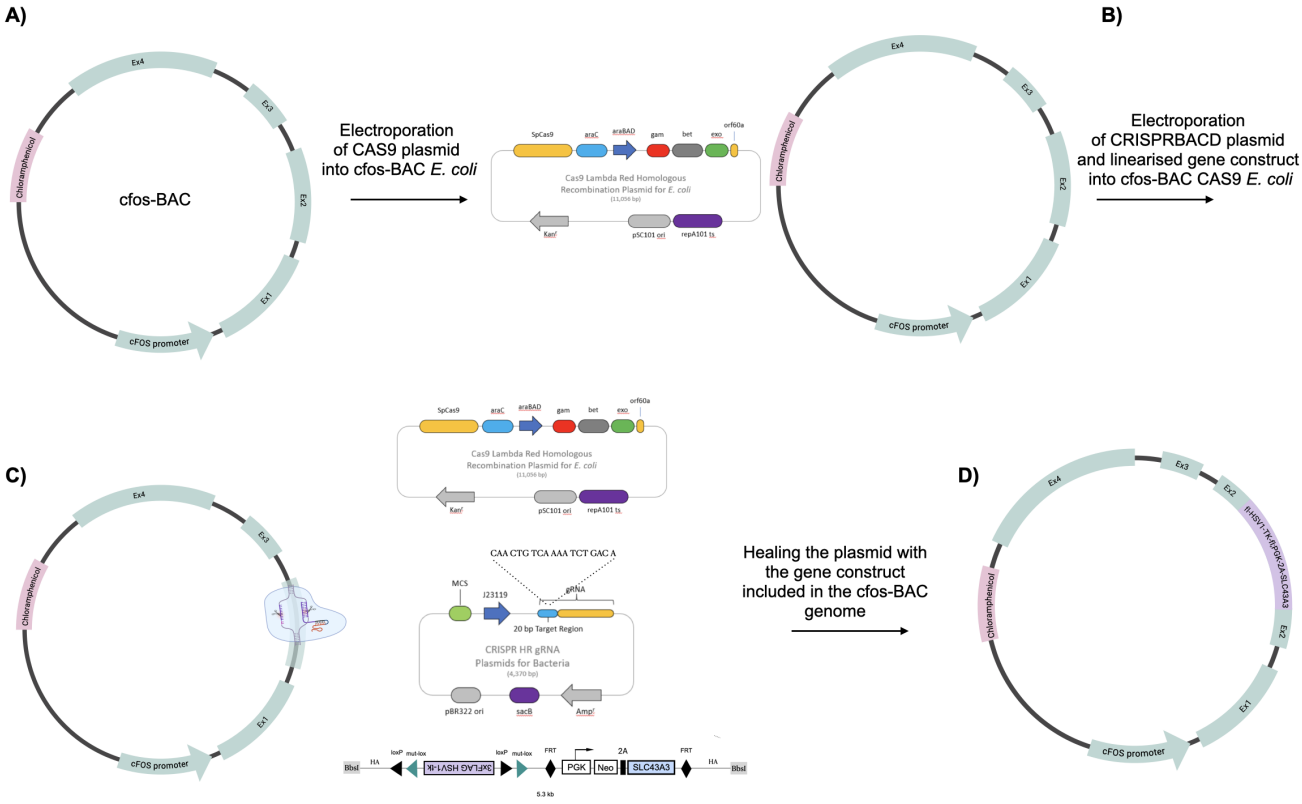

Figure 7: CRISPR/CAS9 Plasmids Used for the Integration of the Gene Construct into the Second Exon of *cfos*-BAC: A) Electroporation of the CAS9 plasmid into the *cfos*-BAC-containing *E. coli*. B) Electroporation of the CRISPRBACD plasmid along with the linearized gene construct into the *cfos*-BAC-containing *E. coli*. C) Recombination is induced by adding L-arabinose, which activates the expression of the *gam*, *bet*, and *exo* enzymes. This, combined with the presence of CAS9 for double-strand breaks and CRISPRBACD as the guide RNA (gRNA), facilitates the integration of the gene construct. D) Final plasmid is prepared, containing the gene construct integrated into the *cfos*-BAC, ready for pronuclear injection.

Upon the second transformation step, PCR was used to screen for the integration of the gene construct into the *cfos*-BAC. Four primers were used in this process. The primers used were: typing primers (5 new correct Fw and 3 new correct Rev) and wild-type primers (55 new Fw and 33 Fostyp Rev). This design allowed for the analysis of both the wild-type and modified *cfos* genes. The specific primers used for both ends of the construct ensured accurate targeting and amplification of the desired regions. To provide a clear overview of the primers used, a detailed table is included in the Materials section 2.2.1. The primers and the resulting amplicons are illustrated in Figure 8. As a final verification step, sequencing was done to confirm the successful integration of the gene construct before proceeding to the next step.

Following the introduction of the double-strand break, the gene construct, flanked by homology arms, was integrated into the second exon of *cfos*, resulting in the desired genetic alteration.

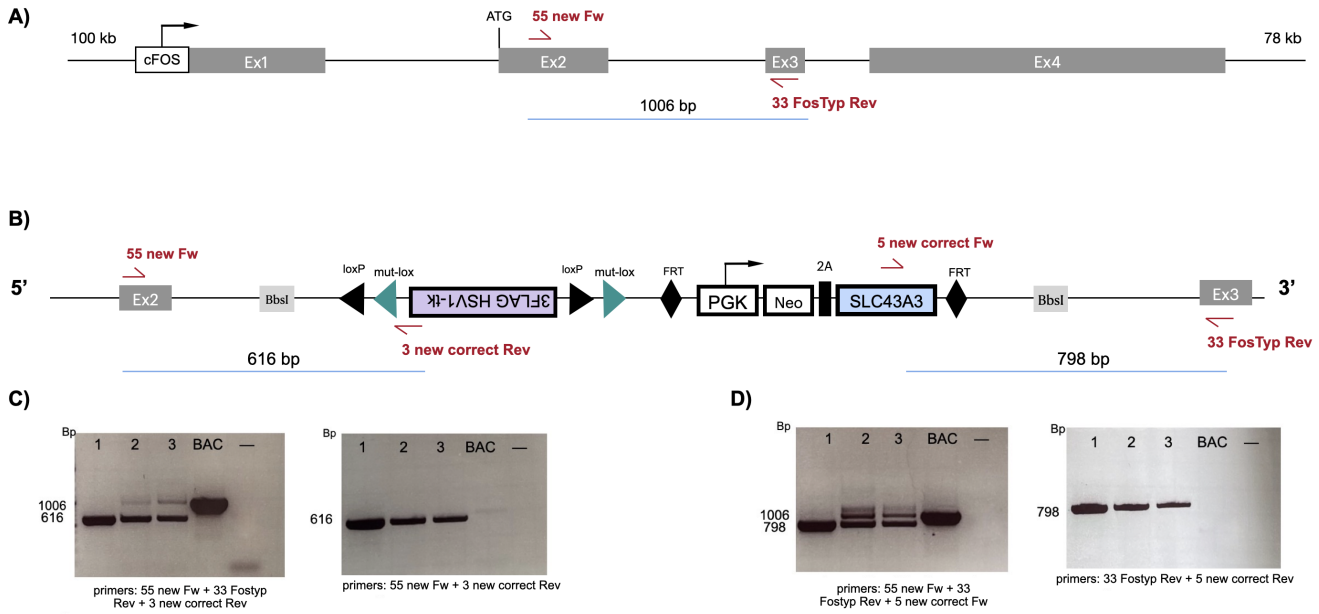

Figure 8: Gene Construct Integration and Primer Design for Verification of *cfos*-BAC Modifications: A) wild-type *cfos* gene (WT), primers shown in red, with the resulting amplicon size in the blue line. B) Gene construct integration into the *cfos* gene, with primers in red and amplicons represented by blue lines. C) Amplification of the 5' end of the modified *cfos*-BAC using specific primers (red) (55 new Fw + 33 Fostyp Rev + 3 new correct Rev) and corresponding amplicons (blue). D) Amplification of the 3' end of the modified *cfos*-BAC using primers in red (55 new Fw + 33 Fostyp Rev + 5 new correct Fw) and amplicons indicated by blue lines.

3.1.3 Linearization and Purification of *cfos*-BAC for Pronuclear Injection

To prepare the plasmid DNA for nuclear injection, the construct was first linearized using the rare-cutting homing endonuclease *PI-SceI* (New England Biolabs) (Fig.9 A)). Linearization is a crucial step, as linear DNA is more likely to integrate into the host genome compared to circular plasmid DNA, thereby increasing the efficiency of generating transgenic animals.

After *PI-SceI* digestion, the DNA was purified to remove any by-products such as residual enzymes, remaining plasmids from earlier transformations (CAS9 and gRNA plasmids), salts, and unwanted vector fragments from the reaction, which could otherwise interfere with subsequent experimental steps.

Purification was carried out using a self-made Sepharose column, which effectively separates linearized DNA from smaller contaminants through size exclusion chromatography (Fig. 9 B)). As the digested DNA passed through the column, the high-molecular-weight linear DNA was isolated, while smaller impurities were efficiently removed.

After purification, the quality and integrity of the DNA were assessed by loading the collected elution samples onto a 1% agarose gel. To further confirm the presence of the transgene, a separate PCR analysis was performed using typing primers specific to the transgene sequence on the most refined elutions. The results, shown in Figure 9, verified the successful presence of the transgene in these selected DNA preparations.

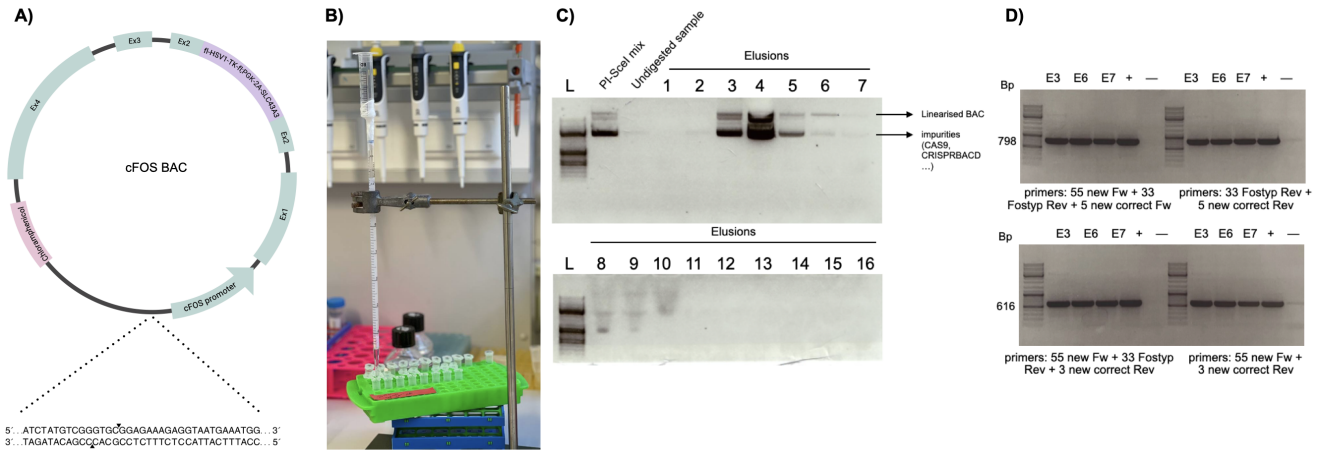

Figure 9: Preparation of Linearized *cfos*-BAC / Purification: A) Overnight digestion with PI-SceI B) Purification step using the self-made Sepharose column C) Agarose gel electrophoresis of the elutions obtained from the Sepharose column D) PCR verification of transgene presence in the selected top elutions.

As depicted in Figure 9 C), elution number 6 exhibited the desired characteristics of the linearized gene construct and passed the PCR confirmation. This particular elution was then sent for nuclear injection to MPI Dresden, Germany. This purification and verification process was critical in ensuring that the DNA used for nuclear injection contained the correct genetic material, thus increasing the likelihood of successful transgene expression in the resulting transgenic mice.

3.1.4 Pronuclear Injection for Generating the Conditional *cfos-fl-HSV1TK:PGK-FRT-SLC43A3* Mice

The generation of *cfos-fl-HSV1TK:PGK-FRT-SLC43A3*-BAC transgenic mice was accomplished through the pronuclear injection technique by our collaborator Ronald Naumann, head of the Transgenic Core Facility at the MPI of Molecular Cell Biology and Genetics in Dresden, Germany. This method involves the microinjection of a linearized BAC DNA construct containing the desired transgene into the pronucleus of mouse oocytes. Pronuclear injection allows for efficient integration of the BAC construct into the genome of the developing embryo, enabling the study of the BAC *cfos-fl-HSV1TK:PGK-FRT-SLC43A3* construct's function in the mouse model system. During the pronuclear injection, mouse oocytes were first collected from donor mice. The DNA construct was injected into the pronucleus of the fertilized eggs using a glass micropipette. The injected eggs were then implanted into the uterus of a foster mother and allowed to develop into offspring (Fig. 10 A)). Finally, 84 tail biopsies were screened for the presense of the transgene using specific primers (combined typing primers: 5 new correct Fw and 3 new correct Rev; and wild-type primers: 55 new Fw and 33 Fostyp Rev). Out of the 84 received biopsies, 9 were positive and subsequently delivered to the Cologne animal facility.

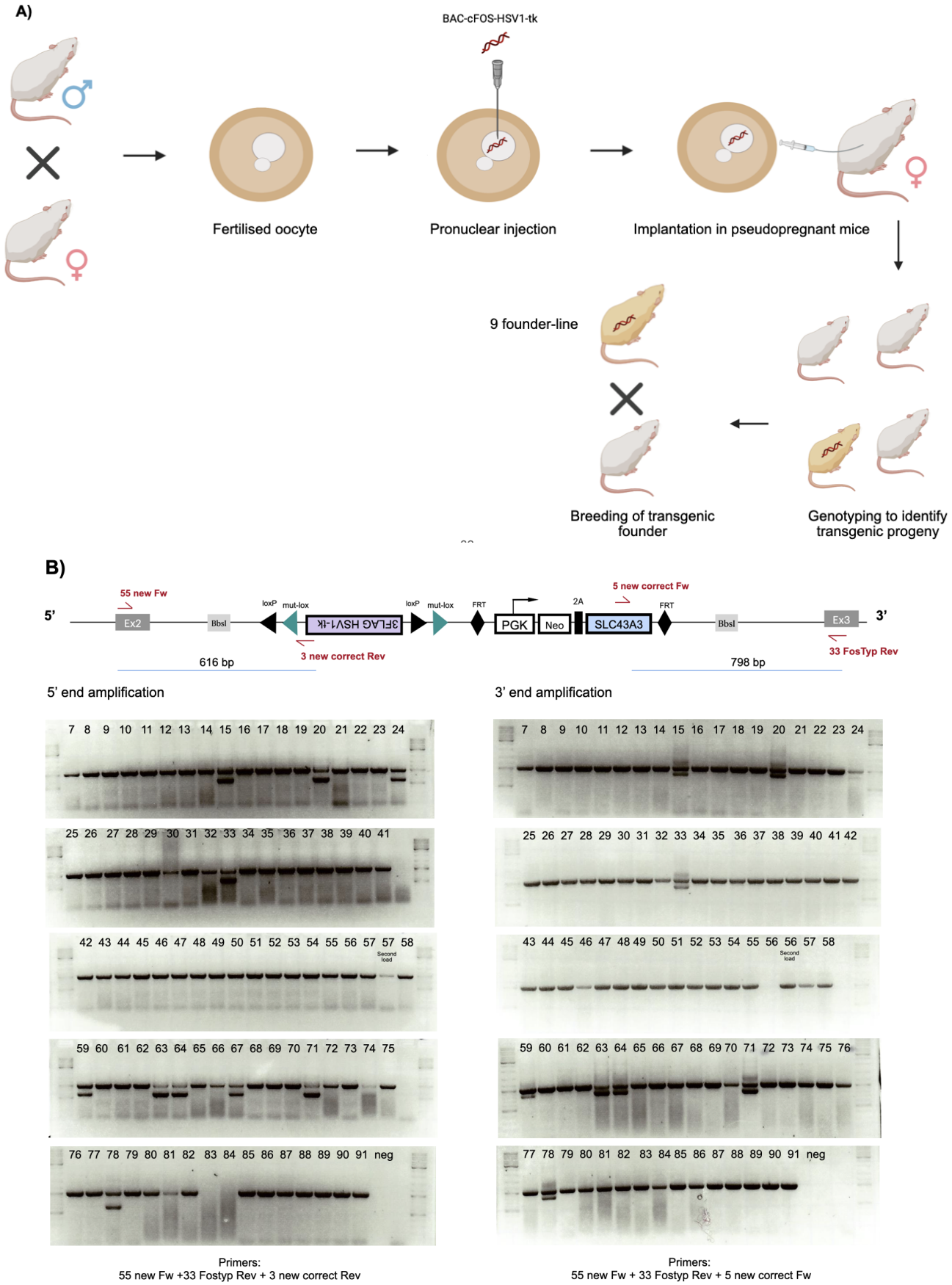

Figure 10: A) The diagram illustrates the process of pronuclear injection in mice. A fertilized egg containing male and female pronucleus is used, and a linearized DNA construct was injected into the male pronucleus with a micropipette. The injected egg was then implanted into a foster mother, where it develops into a transgenic mouse (BioRender.com). B) Agarose gel electrophoresis of tail biopsies from pronuclear injection of *cfos* BAC. Gel images on the left show the 5' amplification, while those on the right display the 3' amplification. Primer names are indicated below the images, with sequences listed in the Materials section 2.2.1.

3.1.5 Evaluating the *cfos* Copy Number in Conditional *cfos*-BAC Transgenic Mice

Pronuclear injection is a commonly used method for generating transgenic mice, but it has several drawbacks and limitations. One limitation is that transgene expression can be influenced by factors such as the site of integration, the copy number, and the position effect, which can lead to unpredictable effects on transgene expression and mouse phenotype. Additionally, there is a risk of random insertion of the transgene into a critical genomic region, which could disrupt endogenous genes.

Therefore, it is important to verify that the transgene is expressing at the expected level, depending on the copy number of the integrated *cfos*-BAC. Due to animal ethics considerations, we were limited to using only five transgenic animals for our experiment. As a result, we focused on identifying the most viable and productive lines for further experiments.

To assess the *cfos*-BAC copy number integrated into the genome of each mouse line, qPCR analysis of genomic DNA was performed. For this purpose, a custom qPCR probe (*cfos* copy number probe) and two primers (*cfos* copy number Fw and *cfos* copy number Rev) were designed to target the *cfos* third exon and intron region (sequence is listed in Materials section 2.2.1). This allowed for the quantification of *cfos*-BAC copy number in each mouse line.

Based on the data shown in the graph of Figure 11, mice numbered 33, 63, 64, 71, and 78 exhibited the highest *cfos* copy number compared to the rest. Mouse number 78 did not transmit on the transgene to its offspring and was therefore excluded from further experimentation.

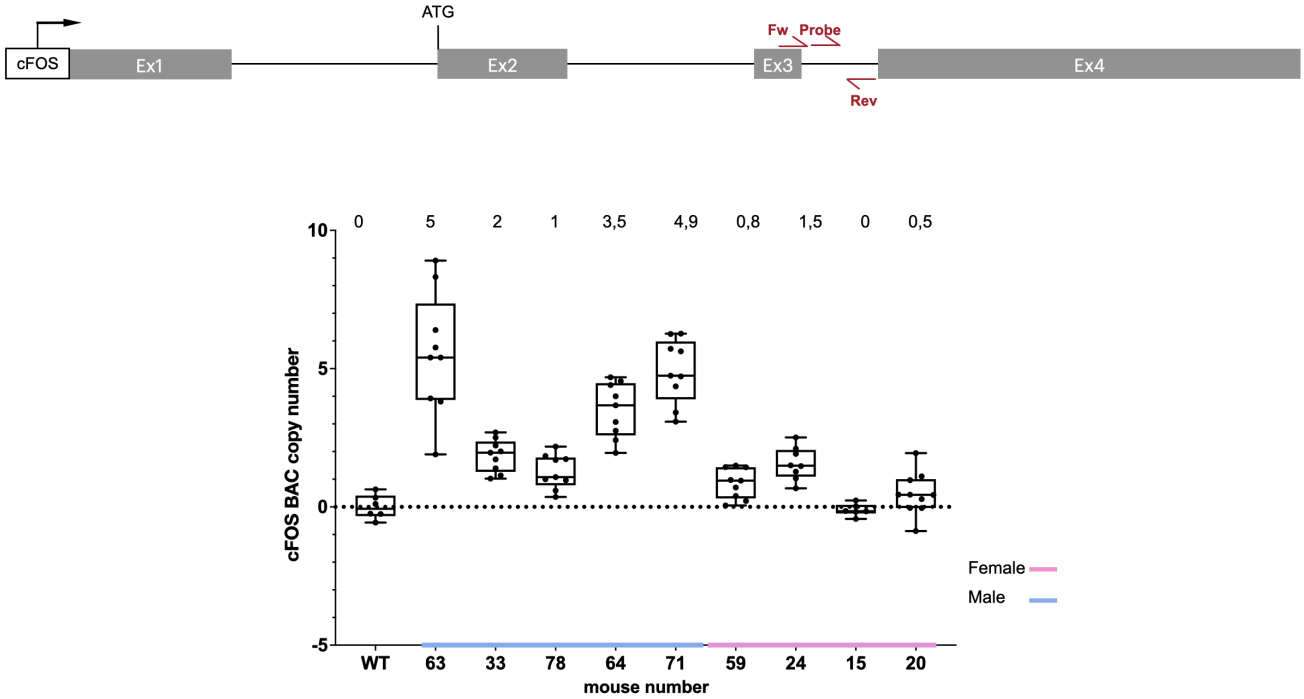

Figure 11: The graph illustrates the copy number of *cfos*-BAC in the genome of nine founder mice. The female mice are indicated by the pink lines, while the male mice are in blue. Numbers on top of the graph show the proportional *cfos* copy number. primers and probe location are shown in red on the scheme.

3.2 *ex vivo* Verification Experiments in MEFs

In total, nine founder mouse lines were obtained from MPI Dresden, each with the BAC construct randomly integrated into the mouse genome at varying copy numbers. After checking the copy number, we continued to work with four lines. To preselect the most suitable founder lines for our *in vivo* experiments, we first aimed to establish a reliable *in vitro* test. For this purpose, mouse embryonic fibroblasts were isolated from the selected founder lines for *in vitro* experiments.

3.2.1 Find the Best Substance to Induce *cfos* Expression in MEFs

To investigate the activation of the *cfos* promoter-controlled *HSV1-TK* expression *ex vivo*, it was necessary to identify the most effective *cfos* stimulator in MEF. Therefore, an experiment was conducted to determine the optimal stimulus for inducing *cfos* activation *ex vivo*. PMA, TNF-alpha, and LPS were chosen as potential stimuli due to their previously demonstrated ability to induce *cfos* expression *in vitro* [24, 41].

In this experiment, wild-type MEFs were treated with the selected stimuli at four different time points to induce *cfos* expression: 30 minutes, 30 minutes incubation with the stimulus followed by washing out and incubating the cells for another 30 minutes, 1 hour, and 4 hours. The activation of *cfos* was then measured using a *cfos* qPCR FAM probe, and the expression levels were normalized to TBP VIC, which served as the housekeeping gene.

The results (Fig. 12) demonstrated that the PMA 30-minute induction exhibited the most robust activation of *cfos* among the tested conditions. This was evidenced by significantly higher levels of *cfos* expression compared to TNF-alpha and LPS treatments. The effectiveness of PMA as a *cfos* stimulator was consistent. Thus, PMA at 20 nM was determined to be the ideal and reliable inducer for inducing *cfos* activity in MEFs.

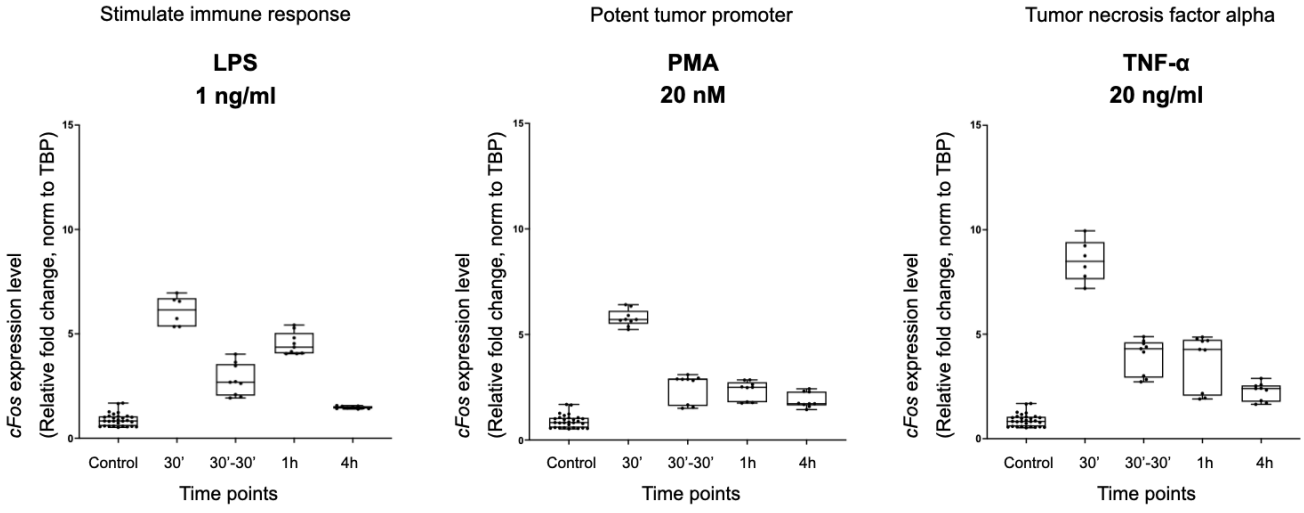

Figure 12: Various stimuli, including PMA, TNF-alpha, and LPS, were tested to induce the expression of *cfos* in wild-type MEFs. The level of *cfos* activation was measured at four different time points.

3.2.2 Evaluate the *SLC43A3* in MEFs of the Conditional *cfos*-BAC Transgenic Mice *ex vivo*

In the transgenic mice, *SLC43A3* is designed to be expressed ubiquitously under the PGK promoter. Therefore, Verification was performed *ex vivo* by generating mouse embryonic fibroblasts (MEFs) from each founder mouse, as described in Methods Section 2.3.2. A *SLC43A3* FAM qPCR probe was used, with the TATA-binding protein (TBP) VIC probe as the housekeeping gene (HKG) for this experiment. TBP was used as a reference in qPCR because its expression remains stable across different experimental conditions.

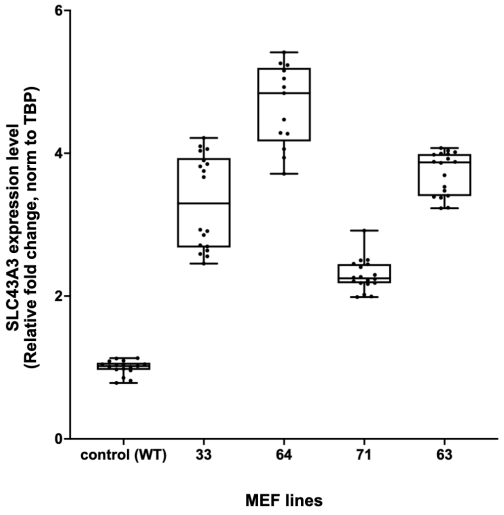

Figure 13: mRNA levels of *SLC43A3* in various transgenic MEF lines compared to wild-type.

The resulting Graph 13 shows the expression of the transporter in various MEF lines compared to wild-type MEF, all of which exhibit higher expression levels, as expected.

3.2.3 Verify the FLEx System in MEFs of the Conditional *cfos*-BAC Transgenic Mice *ex vivo*

In order to verify the functionality of the FLEx system before starting the *in vivo* experiment, MEFs from each line were treated with HTNCre protein, to flip *HSV1-TK* into the correct transcriptional orientation. RT-PCR was conducted using the designed primers and probe (RT-PCR *hsvtk* Fw, RT-PCR *hsvtk* Rev, and probe *hsvtk*) to quantify the expression of the *HSV1-TK-tk* gene in MEFs from each mouse line treated with HTNCre protein *in vitro*. Original, untreated MEFs from each line were used in this experiment as negative controls (Figure 14. A)).

Notably, as shown in the gel picture in Figure 14. B), mouse number 33 showed leaky expression of *HSV1-TK-tk* in untreated cells, leading us to terminate further exploration of this line.

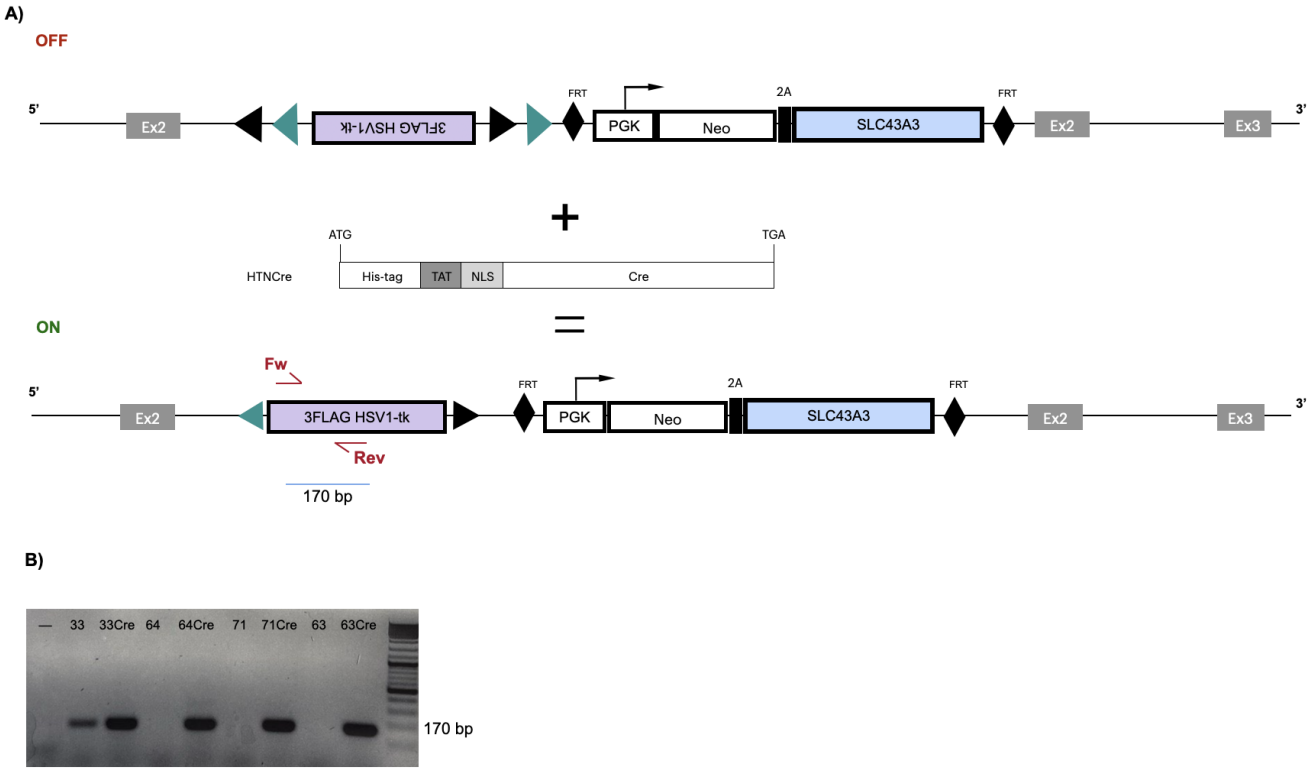

Figure 14: A) Treatment of MEFs with HTNCre protein and quantification of *HSV1-TK* expression levels. The top section shows the original construct, which, after treatment with HTNCre protein (containing TAT, the Trans-Activator of Transcription, which enhances viral transcription efficiency, and NLS, the nuclear localization signal/sequence, which tags the protein for import into the cell nucleus via nuclear transport), inverts the *HSV1-TK* gene into an open reading frame orientation, resulting in the final construct. Primers are indicated by the red arrows, and the amplicon is represented by the blue line. B) RT-PCR quantification of *HSV1-TK* expression in HTNCre treated versus non-treated MEFs.

The leaky expression in line 33 suggests the FLEx system is not working as expected. FLEx keeps the *HSV1-TK* silent until activated by Cre recombination. But *HSV1-TK* is expressed in untreated MEFs. This could be due to imprecise integration of the *cfos*-BAC into the genome and incomplete silencing. Mutations or rearrangements in the loxP sites could also prevent the gene from being locked. Insufficient silencing of the FLEx cassette, epigenetic changes or basal promoter activity even when the gene is inverted contribute to the leaky expression in this line.

3.2.4 Quantifying the Dynamics of *cfos* and *HSV1-TK* mRNA Levels After PMA Stimulation in Different Transgenic MEF Lines

Since *cfos* expression is measured indirectly through the expressed amount of *HSV1-TK* using ^{18}F-FHBG/PET experiments, it was necessary to evaluate whether the expression of these two genes is correlated *in vitro* before starting the *in vivo* experiments.

For this purpose, an experiment was performed in transgenic HTNCre-treated and non-treated MEFs with 20 nM PMA *cfos* induction for 30 minutes and 1 hour, analyzing the mRNA levels of both *HSV1-TK* and *cfos* under these different conditions.

Figure 15 illustrates that *cfos* expression peaked after 30 minutes of PMA treatment, indepen-

dent of HTNCre treatment. However, in the absence of HTNCre, *HSV1-TK* expression remained at basal low levels, even when PMA was present. In contrast, when HTNCre was introduced and followed by PMA treatment, a significant increase in *HSV1-TK* expression was observed.

These findings indicate that the successful activation of *HSV1-TK* was mediated by HTNCre. On the other hand, *cfos* was expressed independently of HTNCre, with the highest levels observed after 30 minutes of stimulation, showing a direct correlation between *cfos* stimulation and elevated *HSV1-TK* expression.

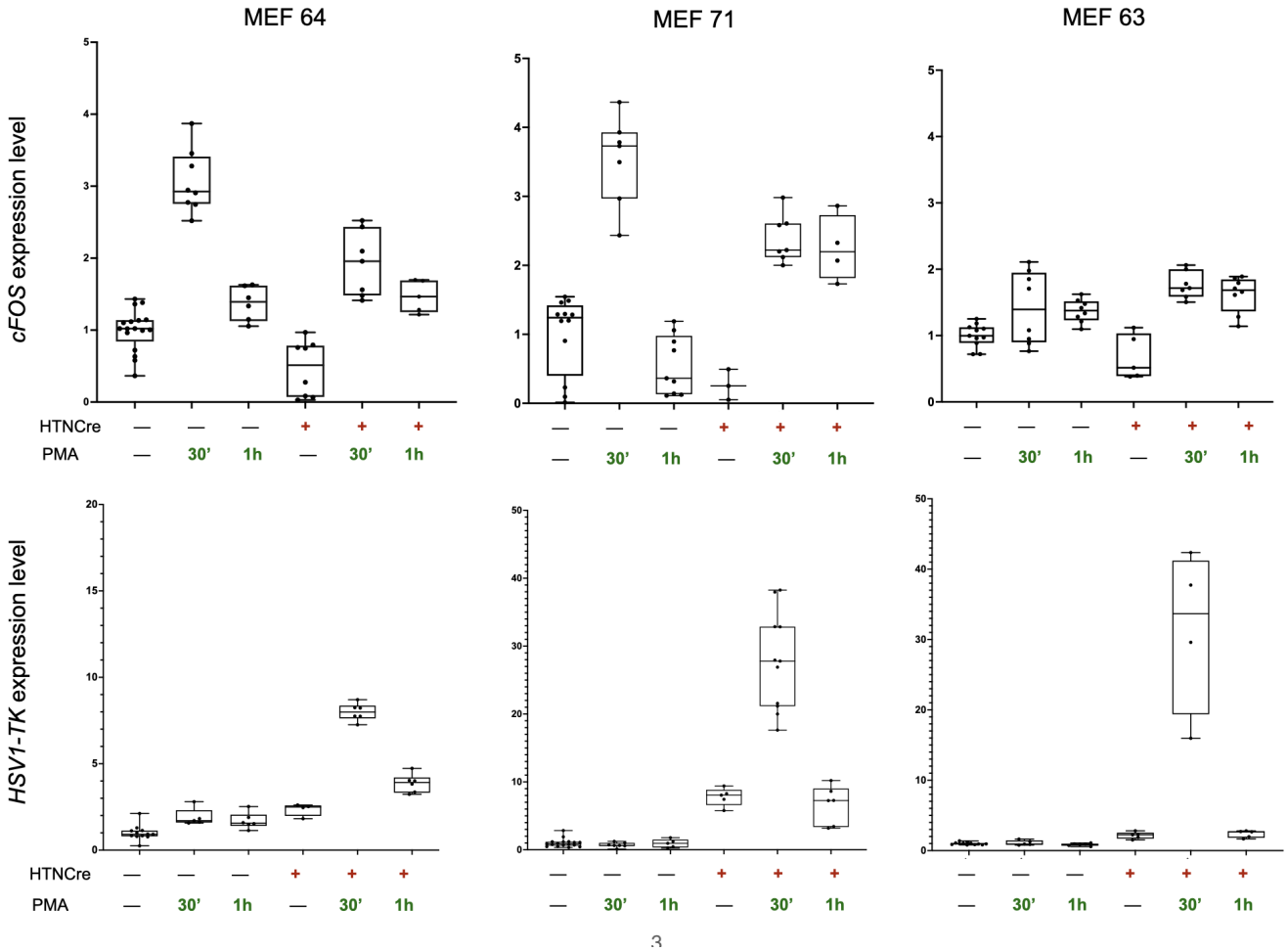

Figure 15: Analysis of *cfos* and *HSV1-TK* mRNA expression in MEFs treated with HTNCre and without treatment, following stimulation with 20 nM PMA for 30 minutes and 1 hour. *cfos* expression reaches its peak at 30 minutes, regardless of HTNCre treatment. A significant increase in *HSV1-TK* expression is observed exclusively in HTNCre-treated cells, indicating that *HSV1-TK* activation is dependent on HTNCre.

3.2.5 Quantifying the Dynamics of *cfos* and *HSV1-TK* mRNA Levels After Removing PMA in MEFs

After confirming that the *HSV1-TK* gene is successfully activated in HTNCre-treated MEFs and that *cfos* is effectively stimulated with 20 nM PMA, correlating with *HSV1-TK*, we needed to verify whether the downregulation of these two genes follows a similar pattern. This would allow us to use *HSV1-TK* as an indirect measure of *cfos* activity.

To address this, an experiment was designed where HTNCre-positive MEF cells were stimulated with 20 nM PMA for 30 minutes. After the 30-minute stimulation, the cells were washed and incubated in 4% FCS media for designated time points. The cells were collected at 0 min, 15 min, 30 min, and 3 hours post-washout, where 0 min indicates the cells were collected immediately after washing out the stimulus.

The expression levels of *HSV1-TK* and *cfos* mRNA were analyzed at each time point across all MEF lines (Figure 16).

As expected, both *cfos* and *HSV1-TK* expression levels were upregulated at the initial time points (0 min, 15 min, 30 min, and 1 hour post-washout), and then downregulated to near basal levels by 3 hours.

These results suggest a correlation between *HSV1-TK* and *cfos* expression levels, indicating that the regulation of *HSV1-TK* expression is dependent on *cfos*, with similar expression dynamics observed for both genes.

Additionally, Figure 17 shows a graph generated from the data presented in Figure 16. The graph plots *cfos* expression on the X-axis and *HSV1-TK* expression on the Y-axis, illustrating that *cfos* and *HSV1-TK* mRNA levels are significantly correlated. This further supports the conclusion that *HSV1-TK* can be used as an indirect measure of *cfos* activity.

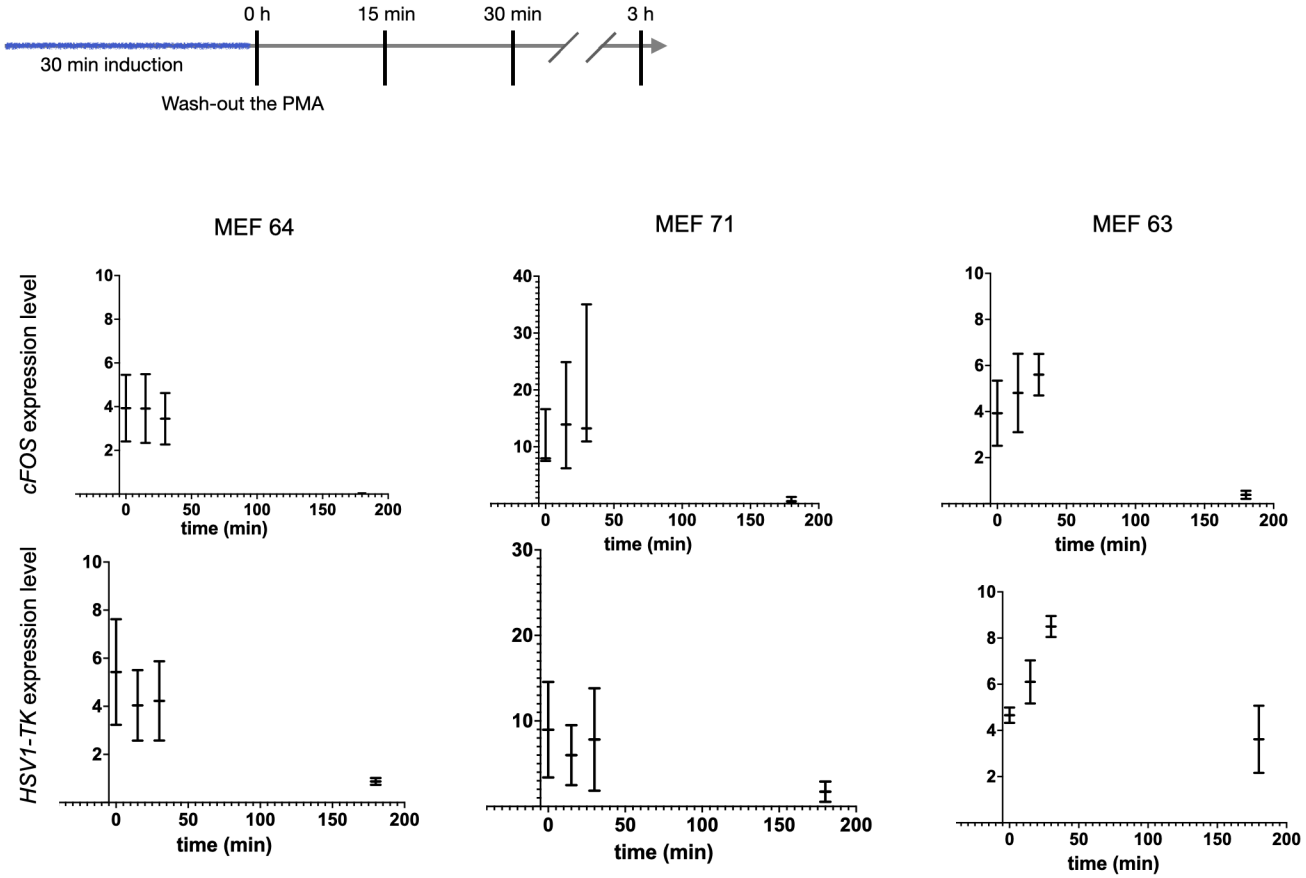

Figure 16: mRNA expression levels of *cfos* and *HSV1-TK* at different time points after PMA stimulation. HTNCre-treated MEFs from various mouse lines were incubated with 20 nM PMA for 30 minutes, washed, and collected at 0 min, 15 min, 30 min, and 3 hours post-washout. The first row shows *cfos* expression levels, and the second row shows *HSV1-TK* expression levels.

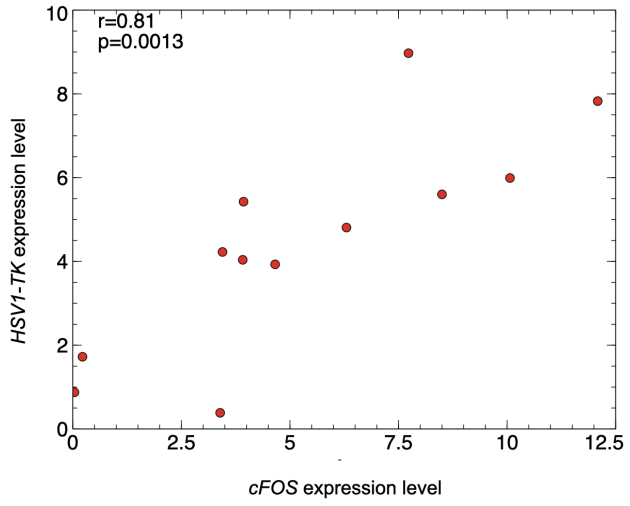

Figure 17: The graph shows *cfos* expression on the X-axis and *HSV1-TK* expression on the Y-axis. It demonstrates that *cfos* and *HSV1-TK* expression levels are significantly correlated at the mRNA level.

3.2.6 Summary of the *in vitro* Experiments in MEFs

After the MEF experiments, we conclude that:

- The FLEx system functions properly after treatment of the lines with HTNCre proteins.
- *SLC43A3* is expressed at higher levels in transgenic MEFs compared to the wild type, as expected.
- PMA successfully induces *cfos* expression, and the expression of both *cfos* and *HSV1-TK* are significantly correlated at the mRNA level.

3.3 *In Vivo* Experiments

3.3.1 *Ex Vivo SLC43A3* Expression Verification in Brain Tissues

SLC43A3 expression was analyzed in the MEFs but still needed to be specifically verified in the brain, as it is the main tissue where we want the transporter to be expressed to facilitate ^{18}F-FHBG crossing the BBB.

To evaluate the ubiquitous expression of *SLC43A3* in the brain of the transgenic animals, brains from the original lines 63 and 64 were collected and subjected to RNA and protein extraction. Among the transgenic lines, line 71 exhibited the lowest *SLC43A3* expression and did not transmit the gene to the next generation very well. Consequently, there were not enough animals available for the mRNA analysis experiment, and priority was given to the protein analysis and the main ^{18}F-FHBG/PET experiment.

For *SLC43A3* expression at the mRNA level, the qPCR technique was employed using SYBR Green with designed primers (qPCR slc Rev + qPCR slc Fw) targeting *SLC43A3* and TBP as the housekeeping gene (HKG). The resulting graph (Fig. 18) illustrates the expression levels of the *SLC43A3* transporter across the two mouse lines compared to wild-type (WT) mice. As anticipated, both transgenic lines showed higher expression levels than WT, confirming the successful overexpression of *SLC43A3*.

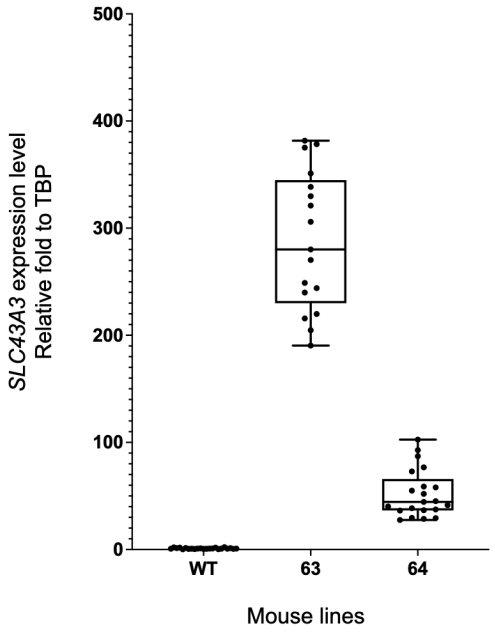

Figure 18: mRNA levels of *SLC43A3* in the brain of transgenic mouse lines 63 and 64 compared to wild-type (WT). The expression levels were quantified using qPCR and normalized to TBP as the housekeeping gene. Transgenic lines 63 and 64 exhibited significantly higher *SLC43A3* expression than WT, confirming successful overexpression.

The difference in *SLC43A3* expression in MEFs and brain tissues in line 64 and 63 can be due to tissue specific regulation, epigenetic differences and variation in transgene transmission

between animals. Since MEFs and brain tissues were from different animals within the same line, differences in copy number inheritance or cellular context could also be a factor. Further studies, such as copy number quantification in brain tissues and a detailed look at transcriptional activity would help to elucidate.

In addition to the qPCR analysis, a Western blot was conducted to compare the protein content of *SLC43A3* in the brains of both transgenic and WT mice. Furthermore, the liver of the wild-type mouse was used as the positive control.

This comparative analysis depicted the differential protein expression levels, demonstrating the abundance of *SLC43A3* in the transgenic mice (Fig. 19).

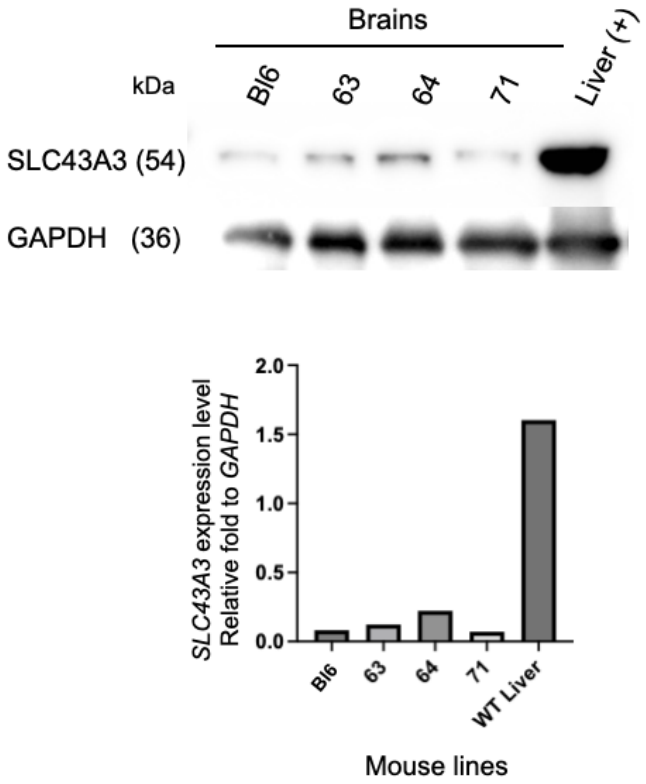

Figure 19: Western blot analysis *SLC43A3* in transgenic mouse lines compared to wild-type and mouse liver

Overall, these combined methods, qPCR for gene expression and Western blot for protein content of the brains, provided a comprehensive evaluation of *SLC43A3* overexpression at both mRNA and protein levels in our *cfos-BAC-HSV1TK:SLC43A3* mice.

3.3.2 *Ex Vivo* HSV1-TK Expression Verification through Brain Extraction

Within the same brain tissues used for the expression analysis of *SLC43A3*, another Western blot was conducted to evaluate *HSV1-TK* expression. Additionally, two mouse lines that were crossed with the Del-Cre line and have *HSV1-TK* in the open reading frame were included as positive controls. An anti-FLAG antibody was used to detect *HSV1-TK* in this experiment.

Figure 20 shows that the mouse lines crossed with Del-Cre exhibit the highest *HSV1-TK* expression, as expected, while the others remain at baseline expression levels.

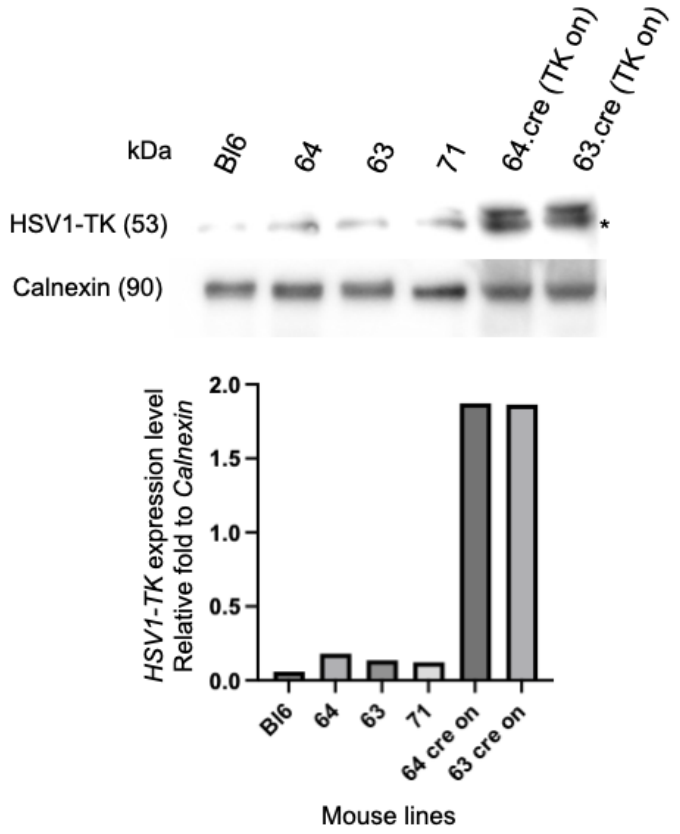

Figure 20: Western blot analysis of *HSV1-TK* expression in transgenic mouse lines compared to wild-type. The mouse lines crossed with Del-Cre show higher expression levels, while other lines exhibit baseline expression.

3.3.3 First Round of ^{18}F-FHBG/PET in Founder *cfos*-BAC Mice

After confirming *SLC43A3* overexpression in both the brain and MEFs, as well as verifying *HSV1-TK* expression in the FLEx system, we set up an experiment to measure ^{18}F-FHBG accumulation in the brains of these mice compared to wild-type.

Pentylenetetrazole (PTZ), a substance commonly used to activate *cfos* expression [42], was administered to experimental groups, while saline was given to control mice.

As the result of the measurement is shown in blue on graph in Figure 21, there was almost no entry of the tracer into the brain. The red line represents ^{18}F-FHBG levels in the blood, showing that it is gradually washed out of the bloodstream and eliminated from the body over time.

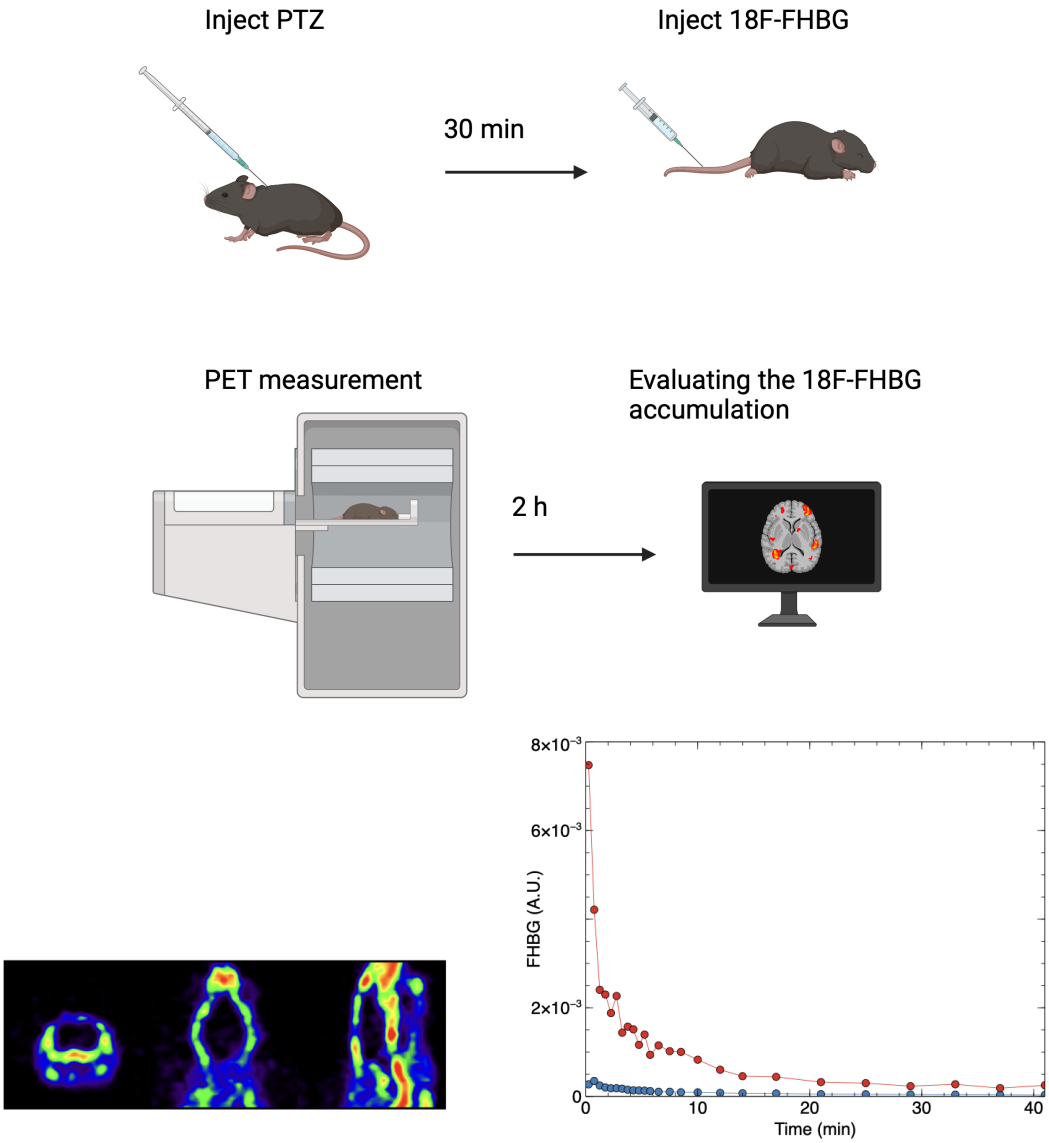

Figure 21: Schematic representation of the experimental setup for ^{18}F-FHBG/PET imaging. PTZ was injected into transgenic and wild-type mice to activate *cfos* expression, followed by the administration of ^{18}F-FHBG as a PET tracer (BioRender). Below shows the results of ^{18}F-FHBG/PET imaging in the founder lines. The blue line indicates ^{18}F-FHBG levels in the brain, while the red line represents levels in the bloodstream. The CT-PET image below the graph clearly shows the absence of ^{18}F-FHBG in the brain.

3.3.4 Immunostaining to Evaluate the Expression of *SLC43A3* in Brain Tissue

After the ^{18}F-FHBG/PET, the mice were perfused and fixed in 4% PFA for cryosectioning. It was important to determine where *SLC43A3* is actually being expressed, as its expression in blood vessels is crucial to facilitate ^{18}F-FHBG entry.

In this experiment, brain slices were subjected to staining with lectin to mark blood vessels, and the same *SLC43A3* antibody used in the Western blot was applied to detect *SLC43A3* expression. The slices were co-stained to visualize *SLC43A3* within the blood vessels. Human liver slices were used as the positive controls, as shown in the paper of Furukawa et al. [10].

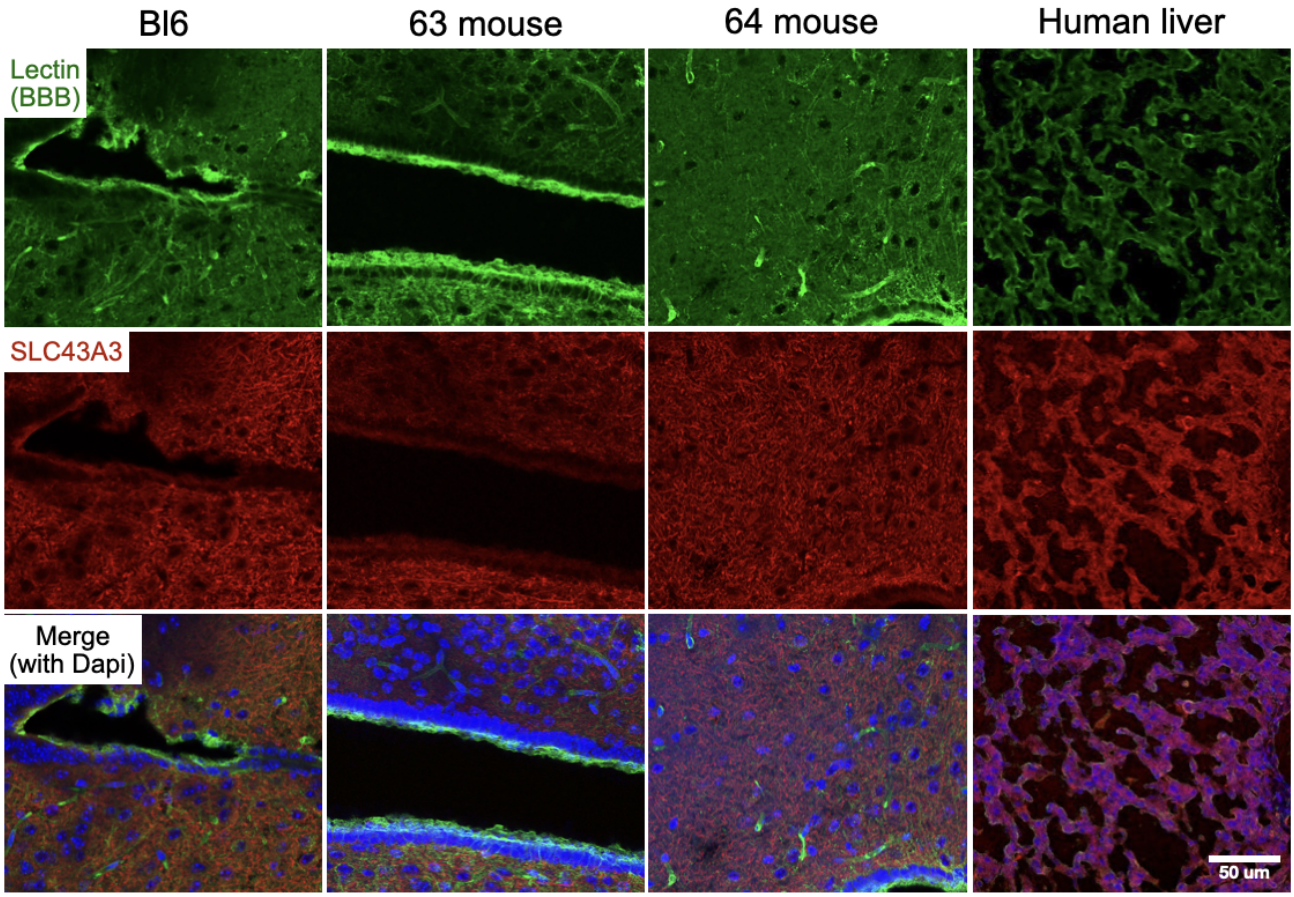

Figure 22: Confocal microscopy images illustrating the immunostaining of *SLC43A3* in brain sections from WT and transgenic mice next to the slices from human liver tissue as positive control. The brains were fixed in PFA and stained with antibodies against (A) *SLC43A3* (red). Lectin (green) was used as a blood vessel marker, and the sections were mounted with Antifade Mounting Medium containing DAPI.

As shown in Figure 22, the confocal images indicate no overlap between the *SLC43A3* protein and the blood vessels. However, *SLC43A3* protein appears to be highly expressed throughout the brain tissue.

This lack of overlap may explain why ^{18}F-FHBG does not enter the brain, as the *SLC43A3* transporter is not expressed in the blood vessels.

Since *SLC43A3* expression appears throughout the brain except in the blood vessels, further

investigation was necessary to validate the antibody and determine where *SLC43A3* is specifically expressed. Therefore, additional *SLC43A3* co-staining was performed with GFAP to label astrocytes and NeuN for neurons. The results of this confocal analysis are shown in Figure 23.

As demonstrated, there is slight overlap of *SLC43A3* with both neurons and astrocytes; however, greater expression of *SLC43A3*/transporter, including in the blood vessels, might be necessary to facilitate ^{18}F-FHBG entry into the brain.

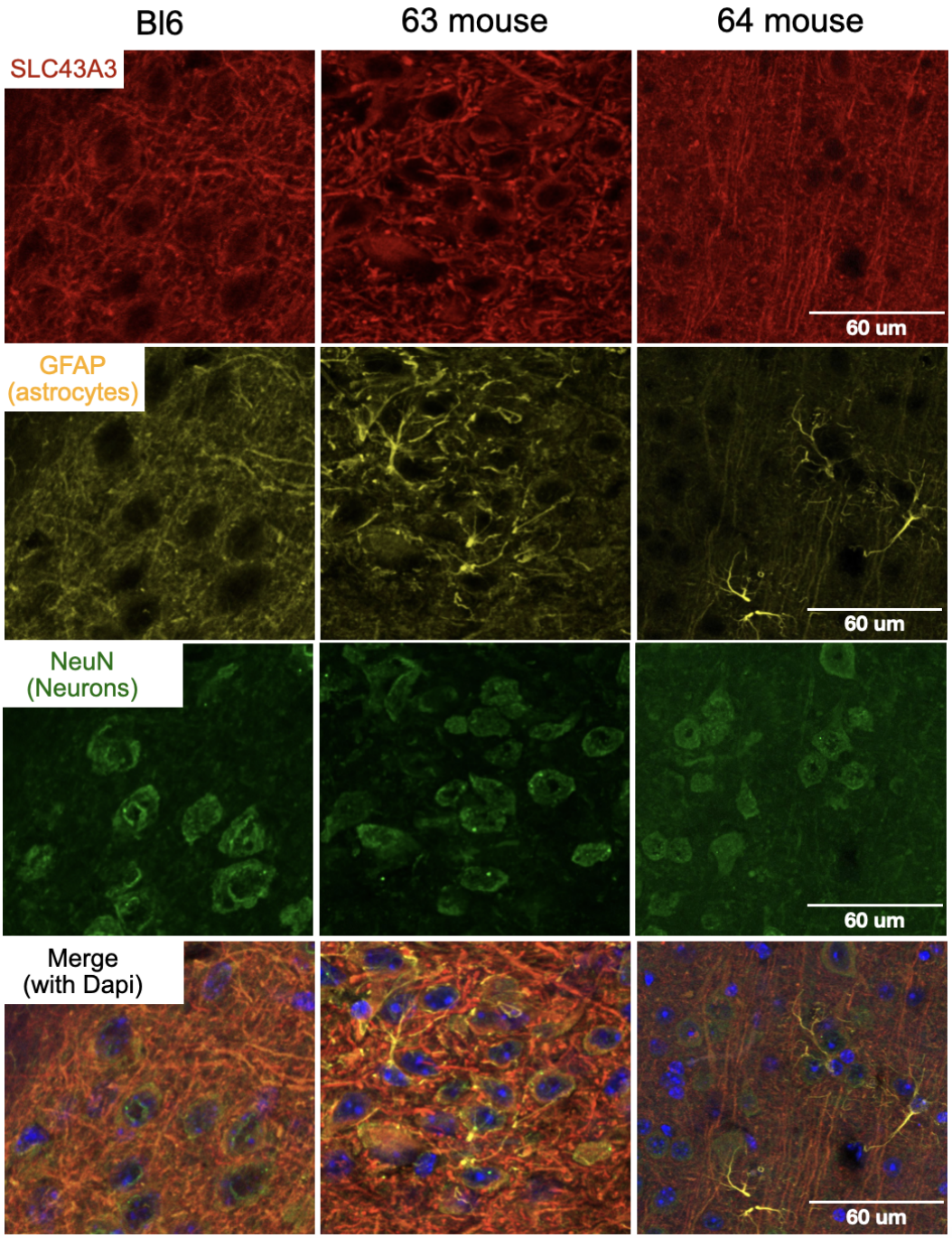

Figure 23: Confocal microscopy images illustrating the immunostaining of *SLC43A3* in brain sections from WT and transgenic mice. The brains were fixed in PFA and stained with antibodies against (A) *SLC43A3* (red), with lectin (green) used as a blood vessel marker, and (B) NeuN (green) as a neuronal marker and GFAP (yellow) as an astrocyte marker. Moderate colocalization with NeuN and GFAP demonstrates that *SLC43A3* is predominantly expressed in neurons and astrocytes

3.3.5 RNAscope to Evaluate the Expression of *SLC43A3* in Brain Tissue

After immunostaining did not produce clear or specific signals for *SLC43A3* protein, *in situ* RNA hybridization was used to verify *SLC43A3* expression at the mRNA level. This method was chosen because it is highly sensitive and specific which is capable of detecting single RNA molecules with subcellular resolution. Human liver slices from normal adult frozen tissue (BioChain Institute, Inc., Newark, CA) were used as the positive control.

For this, a custom *SLC43A3* probe was designed by the Probe Design Team at Advanced Cell Diagnostics, targeting the exact sequence used in the gene construct, which corresponds to human *SLC43A3*. RNAscope was then performed to co-stain *SLC43A3* with lectin antibody and NeuroTrace as a neuronal marker, as shown in Figure 24.

As shown in Figure 24, *SLC43A3* is most strongly expressed in the human liver, followed by the transgenic mice, with almost no expression in wild-type animals.

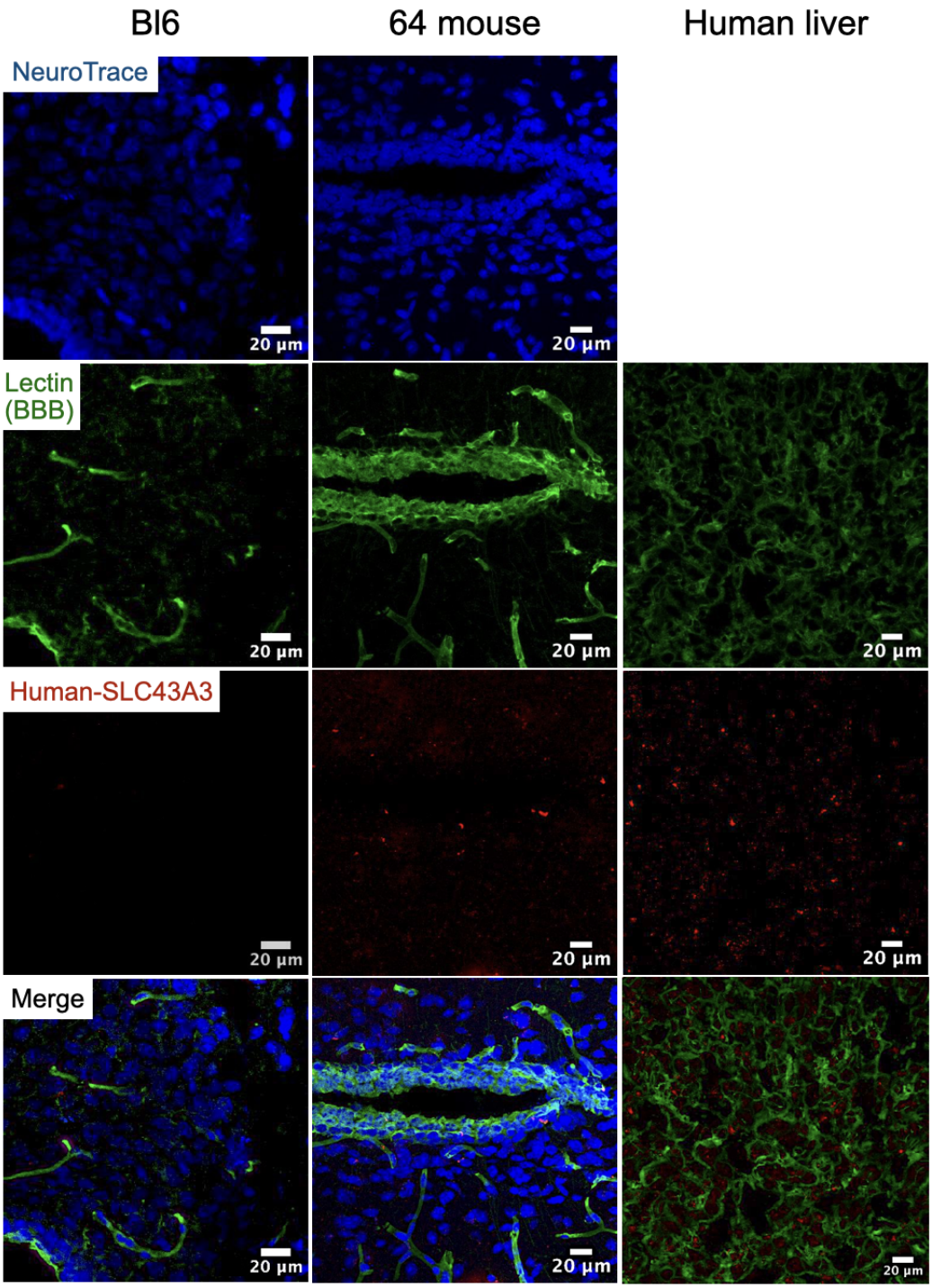

Figure 24: Confocal microscopy images illustrating *SLC43A3* mRNA expression detected via RNAscope in brain sections from wild-type (Bl6) mice, transgenic line 64 mice, and human liver tissue (positive control). NeuroTrace (blue) marks neurons, lectin (green) marks blood vessels, and Human-*SLC43A3* (red) represents the *SLC43A3* mRNA signal. The merged images indicate co-localization. Human liver tissue exhibits the strongest *SLC43A3* expression, while transgenic line 64 shows moderate expression and wild-type tissue shows almost no expression.

3.4 Changing the *SLC43A3* Promoter to CAG and use AAV for the Overexpression of *SLC43A3* in the Brain Endothelial Cells

3.4.1 Improving *SLC43A3* Expression via CAG Promoter Integration

To address the lack of sufficient *SLC43A3* expression in the blood vessels, we decided to replace the PGK promoter, a moderate promoter, with the stronger CAG promoter. To implement this, the *SLC43A3-2A-EYFP* gene was ordered from GENEART and received in a KAN-resistant plasmid. After cutting the backbone with BglII, EcoRI, and BamHI, the digestion was loaded onto a 1% agarose gel, and the 2.3 kbp band was excised and purified using a gel extraction kit. Meanwhile, the same process was performed on the CAG-EYFP plasmid using EcoRI and BamHI to isolate the 4.7 kbp band, which was also purified.

The ligation was set up at a 3:1 insert-to-vector ratio, followed by heat-shock transformation into *STBL3* cells, which were then grown overnight at 37°C on AMP-resistant agar plates. Single colonies were picked and subjected to SmaI/XmaI digestion to check for the presence of ITR sites necessary for AAV packaging, as well as NcoI digestion to confirm the presence of the insertion (Fig. 25).

By using the CAG promoter, it was anticipated to achieve a stronger expression of *SLC43A3*, which should facilitate improved tracer uptake and better experimental outcomes.

The prepared *CAG-SLC43A3-2A-EYFP* plasmid was then ready and set for packaging into different AAVs for direct administration into mice.

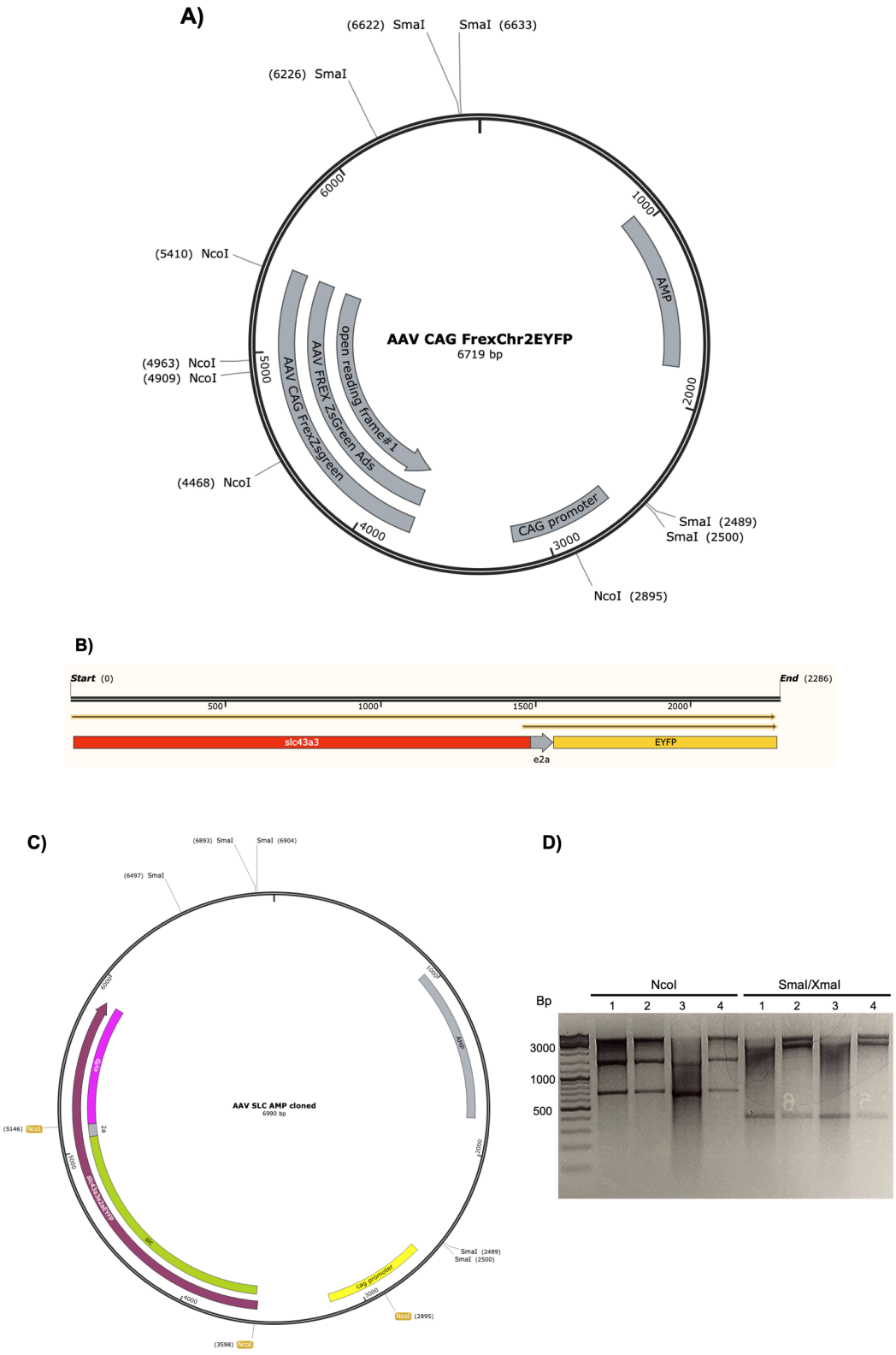

Figure 25: *SLC43A3-2A-EYFP* cloning into the CAG AAV Plasmid: A) Shows the CAG AAV plasmid, which includes Inverted Terminal Repeats (ITRs) essential for AAV packaging and replication. B) Depicts the linearized *SLC43A3-2A-EYFP* gene construct. C) Presents the plasmid map after the successful cloning and integration of *SLC43A3-2A-EYFP* into the CAG plasmid. Integration was confirmed using the NcoI enzyme, and the presence of ITRs was verified with the SmaI enzyme, as indicated on the map. D) Agarose gel electrophoresis results show the digestion of the *SLC43A3-2A-EYFP* construct cloned into the CAG plasmid. The left panel (NcoI lanes) confirms successful integration of *SLC43A3-2A-EYFP*, with expected fragment sizes visible. The right panel (SmaI/XmaI lanes) verifies the presence of ITR sites (396 bp), crucial for AAV functionality. Lane numbers correspond to individual clones tested, with molecular size markers shown on the far left.

3.4.2 Packaging *CAG-SLC43A3-EYFP* into AAV-BI30 for Ubiquitous Expression of SLC43A3 in Endothelial Cells

The first AAV chosen was AAV-BI30, a mutant version of AAV9 designed to target endothelial cells within the CNS. This vector has a unique ability to transduce brain microvascular endothelial cells with high specificity and was packaged by Vector BioLabs.

Initially, the method followed Krolak et al.[27], in which AAV-BI30 was administered via the lateral tail vein of the mouse, allowing the virus to enter the bloodstream and subsequently transduce endothelial cells across the CNS. Three weeks post-injection, a ^{18}F-FHBG/PET scan was conducted; however, no ^{18}F-FHBG uptake was observed in the brain as is shown in the graph in Figure 26.

Subsequently, mice were perfused and subjected to immunostaining for anti-GFP and lectin. The results showed only minimal expression of *SLC43A3-EYFP*, with complete overlap with lectin. This suggests that expression in the brain was insufficient to facilitate -^{18}F-FHBG entry (Figure 26).

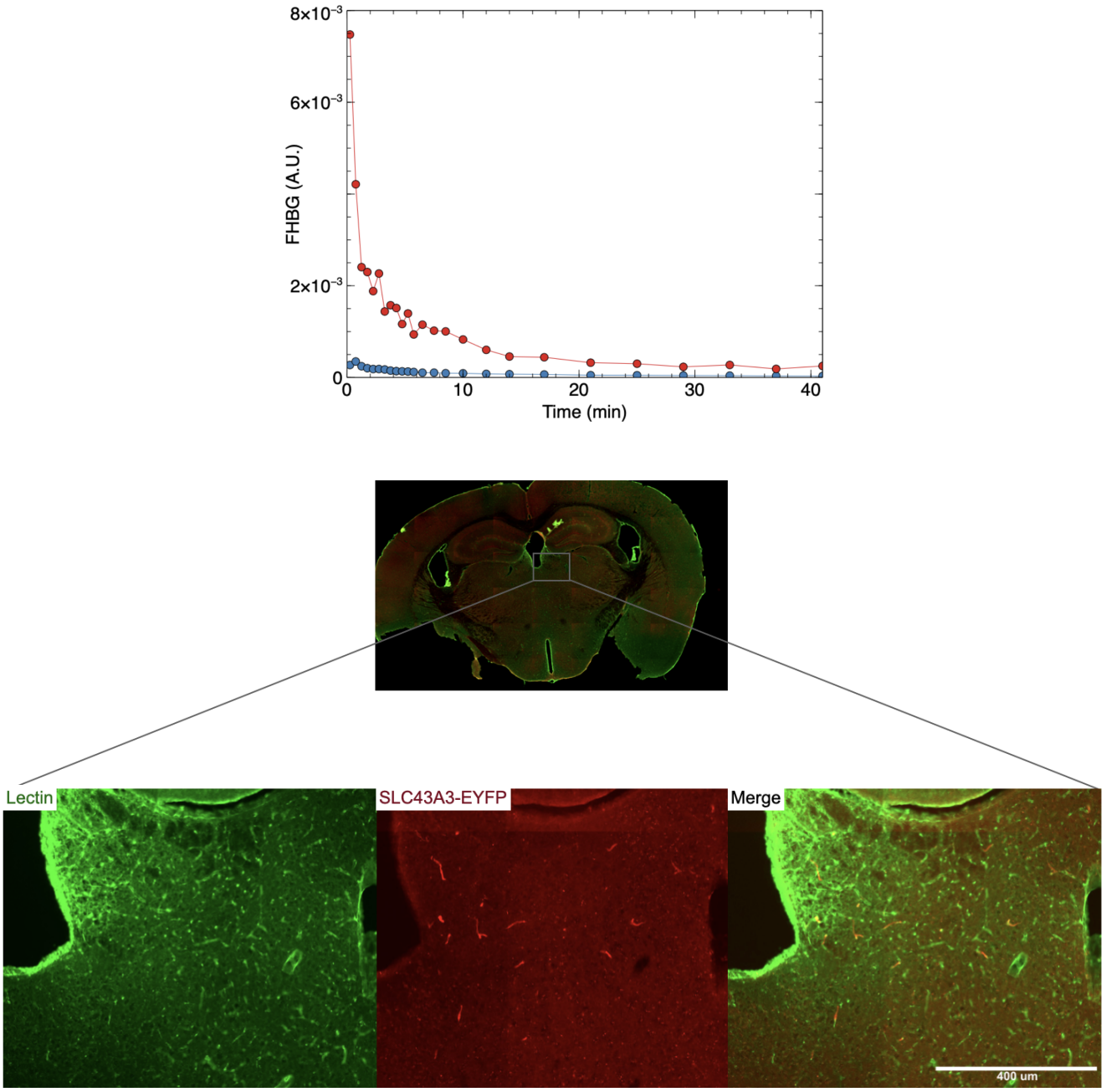

Figure 26: AAV-BI30 tail vein injection results. Top panel is ^{18}F-FHBG/PET graph. Blue line indicated the brain uptake and red line is bloodstream. Bottom confocal images is immunostaining of fixed brain tissue after perfusion. There is some overlap between *SLC43A3* and lectin (green) staining but *SLC43A3* expression is very low and not enough to allow tracer entry into the brain

The next approach involved the direct injection of AAV-BI30 into the brain, as described in the Methods section 2.3.3, to achieve full *SLC43A3* expression within the brain using the same AAV batch. Three weeks post-injection, a ^{18}F-FHBG/PET measurement was performed, but it was still unsuccessful regarding the entry of ^{18}F-FHBG into the brain (Figure 27). Following the ^{18}F-FHBG/PET measurement, perfusion, immunostaining and RNAscope were conducted.

As shown in Figure 27, there is high *SLC43A3* expression around the injection site in the brain, though with limited overlap with lectin.

AAV-BI30 wasn't recommended for direct brain injection to transduce endothelial cells. This limitation arises because AAV-BI30 via tail injection transduces endothelial cells with low efficiency. Therefore, since our aim was to achieve widespread transduction across all cell types in the brain, including endothelial cells, we decided to explore this method. While *SLC43A3* expression was observed around the injection site, the limited overlap with lectin indicates insufficient transduction of endothelial cells within the direct brain injection, consistent with the known characteristics of AAV-BI30.

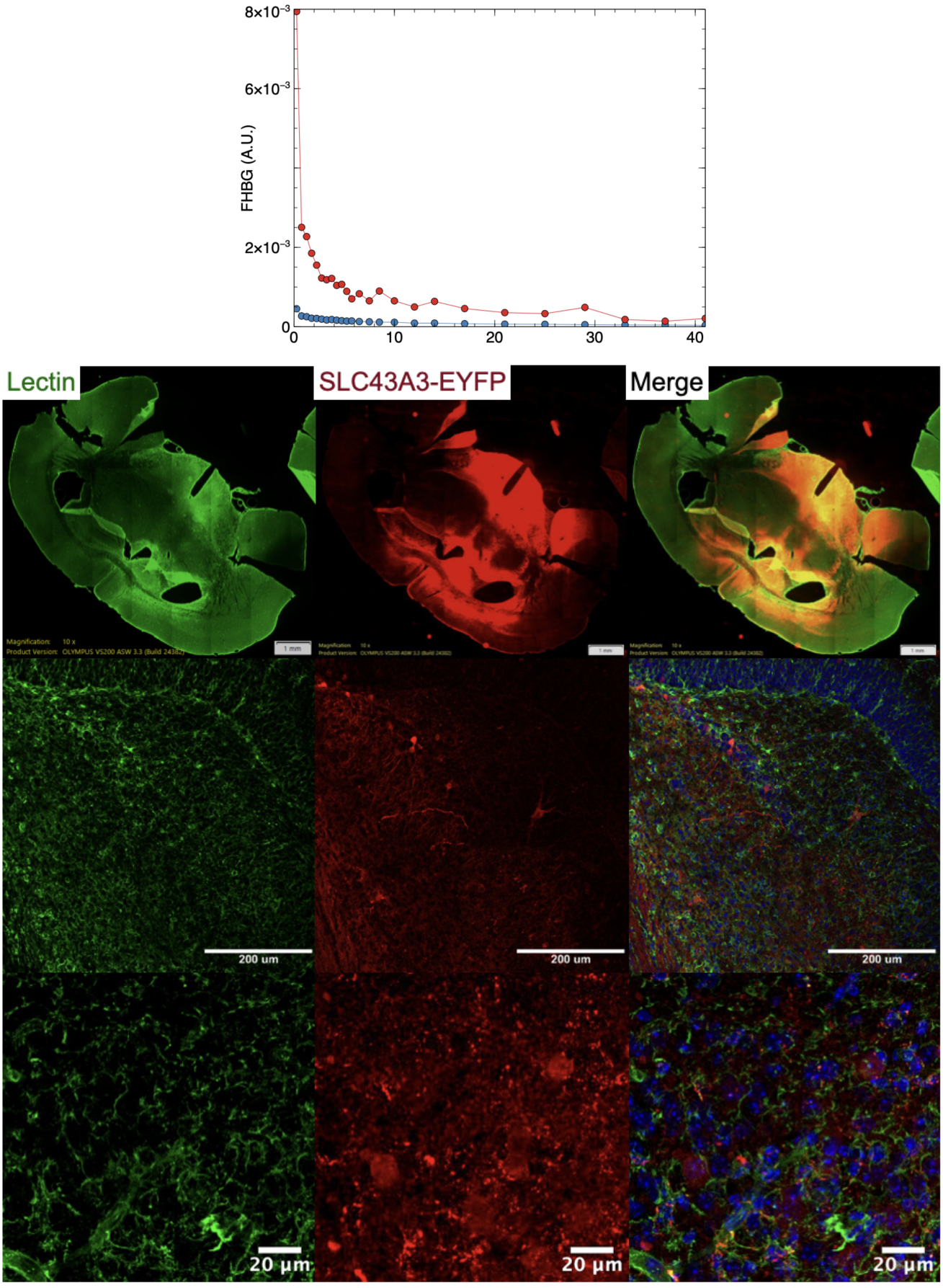

Figure 27: results of the AAV-BI30 brain-injection. Top panel is ^{18}F-FHBG/PET graph. Blue line indicated the brain uptake and red line is bloodstream. Bottom shows the confocal images showing immunostaining of *SLC43A3-EYFP* (red) co-stained with lectin (green) in AAV-BI30 brain-injected mice. The expression of *SLC43A3* is observed around the injection site, with limited overlap with lectin, indicating partial localization to blood vessels.

RNAscope was used as an additional validation tool to check *SLC43A3* expression and localization in brain tissue as is shown in Figure 28. This super sensitive and specific in situ hybridization technique allows to detect single RNA molecules so you can see the target mRNA at the subcellular level. To ensure signal specificity, a custom human *SLC43A3* probe and an EYFP probe were used as separate validation. NeuroTrace was used to stain the neurons.

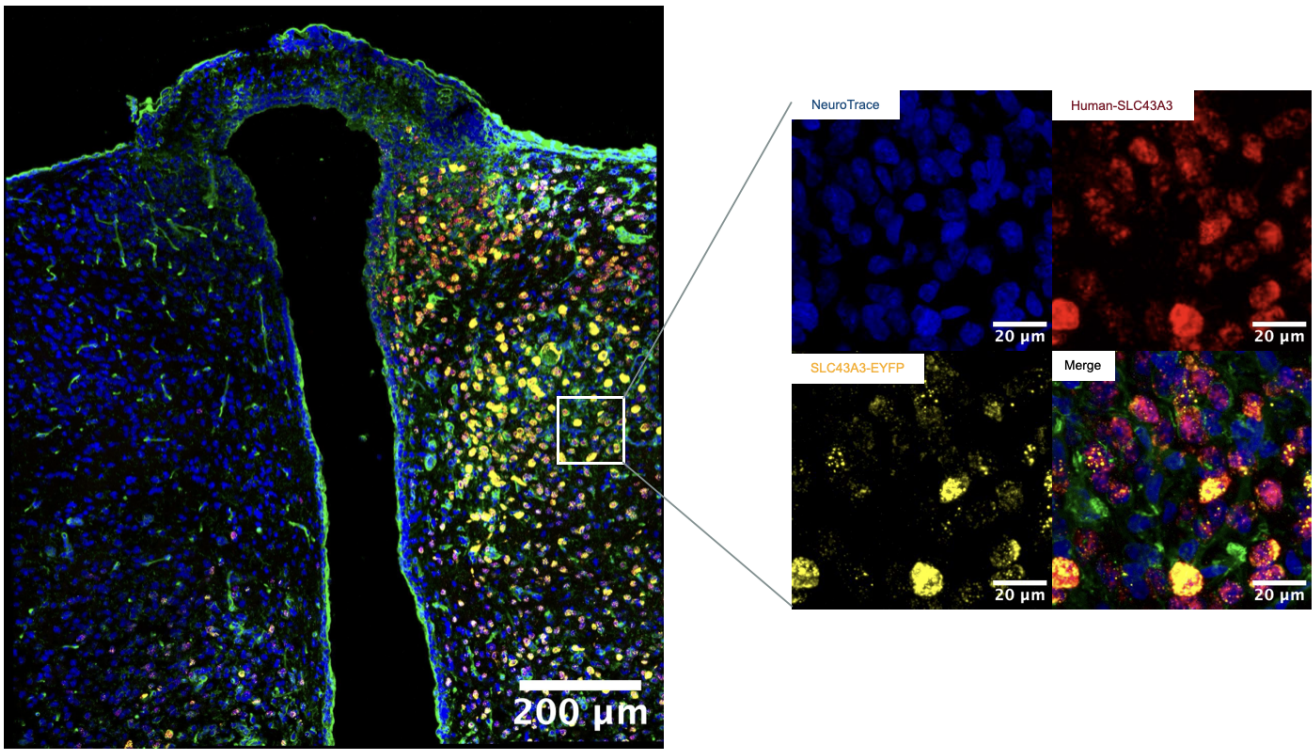

Figure 28: RNAscope of brain sections from AAV-BI30 brain injected mice. Human *SLC43A3* probe and EYFP probe were used to validate signal specificity. NeuroTrace (blue) was used to stain the neurons, *SLC43A3-EYFP* (yellow) and human *SLC43A3* (red) were co-stained with lectin (green) to check overlap with blood vessels. Results show minimal overlap of *SLC43A3* with lectin.

As shown in Figure 28, *SLC43A3-2A-EYFP* is clearly expressed at high levels following the injection of AAV-BI30 into the brain. To confirm the signal, an additional EYFP probe was used as a control, and both probes showed clear overlap. Lectin was used as a marker for blood vessels; however, no overlap was observed between *SLC43A3* expression and blood vessels.

3.4.3 Packaging into AAV-PHP.eB for full Overexpression of *CAG-SLC43A3-EYFP* Throughout the Whole Brain

After the failure of AAV-BI30 to transduce brain endothelial cells, we decided to pursue full overexpression of *CAG-SLC43A3-2A-EYFP* throughout the brain. AAV9 was one option; however, AAV-PHP.eB, discovered by Chan et al.[5], demonstrated a significantly increased ability to transduce the CNS, highlighting its superior performance in gene delivery compared to AAV9.

The *SLC43A3-2A-EYFP* construct was sent to Vector BioLabs company, for packaging. The virus was administered directly into the brain, as detailed in Method 2.3.3, to achieve widespread expression across the brain. The animals were monitored, and three weeks post-injection, they were subjected to a ^{18}F-FHBG/PET measurement to assess tracer uptake. However, ^{18}F-FHBG uptake was still unsuccessful, indicating that the tracer did not effectively penetrate the brain (Figure 29).

Further immunostaining was performed to evaluate *SLC43A3* expression levels within the brain. Figure 29 shows the results, with high *SLC43A3* expression across various brain regions, particularly around the injection site, but with minimal overlap with lectin staining which can be a potential reason for the *SLC43A3* to not to transport the ^{18}F-FHBG efficiently.

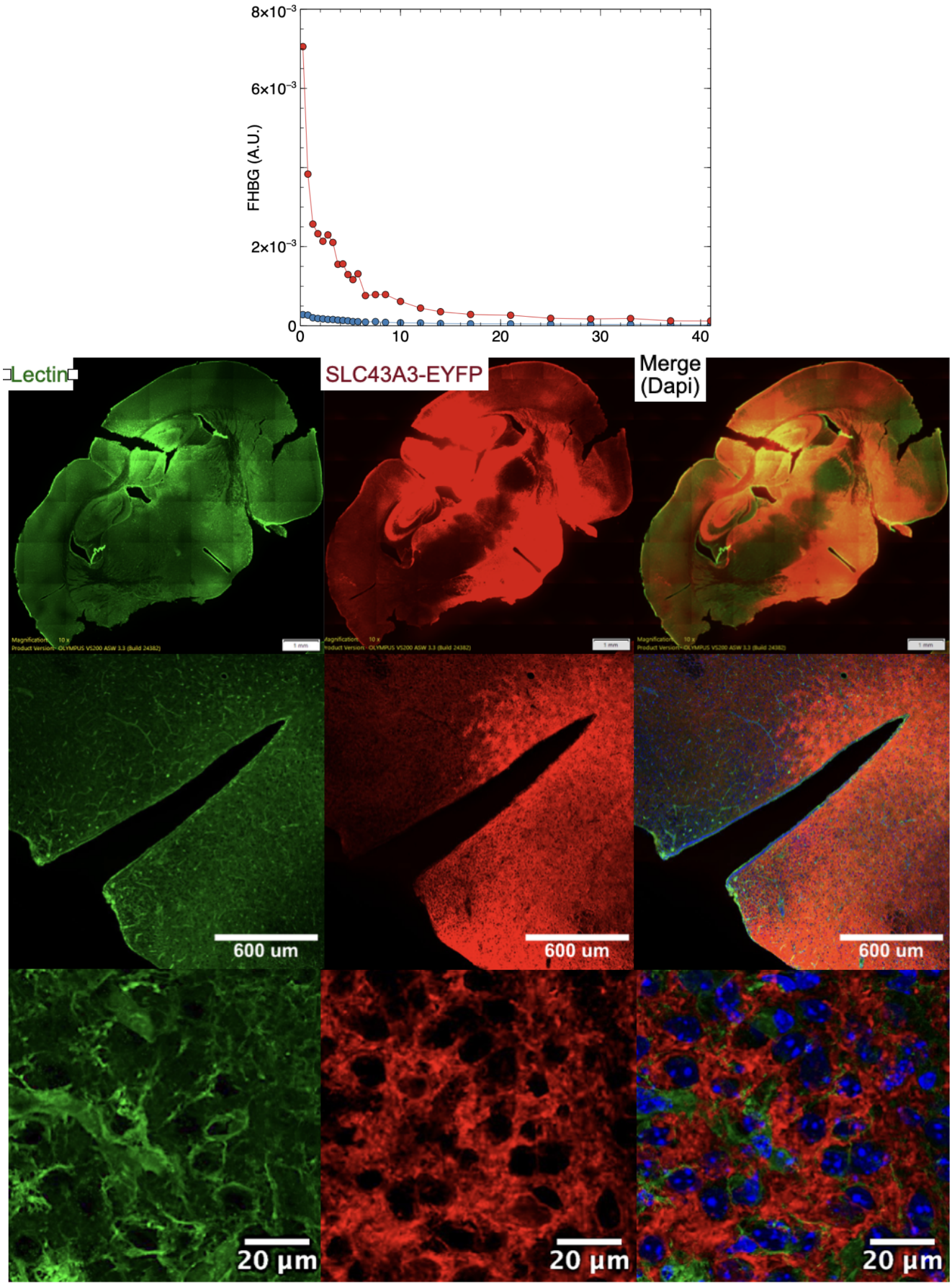

Figure 29: results of the AAV-PHP.eB brain-injection. Top panel is ^{18}F-FHBG/PET graph. Blue line indicated the brain uptake and red line is bloodstream. Bottom shows the immunohistochemistry (IHC) analysis. An anti-EYFP antibody was used to detect *SLC43A3* expression (red), co-stained with lectin (green) to visualize blood vessels. While widespread *SLC43A3* expression is observed throughout the brain, minimal overlap with blood vessels is evident, indicating limited targeting of endothelial cells despite significant transduction in the brain.

RNAscope was also conducted as an additional verification method, using EYFP and a specially designed *SLC43A3* probe co-stained with lectin. As shown in Figure 30, there is only minimal overlap between *SLC43A3* and lectin.

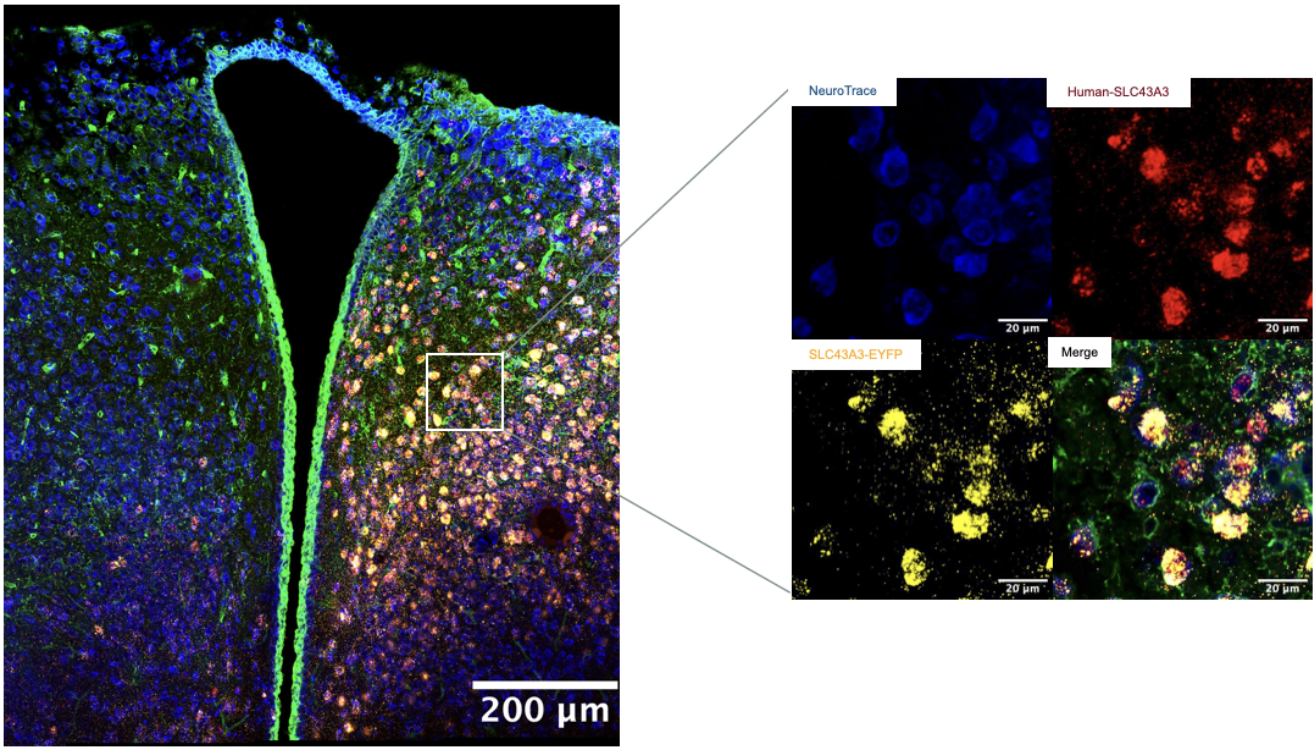

Figure 30: RNAscope of brain sections from AAV-PHP.eB brain injected mice. Human *SLC43A3* probe and EYFP probe were used to validate signal specificity. NeuroTrace (blue) was used to stain the neurons, *SLC43A3-EYFP* (yellow) and human *SLC43A3* (red) were co-stained with lectin (green) to check overlap with blood vessels. Results show minimal overlap of *SLC43A3* with lectin.

Despite strong expression of *SLC43A3-2A-EYFP* in the brain with AAV-PHP.eB, ^{18}F-FHBG failed to enter the brain. This suggests there are other factors here that are preventing tracer uptake. One potential reason is that the *SLC43A3* is not expressed strong enough in brain endothelial cells to be targeted by AAV injection or there are limitations of the transport mechanisms of *SLC43A3* for ^{18}F-FHBG.

In general, both AAV-BI30 and AAV-PHP.eB had difficulty transducing endothelial cells throughout the brain *in vivo*. AAV-BI30, when injected via tail vein, had specific expression in endothelial cells but at very low levels, potentially not enough for *SLC43A3* to allow ^{18}F-FHBG to enter the brain. AAV-PHP.eB had widespread overexpression of *SLC43A3* in the brain but minimal expression in endothelial cells as indicated by lack of overlap with lectin staining.

To conclude, AAV can give strong expression but targeting endothelial cells in sufficient numbers to allow functional transport of ^{18}F-FHBG into the brain is still a big challenge for our purpose. We need alternative approaches or gene delivery system refinements to transduce brain endothelial cells specifically and enough for tracer uptake.

3.5 Reproducing Experimental Conditions for *SLC43A3* and *HSV1-TK* in Ganciclovir ([^{8}H]GCV) Uptake

Since we were unable to achieve optimal conditions for overexpressing *SLC43A3* in the blood vessels of mice without damaging the tissues, we decided to test the hypothesis *in vitro*. Meanwhile, we aimed to replicate the published data by Furukawa et al. (2016) [11] using the plasmid kindly provided by Dr. Tomoya Yasujima, one of the authors of the Furukawa et al.[11].

The protocol was adapted from Furukawa et al. (2016) [11]. For stable plasmid expression, HEK293 cells were transfected with *SLC43A3-GFP-neo*, *HSV1-tk-neo*, and/or *mCherry*-reporter plasmids using LipofectAMINE 2000. These cells were cultured in DMEM supplemented with 10% FBS and Geneticin for 2-3 weeks to select antibiotic-resistant clones stably expressing the specified plasmids.

For transient transfection, HEK293 cells were seeded and transfected with *SLC43A3-GFP-neo*, *HSV1-TK-neo*, and/or *mCherry*-reporter plasmids using LipofectAMINE 2000. Co-expression experiments were conducted by transfecting cells with a 1:1 ratio of *SLC43A3-GFP-neo* to *HSV1-TK-neo* plasmids. The cells were then cultured for 48 hours to allow for transient expression.

As shown in Figure 31 A), GFP (*SLC43A3* tagged) and mCherry (reporter plasmid for the transfection efficiency) fluorescence were visually inspected to confirm the presence of the transporter in transfected cells.

At the same time, the cells were stained with phalloidin and co-stained with an *SLC43A3* antibody to determine if *SLC43A3* was expressed on the cell membrane, as expected. Image 31 B) displays microscopy images showing significant co-localization of *SLC43A3* with phalloidin. Phalloidin, a toxin that binds specifically to F-actin (filamentous actin), was used to stain the cytoskeleton, aiding in the visualization of cellular structure and membrane-associated proteins.

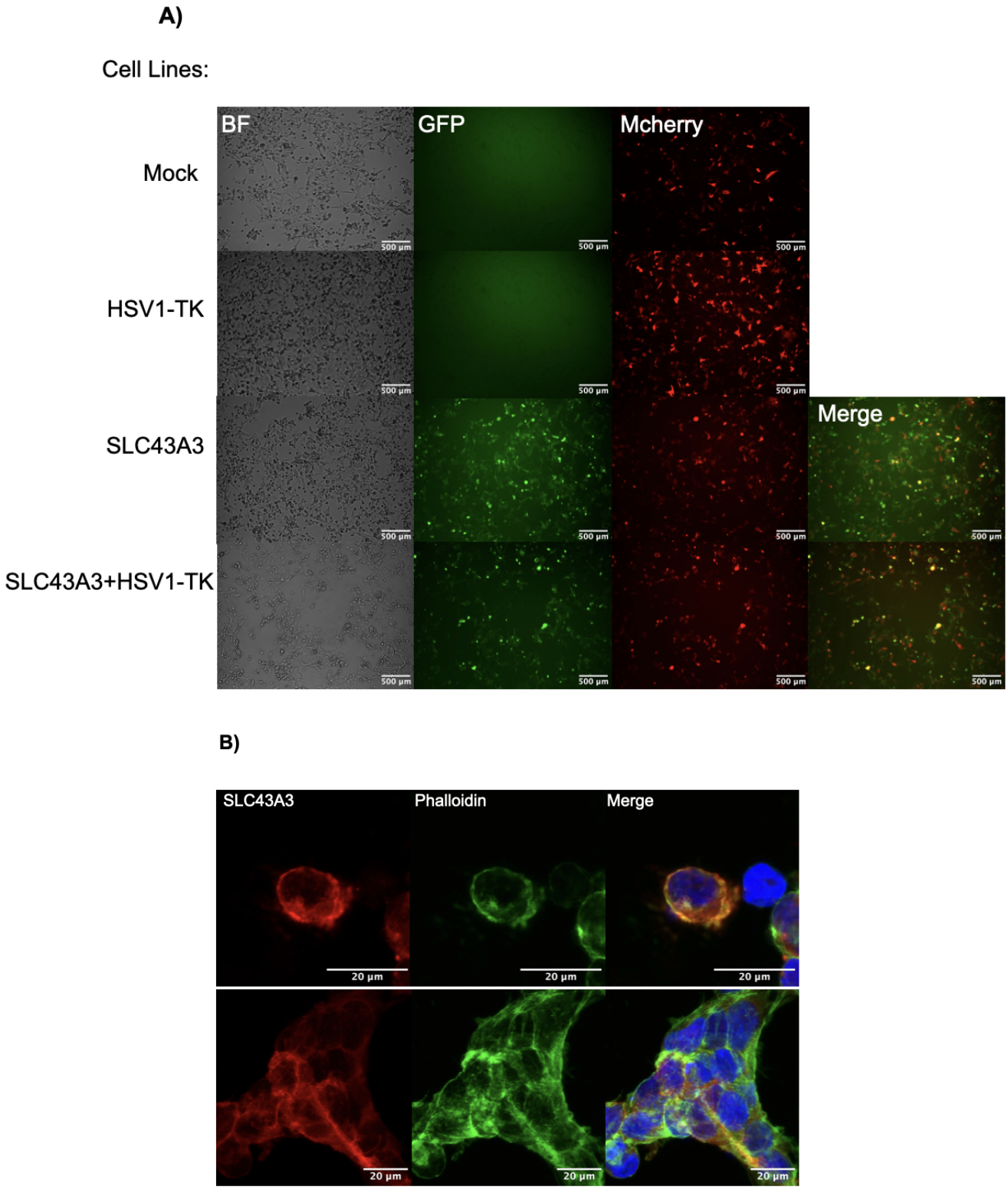

Figure 31: A) HEK293 cells stably expressing different plasmids were confirmed three weeks post-transfection and selection with G418 under a fluorescence microscope. mCherry was used as a control plasmid to assess transfection efficiency, and *SLC43A3* was GFP-tagged to visualize its expression. B) Staining of the cells for *SLC43A3* was performed using an antibody and co-stained with phalloidin to confirm the localization of *SLC43A3* on the cell membrane.

For the data replication experiment as per Furukawa et al. (2016) [11], cells were incubated with ^{18}F-FHBG and [^{3}H]GCV for 5 and 30 minutes. The reaction was stopped by adding ice-cold substrate-free uptake buffer, followed by two washes to remove any unbound substrate. Cells were then lysed for 1 hour at room temperature and radioactivity was measured using a scintillation counter. Figure 32 shows the results but they don't match our expectations of Furukawa et al. (2016) [11]. Specifically, there is no clear trend for [^{3}H]GCV or ^{18}F-FHBG accumulation. Due to low transfection efficiency in MDCKII cells, these cells were excluded from the results in this study.

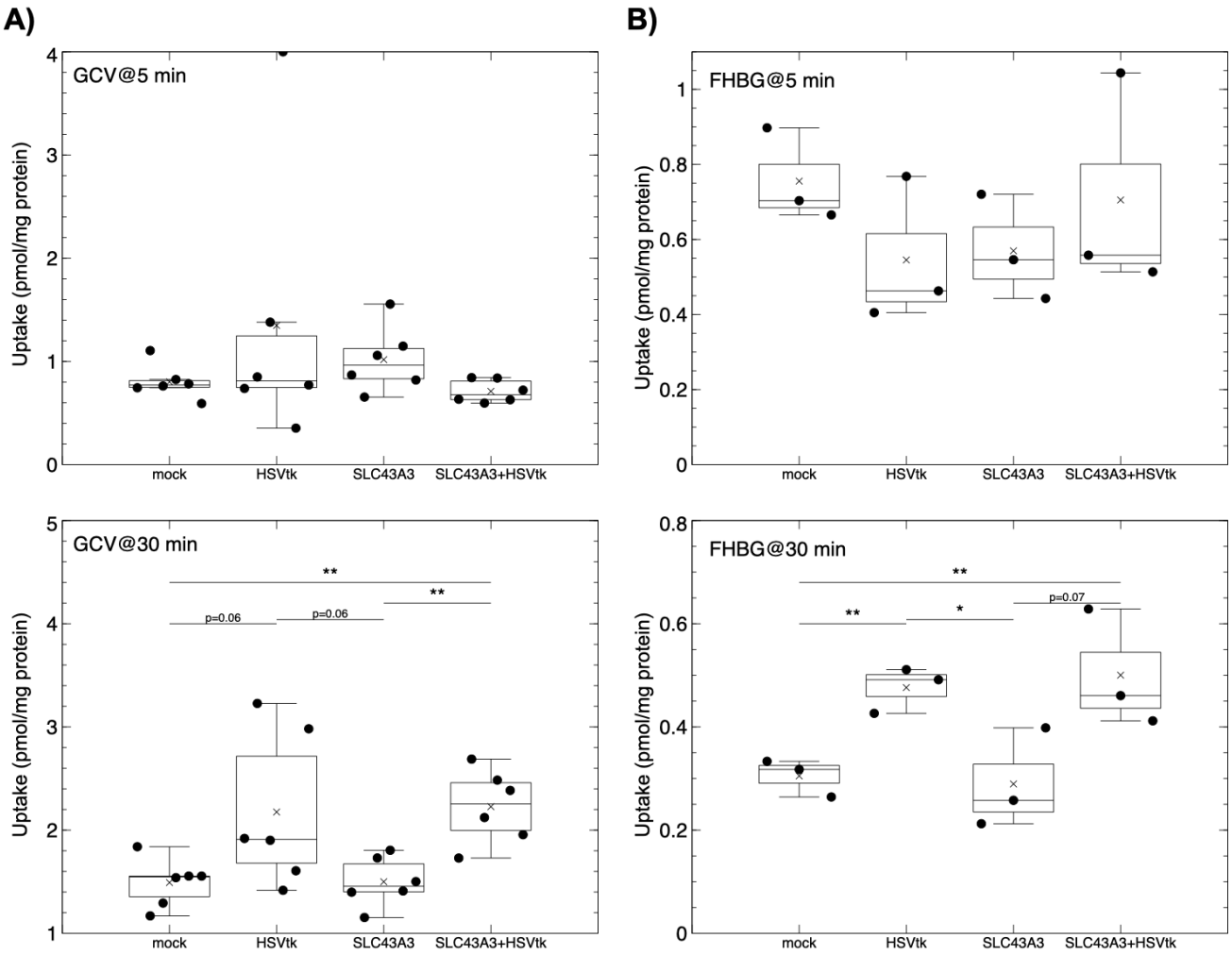

Figure 32: The graphs show: A) ^{18}F-FHBG and B) [^{3}H]GCV accumulation in transfected HEK293 cells compared to mock-transfected cells at 5 and 30 minutes.

The data from reproducing the results published by Furukawa et al., using the provided *SLC43A3-GFP* plasmid, did not show any clear trend after a 5-minute incubation with either ^{18}F-FHBG or [^{3}H]GCV. However, after 30 minutes, a slight accumulation of both ^{18}F-FHBG and [^{3}H]GCV was observed in cells expressing *HSV1-TK*, but not in those expressing *SLC43A3*. This accumulation can likely be attributed to the phosphorylation of both substances over time, leading to their intracellular trapping and gradual accumulation.

4 Discussion

Measuring neuronal activity is key to quantifying and identifying neuronal pathways or activations in response to stress, food smells, or external stimuli. In current scientific method, animals are sacrificed and molecular techniques are used to investigate gene expression or neuronal activity. *cfos* is a widely used marker for neuronal activity. As an immediate early gene *cfos* is expressed at basal levels but responds rapidly and strongly to many stimuli [21, 28]. Despite its popularity *cfos* has not been yet measured in the brain of the living animal, which is a major limitation for neuroscience research.

9-[4-[(^{18}F)fluoro-3 (hydroxymethyl)butyl]guanine (^{18}F-FHBG) is a Food and Drug Administration (FDA) approved PET tracer that allows for therapy monitoring by detecting viable *HSV1-TK* transfected cells at different stages [23, 44]. *HSV1-TK* (Herpes Simplex Virus Type 1 Thymidine Kinase) is a commonly used reporter gene, particularly in cancer gene therapy. Combined with ganciclovir (GCV) as its prodrug, *HSV1-TK* allows for the targeted killing of transfected cells. This system has been shown to work in organs like liver and lungs but cannot cross the BBB which limits its ability to quantify the *HSV1-TK* in the brain [8, 35].

The major limitation of this system in the central nervous system (CNS) is that ^{18}F-FHBG cannot cross the blood-brain barrier (BBB). The BBB is a highly selective barrier composed of tightly joined endothelial cells, supported by pericytes, astrocytes, and neurons. This complex structure is essential for maintaining neural homeostasis but blocks many drugs and imaging agents including ^{18}F-FHBG from entering the CNS [49].

Given this, Furukawa et al. (2016) found an equilibrative purine nucleobase transporter, *SLC43A3*, which is endogenously expressed in many tissues with the highest in liver and lungs and the lowest in brain [10]. Furukawa's *in vitro* studies showed that *SLC43A3* is necessary for GCV uptake into cells and facilitates the entry of GCV into the cells expressing *SLC43A3* [11]. Therefore the reason why ^{18}F-FHBG/*HSV1-TK* system works in liver and lungs but not in brain can be because of lack of *SLC43A3* expression in the brain. Both GCV and ^{18}F-FHBG are acycloguanosine analogs and substrates of *SLC43A3*. *HSV1-TK* phosphorylates these compounds and once phosphorylated they are trapped inside the cells and can be detected via PET scanner.

Based on the results of Furukawa et al., the goal of this project was to build upon Furukawa's study on tritium-labeled GCV uptake by making *SLC43A3* ubiquitously expressed in our transgenic mice model and expressing *HSV1TK* under *cfos* promoter. This would allow indirect measurement of *cfos* activation through ^{18}F-FHBG/PET imaging in the brain. By overcoming the current limitation, this approach provides a robust way to study neuronal activity *in vivo*. It will allow neuroscientists to measure *cfos* or other genes of interest in brain *in vivo* using ^{18}F-FHBG/PET. Placing the gene of interest and *HSV1TK* under the same promoter offers

remarkable specificity and flexibility in studying neuronal activation.

This will allow gene expression studies to be done in a non-invasive, more ethical, and cost-effective way in the brain and other organs. It will open up new opportunities in neuroscience and related fields to study complex neuronal pathways and gene regulation with precision and minimal disruption.

4.1 *HSV1-TK* as a Reporter Gene for *cfos* Expression

In this study, we explored the correlation between *cfos* and *HSV1-TK* expression in MEFs to investigate the potential of the studied *HSV1-TK* as an indirect reporter for *cfos* activity. *cfos*, an early immediate gene rapidly induced by external stimuli such as PMA *in vitro*, plays a critical role in cellular signaling pathways [15, 7]. Since *cfos* is transient and stimulus-responsive, it is widely used as a marker for neuronal activation. By designing *HSV1-TK* expression to be controlled by the *cfos* promoter, we aimed to establish *HSV1-TK* as a reliable indicator of *cfos* activity.

We tested this by stimulating MEFs with 20 nM PMA and quantifying the mRNA levels of *cfos* and *HSV1-TK* over time. MEFs were treated with HTNCre to activate *HSV1-TK* expression by removing the LoxP cassettes in the FLEx system, while untreated MEFs were controls. The original MEFs were derived from transgenic mice and had *HSV1-TK* silenced due to the FLEx system and required Cre recombination to put the *HSV1-TK* gene in the open reading frame for transcription.

RNA analysis showed *cfos* mRNA levels increased within 30 minutes of PMA stimulation and then decreased as the stimulus was removed as expected for an early response gene. *HSV1-TK* mRNA levels were upregulated in HTNCre treated cells confirming *HSV1-TK* is dependent on Cre recombination. The lack of *HSV1-TK* expression in untreated cells validated the specificity of the FLEx system. These results show *HSV1-TK* is tightly linked to *cfos* promoter and can be used as a reporter for *cfos* activity at the mRNA level (Figure 16).

The temporal patterns of *cfos* and *HSV1-TK* expression show a strong link, as both genes increase after stimulation and decrease over time. This connection indicates that *HSV1-TK* is a reliable indicator of *cfos* activity and offers a measurable way to track its expression. Being able to track *cfos* activity through *HSV1-TK* has important implications for studying neuronal activity in various physiological and pathological conditions as it allows indirect and potentially non-invasive monitoring of *cfos* dependent processes.

Also the FLEx system ensures *HSV1-TK* activation is tightly controlled and restricted to Cre expressing cells reducing background noise and increasing the accuracy of the reporter. However note that while the correlation between *cfos* and *HSV1-TK* was significant in this study, differences in mRNA and protein stability may introduce variability when applied in other con-

texts. Future studies should test this correlation at the protein level and in more complex *in vivo* systems.

In summary, *HSV1-TK* is a good reporter gene for *cfos* expression at the mRNA level and a useful tool for studying stimulus induced gene expression and its role in signaling pathways. The validation of this system in MEFs provides a base for its use in neuronal cells and other cell types and potentially new insights into *cfos* dependent processes. Further optimization of the system including testing in more physiological relevant models will make it useful for basic research and clinical applications.

4.2 Insights into Ubiquitous Expression of *SLC43A3* in Transgenic Mice

According to Furukawa et al. (2016), *SLC43A3* is a potential transporter for purine nucleobases such as adenine and guanine. *In vitro* studies showed it can take up nucleoside analogs including GCV, an acycloguanosine analog [11]. We aimed to ubiquitously express *SLC43A3* in transgenic mice using the PGK promoter. *SLC43A3* overexpression in mouse embryonic fibroblasts (MEFs) from the founder line was confirmed by qPCR. However, PET imaging with ^{18}F-FHBG as a tracer did not show uptake in the brain of the founder line. Since MEFs are from body tissues, not brain tissues, the initial *in vitro* verification of *SLC43A3* expression was limited to somatic tissues. After PET scans, the mice were perfused and immunostaining was performed using an anti-*SLC43A3* antibody. This staining showed similar expression levels in both wild-type and transgenic mice with no significant difference. The gene construct sequence was derived from the human *SLC43A3* gene, which shares 82.70% DNA identity with the mouse *SLC43A3*. Additionally, the antibody used in this study is 100% compatible with both the mouse and human *SLC43A3* proteins. Similarly, the qPCR probe designed for human *SLC43A3* was compatible with both mouse and human sequences, despite mismatches, due to their high degree of similarity. It is known that primers can anneal to a template and amplify sequences even with mismatches, although amplification efficiency is reduced. Studies have shown that mismatches at internal regions are more tolerable while mismatches at the 3' end of the primer can significantly affect PCR efficiency [38, 43]. Mismatches between the qPCR probe and the template were likely accommodated by the polymerase and therefore we were able to amplify mouse *SLC43A3* along with human sequence [39]. As a result, as we got qPCR values for *SLC43A3* in both wild-type and transgenic mice during qPCR which means that the probe and primers amplified both mouse and human *SLC43A3*.

The anti-*SLC43A3* antibody used for brain staining is against a sequence that is conserved in both human and mouse *SLC43A3* so it can detect both in wild-type and transgenic mice. To confirm the specificity of the antibody, we extracted protein from the liver of wild-type mice, a tissue that expresses *SLC43A3* more than the brain to be used as a control. We also stained

human liver tissue for comparison, as Furukawa et al. (2016) did in their study. Initial brain staining showed that *SLC43A3* was not expressed in blood vessels but moderately expressed in neurons and astrocytes. The absence of expression in endothelial cells was further confirmed by the lack of overlap between *SLC43A3* staining and lectin, a vascular marker. The gene construct was designed for ubiquitous expression of *SLC43A3* under PGK promoter. However, the moderate activity of PGK promoter may have contributed to the lack of *SLC43A3* expression in endothelial cells. This highlights the limitation of PGK promoter in achieving high transgene expression in brain endothelial cells especially those of the BBB.

4.3 Promoters and Overexpression of *SLC43A3* in the Brain

Promoters are the key in genetic engineering as they control the expression of the gene of interest in the target cells as well as the level of expression. Choosing the right promoter is very important for consistent and cell-specific expression. They can be ubiquitous or tissue-specific, each used for different biological purposes [4]. In our case for the brain expression, it was essential to consider the target area and determine whether the gene should be expressed specifically in endothelial cells, neurons, other cell types, or universally across all cells. Additionally, it was crucial to ensure that the gene expression did not significantly alter the mice's phenotype or cause significant unintended effects.

The CAG promoter, a hybrid of cytomegalovirus (CMV) early enhancer and chicken β-actin promoter, was designed to drive strong and ubiquitous expression in both neuronal and non-neuronal cells [26]. It is known for its high expression levels across different tissues and is one of the strongest and most widely used promoters in neuroscience. PGK promoter, from the phosphoglycerate kinase gene, gives moderate expression with a more stable and less aggressive profile. This is the main reason why it was used initially in our study to drive ubiquitous expression during the generation of the transgenic mouse line as it minimizes the risk of overexpression-related cellular stress [9]. However, after the failure of ^{18}F-FHBG to enter the brain, follow-up immunostaining showed that *SLC43A3* was present in neurons and astrocytes but not in endothelial cells, as there was no overlap with lectin staining. This indicates the limitation of the PGK promoter in targeting endothelial cells of the BBB. To increase *SLC43A3* expression we decided to use AAV-based delivery under the control of the CAG promoter to overexpress the *SLC43A3* in the brain endothelial cells. This aligns with our goal for consistent transgene expression across different brain cell types.

Vectors with CAG promoters have been shown to drive long-term expression of transgenes during mouse embryonic stem cell differentiation into mesodermal and endothelial cell types [3]. However, the AAV approach in our study with the CAG promoter did not give the maximal desired expression of *SLC43A3* in endothelial cells.

Future trials could use endothelial cell-specific promoters like Tyrosine kinase with immunoglobulin and EGF homology domains 2 (Tie2) to improve transgene expression in these cells. Tie2 promoter, linked to the Tyrosine Kinase Endothelial (*TEK*) gene, drives expression mainly in endothelial cells and has been well-studied for its specificity. It achieves this through Ets(E26 transformation-specific)-binding sites in its regulatory regions, which are crucial for endothelial-specific activity [25]. In addition, studies show Tie2 ensures high and consistent expression in endothelial cells during development with minimal off-target effects [22]. This makes it a better choice than the CAG promoter for targeting endothelial cells in the brain. Alternatively, pairing the CAG promoter with endothelial-specific enhancers, such as sequences from *CLDN5* or *MFSD2A*, could improve targeting efficiency without overloading the blood-brain barrier [50]

4.4 AAV Approaches for Overexpression of the Transporter in the Brain Endothelial Cells

Adeno-associated viruses (AAVs) from the Parvoviridae family are single stranded DNA viruses that are non-pathogenic in humans. They are widely used in research and therapeutic applications. These vectors can be engineered to deliver therapeutic agents to specific tissues for both research and treatment purposes[40, 17]. AAVs are used to control gene expression in specific neuronal populations so researchers can study neural circuits and behavior in animal models. This precise gene delivery has revolutionized neuroscience research and given us tools to study complex neural networks and their function. In addition, their unique properties make them great for understanding the brain and treating neurological conditions [31, 16].

In this study, we chose to use the AAV-BI30, an adeno-associated virus vector designed to transduce endothelial cells in the central nervous system (CNS). This vector is based on AAV9 but has much higher tropism so it can cross the blood-brain barrier (BBB) and deliver transgenes to brain endothelial cells [27]. The AAV-BI30 was optimized for endothelial cell targeting via tail vein injection. Krolak et al.(2022) demonstrated that the AAV-BI30 vector, driven by the CAG promoter, produces strong and consistent transgene expression in endothelial cells across the CNS. Their study confirmed the effectiveness of the CAG promoter for targeting endothelial cells using this AAV system.

After systemic tail delivery as recommended by the authors, we used AAV-BI30 to pack the *CAG-SLC43A3-2A-EYFP* plasmid for PET imaging with ^{18}F-FHBG, a tracer that is expected to be transported by *SLC43A3* and cross the BBB. However, the imaging results showed no ^{18}F-FHBG entry into the brain of the animals. Post perfusion and immunostaining showed partial overlap between *SLC43A3* expression and blood vessels. Despite this overlap, the overall *SLC43A3* expression was low, covering only about 10% of the brain. This suggests that systemic AAV-BI30 delivery under our experimental conditions was not sufficient to allow ^{18}F-FHBG up-

take in the brain [27].

To get *SLC43A3* expression across the brain and target more cell types broadly we decided to do direct brain injection of the AAV vector. While systemic delivery of AAV-BI30 is recommended for endothelial specific targeting, our goal was to get expression throughout the brain, beyond endothelial cells. Direct injections were done to maximize *SLC43A3* expression in the brain parenchyma. But PET imaging with ^{18}F-FHBG was unsuccessful as no tracer entry into the brain was observed. Immunostaining showed widespread *SLC43A3* expression along the injection tract but no overlap between *SLC43A3* and lectin, a blood vessel marker. This lack of overlap explains why ^{18}F-FHBG was not transported by *SLC43A3*. To confirm these results RNAscope was used to look at *SLC43A3* transcript localization with higher resolution. This showed no overlap between *SLC43A3* expression and blood vessels, as expected. A custom-designed probe for *SLC43A3* was used along with an EYFP probe as the AAV construct had an EYFP tag. The results showed that while *SLC43A3* was expressed in the brain parenchyma, it was not targeted to endothelial cells. These results show the challenges of getting both endothelial-specific expression and brain-wide expression with AAV-BI30 delivery. Systemic AAV-BI30 delivery gave partial endothelial targeting but the expression was not enough for ^{18}F-FHBG uptake. Direct brain injection resulted in widespread brain expression but failed to specifically target endothelial cells, leading to unsuccessful PET imaging. The authors of the study did not recommend direct brain injection for endothelial cell targeting. However, since our goal was the whole-brain expression, we chose this method. The AAV-BI30 vector clearly transfects endothelial cells according to the immunostaining results, although not with optimal efficiency. In the future, combining AAV-BI30 with direct brain injection might improve outcomes and achieve better results.

Next, to get *SLC43A3* expression across the whole brain we decided to pack our *CAG-SLC43A3-2A-EYFP* plasmid into AAV-PHP.eB, an engineered AAV9 variant that targets the CNS. AAV-PHP.eB has been shown to increase transduction efficiency in the brain and spinal cord compared to AAV9 [6, 5].

To achieve whole brain expression of *SLC43A3* AAV-PHP.eB was injected directly into the brain to maximize local delivery. After injection the mice were observed for three weeks, as performed by Chan et al.(2027)[5], next PET imaging with ^{18}F-FHBG was conducted to evaluate *SLC43A3* functionality in transporting ^{18}F-FHBG. However, the imaging results showed no detectable ^{18}F-FHBG entry into the brain, indicating that *SLC43A3* was not transporting the tracer. After perfusion and immunostaining, we observed robust *SLC43A3* expression along the injection tract which is still lack of overlapping with lectin. The expression was much higher and stronger than what we saw with AAV-BI30. This confirmed that *AAV-PHP.eB* delivered the *SLC43A3* transgene to the brain but *SLC43A3* was still not functional. To further confirm these results

RNAscope was used as an additional tool to look at *SLC43A3* transcript localization. As we did with AAV-BI30, RNAscope showed extensive *SLC43A3* expression in the brain parenchyma but no overlap with vascular markers, so minimal or no expression in endothelial cells. These results indicate that AAV-PHP.eB drives transgene expression throughout the brain but with low efficiency in endothelial cells. We conclude that the lack of *SLC43A3* expression in endothelial cells may explain why ^{18}F-FHBG was not transported. Achieving functional expression in specific brain cell populations while maintaining whole-brain coverage remains a significant challenge.

In this study, we were not able to get the whole brain including endothelial cells expression of our gene *SLC43A3*. While vectors like AAV-BI30 and AAV-PHP.eB were published as AAVs for efficient gene delivery there are several critical limitations. These include not targeting endothelial cells or very low levels of transfection in endothelial cells. Specifically, systemic delivery with AAV-BI30 resulted to specific but low endothelial targeting of *SLC43A3* while direct brain injection with AAV-PHP.eB resulted in strong expression in the brain parenchyma but minimal overlap with endothelial markers. So we were not able to test our hypothesis *in vivo* that *SLC43A3* will transport ^{18}F-FHBG into the brain. The key takeaway is the limited efficiency of targeting endothelial cells with both AAVs used in this study. Efficient transduction of endothelial cells which are part of the blood brain barrier (BBB) is important to achieve the desired outcome. Another observation is that despite strong *SLC43A3* expression in the brain parenchyma there was no ^{18}F-FHBG entry to the brain. This raises questions for future studies on the functionality of *SLC43A3*. As it is a membrane transporter, its expression in BBB endothelial cells is important for the transport of nucleobases or related substrates.

To address these limitations, develop AAV serotypes that are more efficient in transducing endothelial cells. For example, based on the results with AAV-BI30 and AAV-PHP.eB which are engineered mutants of AAV9, we can further explore how to make them more BBB permeable and efficient in transducing endothelial cells. This will give us more reliable tools to achieve whole brain transgene expression and endothelial cell targeting.

4.5 Reproducibility of Data and Experimental Conditions for *SLC43A3* and *HSV1-TK* in [^{3}H]GCV and ^{18}F-FHBG Uptake

Our hypothesis to improve the *HSV1-TK*/^{18}F-FHBG system by overexpressing the *SLC43A3* transporter in the brain as Furukawa et al.[11] suggested. However, we faced difficulties achieving consistent *SLC43A3* overexpression across the entire brain, including in endothelial cells, *in vivo*. To address this, we decided to reproduce the published data to validate their findings and investigate whether *SLC43A3* can effectively transport ^{18}F-FHBG. Reproducibility is key in science so that results are consistent and reliable across different experiments. In this study, after not being able to overexpress *SLC43A3* in the whole brain, we decided to replicate the work by

Furukawa et al. [11] and test *SLC43A3* as a transporter for ganciclovir (GCV) and to show its role in ^{18}F-FHBG uptake as well, since both are acycloguanosine analogs and substrates for this equilibrative membrane transporter.

Replication was done by stably transfecting HEK293 cells with plasmids encoding *SLC43A3-GFP*, which was kindly provided by the authors, and *HSV1-TK* and mCherry reporter vectors to verify transfection efficiency [11].

Stable transfection was done by selecting antibiotic-resistant clones and culturing for 3 weeks in Geneticin, then counting and plating as described in the original study. Fluorescence microscopy showed successful transfection and expression of *SLC43A3* (tagged with GFP) and the mCherry reporter plasmid for the *HSV1-TK* transfection efficiency verification. To further verify that *SLC43A3* localizes to the cell membrane as reported, co-staining with phalloidin and *SLC43A3* antibodies was done. Phalloidin is a peptide from the mushroom *Amanita phalloides* that binds specifically to filamentous actin (F-actin), which is a major component of the cell's cytoskeleton. F-actin is underneath the plasma membrane and forms a structural network that supports membrane shape and integrity. By staining F-actin, phalloidin helps to visualize the cell membrane. This imaging showed the presence of the transporter on the membrane.

Despite the microscopy results, [^{3}H]GCV and ^{18}F-FHBG uptake in different cell lines did not show a significant difference in uptake in cell lines that express *SLC43A3* compared to those that don't. However, Figure 32 shows that after 30 minutes of incubation with both substances, there was a slightly higher accumulation of [^{3}H]GCV or ^{18}F-FHBG in the *HSV1-TK* expressing cells. This means *HSV1-TK* phosphorylated the compounds and trapped them inside the cells. On the other hand, *SLC43A3*-expressing cells did not show any difference in uptake. Notably, these results prove that the substrates used in this study are functional since [^{3}H]GCV and ^{18}F-FHBG were phosphorylated in *HSV1-TK*-expressing cells, ensuring that the materials remain intact and functional.

At 5 minutes, no difference was seen in the accumulation of either substrate, probably because it's too short for *HSV1-TK* to phosphorylate a significant amount of these compounds. By 30 minutes, enough accumulation of [^{3}H]GCV or ^{18}F-FHBG was measurable using a scintillation liquid counter.

This shows the problems with data in research which can be due to methodological differences, lab settings or biological variability. Reproducibility is hard but necessary to make sure the results are not due to chance or experimental bias [2]. We tried to validate *SLC43A3* in taking up nucleobase analogs, specifically ^{18}F-FHBG a PET reporter probe. But we did not see the affect of *SLC43A3* in either ^{18}F-FHBG nor [^{3}H]GCV uptake. Future studies should focus on optimizing the protocol, including more precise quantification methods, validation of substrate-transporter

interaction and other conditions that might affect transporter activity. Reproducibility matters; small changes in the protocol can make a big difference. This is key to *SLC43A3* research. We checked the protocol with the authors but still failed to reproduce the published data.

4.6 Conclusions and Future Directions

SLC43A3 doesn't transport ^{18}F-FHBG into the brain in our experiments, especially *in vitro*. No significant uptake or accumulation of ^{18}F-FHBG was seen in cells expressing *SLC43A3* despite replicating the experimental conditions described by Furukawa et al., [11]. So we need to look into other transporters in the future studies that have higher affinity for this substrate. Transporters that are highly expressed in the liver where ^{18}F-FHBG is transported but minimally expressed in the brain would be good candidates to look further into.

One way to identify such transporters is to use RNA sequencing (RNAseq), a powerful tool to study gene expression across tissues. RNAseq quantifies RNA transcripts and gives a detailed view of gene expression in specific tissues [29, 37]. Its ability to compare gene expression between tissues makes it perfect to identify transporters that are highly expressed in the liver but low or no expression in the brain are potential candidates for ^{18}F-FHBG transport.

Future studies should combine RNAseq data with functional assays to validate the transport efficiency of these candidates for ^{18}F-FHBG. Combining gene expression analysis with substrate affinity studies is a targeted approach to overcome the current challenges. This will not only increase the delivery of the tracer but also deepen our understanding of transporter biology in tracer metabolism and distribution.

It is also important to look deeper on engineered AAV capsids as a delivery systems to increase targeting and BBB penetration. We chose AAV-BI30 initially based on the work by Krolak et al. (2022)[27] which showed that the combination of the CAG promoter gave high expression in endothelial cells throughout the brain. However the expression level was not high enough to test the transporter function of *SLC43A3* for the ^{18}F-FHBG.

To address this, investigating endothelial specific promoters could increase transgene expression in the brain vasculature. Future work should first reproduce the data with positive controls before doing *in vivo* experiments. *In vitro* assays should also be performed to confirm transporter function with the tracer and delivery conditions. By addressing these limitations future work can establish a more robust and efficient imaging system to monitor transgene expression in the brain.

5 Literature

References

[1] Sara A Collins, Kei Hiraoka, Akihito Inagaki, Noriyuki Kasahara, and Mark Tangney. Pet imaging for gene & cell therapy. *Current gene therapy*, 12(1):20–32, 2012.

[2] Monya Baker. Reproducibility crisis. *nature*, 533(26):353–66, 2016.

[3] Leah O Barrera, Zirong Li, Andrew D Smith, Karen C Arden, Webster K Cavenee, Michael Q Zhang, Roland D Green, and Bing Ren. Genome-wide mapping and analysis of active promoters in mouse embryonic stem cells and adult organs. *Genome research*, 18(1):46–59, 2008.

[4] John Blazeck and Hal S Alper. Promoter engineering: recent advances in controlling transcription at the most fundamental level. *Biotechnology journal*, 8(1):46–58, 2013.

[5] Ken Y Chan, Min J Jang, Bryan B Yoo, Alon Greenbaum, Namita Ravi, Wei-Li Wu, Luis Sánchez-Guardado, Carlos Lois, Sarkis K Mazmanian, Benjamin E Deverman, et al. Engineered aavs for efficient noninvasive gene delivery to the central and peripheral nervous systems. *Nature neuroscience*, 20(8):1172–1179, 2017.

[6] Diptaman Chatterjee, David J Marmion, Jodi L McBride, Fredric P Manfredsson, David Butler, Anne Messer, and Jeffrey H Kordower. Enhanced cns transduction from aav. php. eb infusion into the cisterna magna of older adult rats compared to aav9. *Gene therapy*, 29(6):390–397, 2022.

[7] Tom Curran and James I Morgan. Fos: an immediate-early transcription factor in neurons. *Journal of neurobiology*, 26(3):403–412, 1995.

[8] C Fillat, M Carrio, A Cascante, and B Sangro. Suicide gene therapy mediated by the herpes simplex virus thymidine kinase gene/ganciclovir system: fifteen years of application. *Current gene therapy*, 3(1):13–26, 2003.

[9] Helen L Fitzsimons, Ross J Bland, and Matthew J During. Promoters and regulatory elements that improve adeno-associated virus transgene expression in the brain. *Methods*, 28(2):227–236, 2002.

[10] Junji Furukawa, Katsuhisa Inoue, Junya Maeda, Tomoya Yasujima, Kinya Ohta, Yoshikatsu Kanai, Tappei Takada, Hirotaka Matsuo, and Hiroaki Yuasa. Functional identification of slc43a3 as an equilibrative nucleobase transporter involved in purine salvage in mammals. *Scientific reports*, 5(1):15057, 2015.

[11] Junji Furukawa, Katsuhisa Inoue, Kinya Ohta, Tomoya Yasujima, Yoshihisa Mimura, and Hiroaki Yuasa. Role of equilibrative nucleobase transporter 1/slc43a3 as a ganciclovir transporter in the induction of cytotoxic effect of ganciclovir in a suicide gene therapy with herpes simplex virus thymidine kinase. *Journal of Pharmacology and Experimental Therapeutics*, 360(1):59–68, 2017.

[12] Sanjiv Sam Gambhir. Molecular imaging of cancer with positron emission tomography. *Nature Reviews Cancer*, 2(9):683–693, 2002.

[13] Patricia Giraldo and Lluís Montoliu. Size matters: use of yacs, bacs and pacs in transgenic animals. *Transgenic research*, 10:83–103, 2001.

[14] Leeta A Green, Cecelia S Yap, Khoi Nguyen, Jorge R Barrio, Mohammad Namavari, Nagichettiar Satyamurthy, Michael E Phelps, Eric P Sandgren, Harvey R Herschman, and Sanjiv S Gambhir. Indirect monitoring of endogenous gene expression by positron emission tomography (pet) imaging of reporter gene expression in transgenic mice. *Molecular Imaging & Biology*, 4(1):71–81, 2002.

[15] Michael E Greenberg, Edward B Ziff, and Lloyd A Greene. Stimulation of neuronal acetylcholine receptors induces rapid gene transcription. *Science*, 234(4772):80–83, 1986.

[16] Leila Haery, Benjamin E Deverman, Katherine S Matho, Ali Cetin, Kenton Woodard, Connie Cepko, Karen I Guerin, Meghan A Rego, Ina Ersing, Susanna M Bachle, et al. Adeno-associated virus technologies and methods for targeted neuronal manipulation. *Frontiers in neuroanatomy*, 13:493120, 2019.

[17] David L Haggerty, Gregory G Grecco, Kaitlin C Reeves, and Brady Atwood. Adeno-associated viral vectors in neuroscience research. *Molecular Therapy-Methods & Clinical Development*, 17:69–82, 2020.

[18] Kathrin B Hasbargen, Wen-Jun Shen, Yiqiang Zhang, Xiaoming Hou, Wei Wang, Qui Shuo, David A Bernlohr, Salman Azhar, and Fredric B Kraemer. Slc43a3 is a regulator of free fatty acid flux1. *Journal of lipid research*, 61(5):734–745, 2020.

[19] Harvey R Herschman. Pet reporter genes for noninvasive imaging of gene therapy, cell tracking and transgenic analysis. *Critical reviews in oncology/hematology*, 51(3):191–204, 2004.

[20] Gloria E Hoffman, M Susan Smith, and Joseph G Verbalis. c-fos and related immediate early gene products as markers of activity in neuroendocrine systems. *Frontiers in neuroendocrinology*, 14(3):173–213, 1993.

[21] Stephen P Hunt, Adrian Pini, and Gerard Evan. Induction of c-fos-like protein in spinal cord neurons following sensory stimulation. *Nature*, 328(6131):632–634, 1987.

[22] Kristiina Iljin, Antoinise Dube, Sirpa Kontusaari, Jaana Korhonen, Isto Lahtinen, Peter Oettgen, and Kari Alitalo. Role of ets factors in the activity and endothelial cell specificity of the mouse tie gene promoter. *The FASEB journal*, 13(2):377–386, 1999.

[23] Zahra Karjoo, Xuguang Chen, and Arash Hatefi. Progress and problems with the use of suicide genes for targeted cancer therapy. *Advanced drug delivery reviews*, 99:113–128, 2016.

[24] Yung-Hi Kim, Mi-Ran Choi, Dong-Keun Song, Sung-Oh Huh, Choon-Gon Jang, and Hong-Won Suh. Regulation of c-fos gene expression by lipopolysaccharide and cycloheximide in c6 rat glioma cells. *Brain research*, 872(1-2):227–230, 2000.

[25] Yaz Y Kisanuki, Robert E Hammer, Jun-ichi Miyazaki, S Clay Williams, James A Richardson, and Masashi Yanagisawa. Tie2-cre transgenic mice: a new model for endothelial cell-lineage analysis in vivo. *Developmental biology*, 230(2):230–242, 2001.

[26] Motomichi Kosuga, Shin Enosawa, Xiao-Kang Li, Seiichi Suzuki, Nobutake Matsuo, Masao Yamada, Jayanta Roy-Chowdhury, Osamu Koiwai, and Torayuki Okuyama. Strong, long-term transgene expression in rat liver using chicken β-actin promoter associated with cytomegalovirus immediate-early enhancer (cag promoter). *Cell transplantation*, 9(5):675–680, 2000.

[27] Trevor Krolak, Ken Y Chan, Luke Kaplan, Qin Huang, Jason Wu, Qingxia Zheng, Velina Kozareva, Thomas Beddow, Isabelle G Tobey, Simon Pacouret, et al. A high-efficiency aav for endothelial cell transduction throughout the central nervous system. *Nature cardiovascular research*, 1(4):389–400, 2022.

[28] M Martinez, A Calvo-Torrent, and J Herbert. Mapping brain response to social stress in rodents with c-fos expression: a review. *Stress*, 5(1):3–13, 2002.

[29] Ali Mortazavi, Brian A Williams, Kenneth McCue, Lorian Schaeffer, and Barbara Wold. Mapping and quantifying mammalian transcriptomes by rna-seq. *Nature methods*, 5(7):621–628, 2008.

[30] Michael F Naso, Brian Tomkowicz, William L Perry III, and William R Strohl. Adeno-associated virus (aav) as a vector for gene therapy. *BioDrugs*, 31(4):317–334, 2017.

[31] Alexander R Nectow and Eric J Nestler. Viral tools for neuroscience. *Nature Reviews Neuroscience*, 21(12):669–681, 2020.

[32] Hiroyuki Okuno. Regulation and function of immediate-early genes in the brain: beyond neuronal activity markers. *Neuroscience research*, 69(3):175–186, 2011.

[33] Michael E Phelps. Positron emission tomography and autoradiography: principles and applications for the brain and heart. *Journal of Nuclear Medicine*, 41(9):1512–1512, 2000.

[34] James A Sawitzke, Alessandro Barenghi, Lynn Thomason, Nina Costantino, and Donald Court. Recombineering: a modern approach to genetic engineering. 2023.

[35] TV Sekar, K Foygel, JK Willmann, and R Paulmurugan. Dual-therapeutic reporter genes fusion for enhanced cancer gene therapy and imaging. *Gene therapy*, 20(5):529–537, 2013.

[36] Vijay Sharma, Gary D Luker, and David Piwnica-Worms. Molecular imaging of gene expression and protein function in vivo with pet and spect. *Journal of Magnetic Resonance Imaging: An Official Journal of the International Society for Magnetic Resonance in Medicine*, 16(4):336–351, 2002.

[37] Julia F Söllner, German Leparc, Tobias Hildebrandt, Holger Klein, Leo Thomas, Elia Stupka, and Eric Simon. An rna-seq atlas of gene expression in mouse and rat normal tissues. *Scientific data*, 4(1):1–11, 2017.

[38] Ralph Stadhouders, Suzan D Pas, Jeer Anber, Jolanda Voermans, Ted HM Mes, and Martin Schutten. The effect of primer-template mismatches on the detection and quantification of nucleic acids using the 5 nuclease assay. *The Journal of Molecular Diagnostics*, 12(1):109–117, 2010.

[39] Sébastien Terrat, Eric Peyretaillade, Olivier Gonçalves, Eric Dugat-Bony, Fabrice Gravelat, Anne Moné, Corinne Biderre-Petit, Delphine Boucher, Julien Troquet, and Pierre Peyret. Detecting variants with metabolic design, a new software tool to design probes for explorative functional dna microarray development. *BMC bioinformatics*, 11:1–16, 2010.

[40] S Tiwari and E Menghani. Mode of viral and non-viral gene transfer: an overview. *S. Tiwari and E. Menghani, Mode of Viral and Non-Viral Gene Transfer: An Overview, International Journal of Advanced Research in Engineering and Technology*, 11(11), 2020.

[41] Yu-Cheng Tu, Duen-Yi Huang, Shine-Gwo Shiah, Jang-Shiun Wang, and Wan-Wan Lin. Regulation of c-fos gene expression by nf-κb: a p65 homodimer binding site in mouse embryonic fibroblasts but not human hek293 cells. *PLoS One*, 8(12):e84062, 2013.

[42] Jan Van Erum, Debby Van Dam, and Peter Paul De Deyn. Ptz-induced seizures in mice require a revised racine scale. *Epilepsy & Behavior*, 95:51–55, 2019.

[43] Elizabeth van Pelt-Verkuil, Alex van Belkum, and John P Hays. Pcr primers. *Principles and Technical Aspects of PCR Amplification*, pages 63–90, 2008.

[44] Shahriar Yaghoubi, Jorge R Barrio, Magnus Dahlbom, Meera Iyer, Mohammad Namavari, Nagichettiar Satyamurthy, Robin Goldman, Harvey R Herschman, Michael E Phelps, and Sanjiv S Gambhir. Human pharmacokinetic and dosimetry studies of [18f] fhbg: a reporter probe for imaging herpes simplex virus type-1 thymidine kinase reporter gene expression. *Journal of Nuclear Medicine*, 42(8):1225–1234, 2001.

[45] Shahriar S Yaghoubi. Pet and spect reporter gene imaging. *Molecular Imaging Probes for Cancer Research*, 389:373, 2012.

[46] Shahriar S Yaghoubi, Dean O Campbell, Caius G Radu, and Johannes Czernin. Positron emission tomography reporter genes and reporter probes: gene and cell therapy applications. *Theranostics*, 2(4):374, 2012.

[47] Shahriar S Yaghoubi and Sanjiv S Gambhir. Measuring herpes simplex virus thymidine kinase reporter gene expression in vitro. *Nature protocols*, 1(4):2137–2142, 2006.

[48] Shahriar S Yaghoubi and Sanjiv S Gambhir. Pet imaging of herpes simplex virus type 1 thymidine kinase (hsv1-tk) or mutant hsv1-sr39tk reporter gene expression in mice and humans using [18f] fhbg. *Nature protocols*, 1(6):3069–3074, 2006.

[49] Ming Zhao, Xue-Fan Jiang, Hui-Qin Zhang, Jia-Hui Sun, Hui Pei, Li-Na Ma, Yu Cao, and Hao Li. Interactions between glial cells and the blood-brain barrier and their role in alzheimer's disease. *Ageing research reviews*, 72:101483, 2021.

[50] Zhen Zhao, Amy R Nelson, Christer Betsholtz, and Berislav V Zlokovic. Establishment and dysfunction of the blood-brain barrier. *Cell*, 163(5):1064–1078, 2015.

Acknowledgments

I sincerely thank everyone who contributed to the completion of this project and supported me through the challenges of pursuing a PhD.

First and foremost, I want to thank my amazing mother. Even though we have been miles apart, her endless love, encouragement, and support have been my constant source of strength. Mom, your belief in me kept me going, and I wouldn't have made it through this journey without you. Thank you for always being there for me, no matter the distance. I am endlessly grateful for having you.

I am deeply grateful to my supervisors, Professor Thomas Wunderlich and Dr. Heiko Backes, for their invaluable guidance and support throughout this journey. Their mentorship, patience, and expertise have been the cornerstone of my research and personal growth. Thank you both for believing in my potential, for your thoughtful advice, and for always being there to provide encouragement and feedback.

A huge thank you to my amazing lab mates who have been a constant source of inspiration and support throughout this journey. Peter, Annika, Nasim, Cecile, Sicilia, Rui, Shuntaro, Lionel, Sima, Vivien, Leonie C, Patricia S, Alex, Weiyi, Carlos—and everyone else who has been part of this adventure—you've made my time in the lab so much more enjoyable and meaningful. Your friendship, support, and good humor, both in and out of the lab, have made this journey truly special. I feel so lucky to have had you all with me along the way!

I would like to express my gratitude to my thesis advisory committee, consisting of Prof. Dr. Thomas Wunderlich, Prof. Dr. Bernd Neumaier, and Dr. Sophie Steculorum, for their valuable insights and thoughtful suggestions that greatly improved our experimental strategies during our regular meetings.

I would like to sincerely thank my thesis committee members, Prof. Thomas Wunderlich, Prof. Peter Kloppenburg, Prof. Matteo Bergami, and Dr. Heiko Backes, for their time, effort, and valuable input in reviewing my thesis and being part of my defense committee. Your knowledge and helpful feedback have played a key role in shaping this work.

Finally, to my incredible family, friends, and everyone who stood by me throughout this journey: thank you for being my biggest cheerleaders and my steady source of strength. Your love, support, and encouragement made all the difference, and I couldn't have done it without you!